SYNTHESIS, CHARACTERIZATION AND CATALYTIC PROPERTIES OF VANADIUM SILICATE MOLECULAR SIEVES

A THESIS

SUBMITTED TO THE

UNIVERSITY OF POONA

FOR THE DEGREE OF

DOCTOR OF PHILOSOPHY

(IN CHEMISTRY)

BY

P. RAJA HARI PRASAD RAO

CATALYSIS DIVISION

NATIONAL CHEMICAL LABORATORY

PUNE - 411 008, INDIA

NOVEMBER 1992

Dedicated to

my beloved

Parents

and

Sisters

CERTIFICATE

Certified that the work incorporated in the thesis entitled "**Synthesis, Characterization and Catalytic Properties of Vanadium Silicate Molecular Sieves**" submitted by Mr. **P. Raja Hari Prasad Rao** for the degree of Doctor of Philosophy was carried out by the candidate under my supervision in the National Chemical Laboratory, Pune, India. Such material as has been obtained from other sources has been duly acknowledged.

(Dr. P. RATNASAMY)

Supervisor

ACKNOWLEDGEMENTS

I wish to express my deep sense of gratitude to my supervisor, Dr. P. Ratnasamy, Deputy Director, National Chemical Laboratory, for his valuable guidance and encouragement throughout the course of this investigation.

I am deeply indebted to Dr. A.V. Ramaswamy for his stimulating discussions and constant professional and personal help rendered during the course of the present investigation. Without his help, it would not have been possible for me to complete my research work successfully.

I wish to offer my sincere thanks to Dr. S. Sivasanker, Dr. B.S. Rao, Dr. R. F. Shinde, Dr. I. Balakrishnan, Dr. S.G. Hegde, Dr. Rajiv Kumar and Dr. R. Vetrivel for their valuable discussions and suggestions.

I thank my colleagues and friends for their help and co-operation.

I am thankful to the Director, National Chemical Laboratory, for allowing me to submit this work in the form of a thesis for the award of Ph. D degree. Financial assistance from the Council of Scientific and Industrial Research, New Delhi, is gratefully acknowledged.

My special word of thanks is due to grand mother, brother-in-laws and Madhavi for their inspiration, constant encouragement and moral support.

Date : 24.11.92

(P. RAJA HARI PRASAD RAO)

Contents...

CHAPTER 1

GENERAL INTRODUCTION

1.1 INTRODUCTION

The subject dealing with zeolites is a dynamic and rapidly growing field in which a broad range of chemistry from solid state to organic is being explored. Zeolites introduce both unusual activity and selectivity into heterogeneous adsorption and catalytic processes and are the inorganic analogs of enzymes in living systems. These are used on a large industrial scale for great variety of processes from simple drying to complicated catalytic reactions. These exhibit appreciable acid activity with shape selective features, not available in compositionally equivalent amorphous catalysts[1]. Zeolites can also act as supports for numerous catalytically active metals.

1.2 ZEOLITES

Zeolites are crystalline, hydrated aluminosilicates, both natural and synthetic, whose framework structure is based on an infinitely extending three dimensional network of SiO_4 and AlO_4 tetrahedra linked to each other by sharing all the oxygens. The crystallographic unit cell of zeolites may be represented as:

$$M_{x/n}[(AlO_2)_x(SiO_2)_y]\ z\ H_2O$$

where M is a cation of valence 'n' from group I or II of the periodic table or of a rare earth element or an organic species. The net negative charge and hence the cation content is governed by the Si/Al (y/x) ratio. Si/Al ratio is always greater than or equal to one, because Al^{3+} does not occupy adjacent tetrahedral sites, according to Loewenstein rule[2]. The relatively rigid anionic framework forms the channels with free diameters of 2.5 to 8 Å and inter connected voids which are occupied by the cations and water molecules. The cations are quite mobile and may be usually exchanged to varying degrees by other cations. The intra crystalline water molecules can in general be removed easily by heating to 523 to 623 K.

Al^{3+} ions in the zeolite lattice can be replaced by various metal ions like B^{3+}, Ga^{3+}, Fe^{3+}, Cr^{3+}, Ti^{4+}, Zr^{4+}, V^{4+}/V^{5+} and Sb^{5+}. The resultant materials are generally called metallosilicate analogs of zeolites or metallosilicate molecular sieves.

1.3 CLASSIFICATION

Till todate about 40 natural and more than 160 synthetic zeolites have been identified. Zeolites have been classified based on morphological characteristics[3-6], crystal structure[3,4,7], chemical composition[3,4,8], effective pore diameter[3,4,9] and natural occurrence[3,4].

Bragg[6] classified the zeolites based on their morphology and it was modified by Meier[5] and Barrer[4] according to secondary building units present in them, as presented in Table 1.1. Classification of zeolites according to their chemical composition has been made based on silica to alumina ratios into four types, *viz*, 1. Low silica zeolites (A, X, sodalite *etc.*) 2. Intermediate silica zeolites (Y, L, mordenite *etc.*) 3. High silica zeolites (ZSM-5, ZSM-11, EU-1 *etc.*) and 4. Pure silica zeolites (silicalites or silica molecular sieves) (silicalite-1 and silicalite-2).

Barrer[4] and Sand[8] classified the zeolites based on effective pore diameter into three groups *viz.* 1. Small pore zeolites (eg. Linde A, ZK-5, Rho, Chabazite *etc.*), 2. Medium pore zeolites (ZSM-5, ZSM-11, ZSM-23, ZSM-48, ferririte, Stilbite *etc.*) and 3. Large pore zeolites (Linde X, Y, L, gmelinite, mordenite, ZSM-20 *etc.*). Recently, a very large pore aluminophosphate molecular sieve (VPI-5)[10] and a gallophosphate molecular sieve[11] (cloverite) have been discovered. An isomorph of VPI-5 called MCM-9 containing Si atoms has also been reported[12].

1.4 NOMENCLATURE

There is no systematic nomenclature developed for zeolites and molecular sieves. The early synthetic zeolites discovered by Milton, Breck and coworkers at union carbide were named with Arabic alphabets e.g., zeolite A, B, X, Y and L, and those discovered at Mobil and Union Carbide were named with Greek alphabets e.g., alpha, beta and omega. The zeolites having structures similar to mineral zeolites were assigned the name of minerals e.g., synthetic mordenite, chabazite, erionite, offretite *etc.*

International Zeolite Association Structure Commission (IZA) and International Union of Pure and Applied Chemistry (IUPAC) have assigned structural codes to known synthetic and natural zeolites[5,13]. Designations consisting of three capital letters (excluding numbers and characters other than roman letters), generally derived from the type species have been used to identify structure types. Structure type codes are independent of composition and distribution

Table 1.1

Classification of zeolites according to structure type

	Structure type	Main species	Isostructural species
1.	**Analcime group :** (inter connected 4- and 6 membered rings)	analcime	leucite, pollcite, viseite, wairakite 6-Ca-D, Na-B.
2.	**Natrolite group :** (chains of tetrahedra with 6.6 Å repeat distance)	natrolite	laubanite, mesolite, metanatrolite
3.	**Chabazite group :** (parallel 6- or double 6 membered rings)	chabazite	Linde D, herschelite, Linde R
4	**Phillipsite group :** (approximated parallel 4- membered rings)	phillipsite	harmotome, ZK-19, Na-P_1, Linde W
5	**Heulandite group :** (characteristic configuration with 4 or 5 membered rings)	heulandite	clinoptilolite
6	**Mordenite group :** (each tetrahedra of the framework belongs to at least one 5 membered ring)	mordenite	Na-D, Zeolon, ZSM-21, ZSM-35, ZSM-38, ptilolite
7	**Faujasite group :** (Framework based on polyhedral cages of cubic or near cubic symmetry)	faujasite	Linde X, Linde Y, ZSM-20, ZK-4, ZK-21, ZK-22, N-A, Alpha
8	**Laumontite group :**	laumontite	leonhardite
9	**Pentasil group :**	ZSM-5, ZSM-11	
10	**Clathrate group :**	melanophlogite, ZSM-39	

of various possible T atoms (Si, Al, Ga, Fe, B, Ge, Ti, V, *etc.*) e.g., FAU (Faujasite, X and Y), MFI (Mobil five, ZSM-5), MEL (Mobil eleven, ZSM-11), MTW (Mobil twelve, ZSM-12) MOR (Mordenite), TON (Theta-1) *etc.*

1.5 ZEOLITE SYNTHESIS

The method developed by Milton in the late 1940's involves the hydrothermal crystallization of reactive alkali metal aluminosilicate gels at low temperatures and pressures. During the synthesis of low silica zeolites with alkali aluminosilicates, it has been proposed that hydrated alkali cation "templates" or stabilizes the formation of zeolite structural sub units. Alkali hydroxide, reactive forms of alumina and silica, and H_2O were combined to form gel and crystallization was carried out around 100 °C .

The addition of quarternary ammonium cations to alkali aluminosilicate gels was started in the early 1960's, first to produce intermediate silica zeolites and subsequently led to the discovery of high silica zeolites and silica molecular sieves. The synthetic chemistry of both high silica and early low silica molecular sieves is similar except the addition of quarternary ammonium ions and crystallization temperatures. The pH of the gel in both types of zeolites is high and is around 10 - 14.

The variables which have major influence on the structure crystallized are the gross composition of the reaction mixture, crystallization temperature and time[14].

The silica to alumina ratio, generally determine the framework composition of the zeolite, but the amount of alumina in the zeolite also can determine the structure. Apart from the silica to alumina ratio various other factors in the gross composition of the reaction mixture which influence the zeolite structure and crystallization are organic (template) and inorganic cations, -OH ion concentration. Aging period, stirring, nature of the reaction mixture and order of mixing also influence the crystallization.

During the crystallization both aluminum and silicon will dissolve to form aluminate and silicate anions. These anions are brought together (by template and /or metal ion) to form a gel by condensation or polymerization.

Sand[15] has summarized the following events occurring during the crystallization of the zeolites

Precipitation of the gel
Dissolution of the gel
Nucleation of the zeolite structure
Continued crystallization and crystal growth
Dissolution of the initial meta stable phase
Continued crystallization and crystal growth of more stable crystalline phase, while initial metastable crystals are dissolving.
Dissolution of further meta stable phases
Nucleation of a more stable meta stable phase
Continued crystallization and crystal growth of final crystalline phase

1.6 ISOMORPHOUS SUBSTITUTION

Isomorphous substitution can be performed either during the synthesis or by post-synthesis methods. Isomorphous substitution is also reported by solid-solid interaction at high temperatures between zeolite and metal oxide. Szostak[16] has presented a list of crystalline metallosilicate molecular sieves and their corresponding structure. The first isomorphous substitution in the zeolite framework was reported by Goldsmith[17] in 1952 in the synthesis of germanium containing thomsonite, in which Si was replaced by Ge. Later, Barrer *et al.*[18] reported a number of Ga and Ge substituted zeolites. Isomorphous substitution of tri-, tetra- and pentavalent cations, such as Fe^{3+}, Ga^{3+}, B^{3+}, Ti^{4+}, Ge^{4+} and V^{4+}/V^{5+} during the hydrothermal synthesis[16,19-24] is one of the significant achievements in the last decade. The replacement of the Al by B, Ga, Fe, Ge and Ti are now well established. Recently incorporation of pentavalent metal ions such as V, Sb and P is reported[22-26].

Secondary synthesis methods have also been used to incorporate various metal ions such as Al, Si, Fe, Ga, Ti, V and P into zeolite frame work[26-31]. Introduction of metal ions such as Cr, Mo and V was reported by solid-solid interaction at high temperatures (773 K)[32]. In this method, the introduced metal ions will be normally at cationic positions. Introduction of V ions at cationic positions by chemical vapor deposition method is also reported[31].

Aluminophosphate molecular sieves, structural analogs of zeolites as well as new structures with pore size greater than that of zeolites have been reported by Wilson *et al.*[33]. Davis *et al.*[10] have reported 18-membered ring large pore molecular sieve, designated as VPI-5. Recently,

Estermann *et al.*[11] have reported gallophosphate molecular sieve (cloverite). Metalloaluminumphosphate (**MeALPO**) molecular sieves, where metal ions such as Co, Fe, Mg, Zn, Ga, Cr, Ti, V and Mo has been substituted into the framework of ALPO have been synthesized[34-36]. Silicoaluminumphosphates (SAPO's) by the substitution of the silicon into the framework of the ALPO's has been reported[37]. These exhibit cation exchange and weak acidic properties.

1.7 CHARACTERIZATION

1.7.1 X-RAY DIFFRACTION

X-ray powder diffraction is the most important technique used in the study of zeolites. It gives information about

Zeolite structure[38]
Phase purity
Degree of crystallinity
Crystal size
Unit cell parameters[39]

When Al or Si is substituted by other metal ions a change in unit cell parameters will be observed depending on size of the metal ion. Hence, by measuring the unit cell parameters the extent of incorporation can also be determined. Correlations between the values of unit cell parameters and extent of incorporation of B, Fe, Ga and Ti have been reported[41-45].

The most important use of the XRD technique is the structure determination, especially by single crystal methods[46]. Powder diffraction technique including *ab initio* structure determination and *Rietveld refinements*[47] have helped in structure determination of numerous zeolites.

1.7.2 INFRARED SPECTROSCOPY

Infrared spectroscopy is a sensitive technique for the investigation of structural features of zeolites, isomorphous substitution, acidic properties and nature of adsorbate-zeolite interaction[48-50]. The lattice vibrations of the zeolites in the infrared spectrum will be observed in the range of 300 -1300 cm^{-1}. These vibrations can be classified into two groups[48], (i) internal vibrations of the TO_4 units or structure insensitive vibrations and (ii) vibrations due to external linkages of the TO_4 units or structure sensitive vibrations. The major infrared band assignments are as follows :

Internal Tetrahedra

Assymmetric stretching	1250 - 950 cm^{-1}
Symmetric stretching	720 - 650 cm^{-1}
T - O bond	420 - 500 cm^{-1}

External Linkages

Double ring	650 - 500 cm^{-1}
Pore opening	300 - 420 cm^{-1}
Symmetric stretching	750 - 820 cm^{-1}
Asymmetric stretching	1050 - 1150 cm^{-1}

Systematic studies of the framework vibrations of zeolites A, X, Y, ZK-5 and Omega have been reported[49]. For some structure sensitive bands a linear relation between the wave number and the number of lattice aluminum atoms is reported[49]. Isomorphous substitution shifts both symmetric and asymmetric framework vibrations. The substitution of lighter elements such as B shifts the framework vibrations to higher wave numbers[53], while heavier metal ions such as Fe, Ga and Ti shifts to lower wave numbers[54]. In the case of titanium and vanadium silicates an additional asymmetric stretching vibration at around 960 cm^{-1} was reported. It was attributed to Si-O-M (M = Ti, V) linkages[21,22,24].

IR spectroscopy is an efficient technique to study both the Brönsted and Lewis acidity using probe molecules such as ammonia, pyridine, benzene, carbon monoxide, acetonitrile *etc.,* and is extensively reviewed by Ward[50]. The O-H stretching frequency also changes depending on acidity. Decrease in acidity decreases the stretching frequency. Barthomeuf[55] has measured the exact position of the IR peaks corresponding to acidic -OH groups for a series of zeolites with varying Si/Al ratios.

1.7.3 NUCLEAR MAGNETIC RESONANCE SPECTROSCOPY

High resolution solid state MAS NMR spectroscopy has emerged as a powerful technique for the investigation of zeolite lattice structures and location of various isomorphously substituted metal ions[56,57]. NMR is very sensitive to the local ordering and geometries. Till to date about twenty NMR active nuclei in zeolites have been studied. NMR technique is used to investigate

Si and Al ordering in the zeolite framework[58]

Crystallographically equivalent and non-equivalent Si and Al ions at various sites.[59,60]
Framework Si/Al ratios[61]
Coordination number of Si[62] and Al[63] and
Spectral correlations with Si-O-T bond angles[64] and Si-O bond lengths[65].

Application of ^{29}Si MAS NMR technique to zeolites results in spectra in which a number of separate Si peaks can be observed. For faujasite structure it is possible to distinguish upto five different peaks, which can be attributed to silicon atoms connected through oxygen to 0, 1, 2, 3, and 4 Al atoms[66]. Since the intensity of the peak is proportional to the number of the Si atoms, it is possible to estimate the number of silicon atoms by summation of the peak intensities.

Recently, Fyfe *et al.* have demonstrated three dimensional connectivities in zeolites ZSM-5, ZSM-11, ZSM-22 and ZSM-39[67-70]. High resolution liquid NMR (^{29}Si and ^{27}Al) has provided useful information on the silicate[71,72] and aluminosilicate[73-76] species present in the solution used in the zeolite synthesis. This has enabled the synthesis of titanium rich TS-1. ^{13}C CP/MAS NMR has been used to study the location and configuration of organic templates[76].

^{129}Xe NMR has been used in the characterization of zeolite pore systems, coke formation during catalytic cracking *etc.*[77]. Pfeifer *et al.*[78] have applied ^{1}H MAS NMR to study different types of protons present in the zeolite.

1.7.4 ELECTRON SPIN RESONANCE SPECTROSCOPY

ESR spectroscopy is sensitive to environmental symmetry of paramagnetic metal ions. ESR spectroscopy is used to study the environment of the isomorphously substituted and exchanged cations and metal oxides within the pores or external zeolite matrix[31]. Various paramagnetic metals such as V^{4+}, Fe^{3+}, Cr^{3+}, have been studied extensively using ESR spectroscopy[19,32,79]. Vedrine[80,81] identified three types of Fe^{3+} ions in Fe-ZSM-5 using detailed ESR study complemented by Mössbauer and UV-VIS techniques. ESR technique[32] has been used to characterize solid-solid reaction between zeolite and metal oxide of elements such as Cu, Cr, Fe, V and Mo. The oxidation state, position, environment and redox property of V in vanadium silicate molecular sieves with MFI and MEL structures have been studied[22-24,79].

1.7.5 SORPTION AND DIFFUSION STUDIES

Sorption property of the zeolites has been extensively used in characterizing molecular sieve materials. Sorption studies provide information about **void volume, pore size, crystallinity, crystal size** and **acidity** of the zeolites.

The most commonly used method to measure sorption kinetics is conventional **gravimetry** using microbalence. Other techniques which can be used to study sorption kinetics include **pulse chromatography, tracer diffusion, neutron diffusion** and **pulse field gradient NMR spectroscopy**.

The role of adsorption and diffusion of the molecules within the zeolite pores is important for shape selective properties. Barrer[82], Ruthven[83], Paleker and Rajadyaksha[84] reviewed the sorption properties with special emphasis on catalytic properties. Sorption of various gases and vapors on both natural and synthetic zeolites has been extensively studied[82,85,86] and various thermodynamic parameters such as entropy, heat and free energy of sorption have been estimated.

The diffusion among the zeolites can be classified into three types, namely **Configurational, Knudsen** and **Bulk** diffusions. In configurational diffusion the dimensions of the zeolite pores approaches those of molecules and even a subtle change in the dimensions of the molecule results in a large change in diffusivity. Knudsen diffusion takes place when the mean free path of the molecule is comparable to the zeolite pore diameter. Bulk diffusion occurs when the mean free path of the molecule is smaller than that of the zeolite pore diameter and the rate of diffusion is independent of the pore diameter.

1.8 NATURE OF ACTIVE SITES

The catalytic activity of zeolites is associated with the presence of acid centers in the intracrystalline surface. These acid centers are created by the imbalance in the charge between silicon and aluminum ion of the framework. Each aluminum atom of the framework induces a potential active acid site.

Brönsted acidity arises when the cations balancing the framework anionic charge are replaced by protons (H^+). Trigonally coordinated aluminum atom can accept an electron pair and thus behave as Lewis acid site.

These acid sites on zeolites can be studied by both physical and catalytic characterization techniques. Important among them are infrared spectroscopy, adsorption and desorption properties of probe molecules such as ammonia and pyridine and acid catalyzed reactions including selected cracking and isomerization.

Infrared spectroscopy is a widely used technique to characterize the hydroxyl species on the zeolite surface and to measure the number and strength of Brönsted and Lewis acid sites and is extensively reviewed by Ward[50]. IR studies on ZSM-5 revealed two hydroxyl stretching bands, one at 3605 cm^{-1} and another at 3720 cm^{-1}. The absorption bands between 3600 - 3610 cm^{-1} are due to hydroxyl stretching associated with Al-O(H)-Si bridge[87,88], and the bands between 3720 - 3740 cm^{-1} are due to terminal silanol (Si-OH) groups[88]. Adsorption and desorption of basic probe molecules accompanied by IR spectroscopic method have been used to estimate the number and strength of acid sites[87-90]. Pyridine is frequently used as probe molecule. The reaction of pyridine on Brönsted acid sites results in the formation of pyridinium ion, and form coordinate bond on the Lewis acid sites. Both pyridinium ion and coordinatively bound pyridine have characteristic IR absorption bands. The intensity of these bands gives information about the number of acid sites. Jacobs *et al.*[91] have used less basic probe molecules such as benzene in order to characterize the strength of acidic sites.

Desorption of the bases can also be used to characterize the strength of acid sites. Stronger acid sites adsorb bases more strongly and require higher temperatures to desorb. In this method the zeolite is contacted with a base (ammonia or pyridine) to neutralize the acid sites present. Then the temperature is raised at a constant rate and the amount of desorbed base is recorded. The temperature and area of the desorption of the peaks provide information about strength and number of acid sites. However, this method can not distinguish between ammonia desorbing from Brönsted or Lewis acid sites.

Catalytic probe reactions can also be used to study the acidity of the zeolites. Important among various test reactions used to study are

Cracking of n-hexane
Cracking of n-butane
Cracking of n-decane
Isomerization of xylene
Disproportionation of toluene
Disproportionation of ethylbenzene

Cracking of n-hexane[92] is commonly called as alpha test developed at Mobil laboratories to study the catalytic activity of the zeolites. Cracking of butane[93] as a means of comparing catalytic acid properties of zeolites was developed in the Union Carbide laboratories. Cracking of n-decane provides information on both porosity and acidity[94].

1.9 SHAPE SELECTIVITY IN ZEOLITES

Shape selectively is one of the unique properties exhibited by zeolites which have pore dimensions similar to kinetic diameter of simple organic molecules. Molecular shape selectivities have been classified into four types.
viz. Reactant shape selectivity, Product shape selectivity, Transition state shape selectivity and Molecular traffic control[95].

Reactant shape selectivity results from limited diffusivity of some of the reactants, which can not effectively enter and diffuse inside the zeolite pores.

Product shape selectivity occurs when slowly diffusing product molecules can not rapidly escape from the zeolite pores and undergo secondary reactions.

Restricted transition state shape selectivity is observed when the transition state for a reaction is too large to be accommodated inside the pores.

1.10 APPLICATIONS OF ZEOLITES

The major applications of synthetic zeolites are as cation exchangers in detergent formulations, adsorbents in drying and separation and as catalysts in process industry. The introduction of acid faujasites into industrial catalysts for fluid catalytic cracking in 1962 was the foremost event in zeolite catalysis[96,97]. The characteristic properties such as acidity, shape selectivity and thermal stability enable them to be used for highly selective synthesis in the field of chemical intermediates and fine chemicals. The ion exchange properties, isomorphous substitution, stabilization of functional metal ions and complexes make them useful in various reactions involved in organic synthesis.

1.10.1 ZEOLITES IN PETROCHEMICAL PROCESSES

In 1962 zeolites were incorporated into typical cracking catalysts. The use of zeolite catalysts has resulted in large increase in gasoline selectivity with lower gas and coke yields.

Metal doped Y zeolites were proved to be selective as bifunctional catalysts, in the field of hydrocracking[98,103]. The shape selective catalysis by high silica pentasil zeolites led to new industrial processes[99]. Apart from cracking and hydrocracking, selectoforming[100], olefin oligomerization[101], dewaxing[103] and MTG (methanol to gasoline) process[103] based on zeolite catalysts have been established as industrial processes. Presently, dealuminated zeolite Y in combination with ZSM-5 is used as shape selective cracking catalyst. Table 1.2 describes some of the processes commercialized using zeolite catalysts.

..10.2 ZEOLITES IN ORGANIC SYNTHESES

Recently, zeolites have been successfully applied in organic synthesis as non-acid catalysts in reactions such as oxidation, reduction, olefin oligomerization, hydroformylation *etc.* Venuto[102] has introduced the potential use of zeolites in organic synthesis. Holderich[103] and van Bekkum[104] have extensively reviewed their use in organic synthesis.

A. Isomerization Reactions

Isomerization of the substituted arenes is of industrial interest and frequently serves as model for shape selectivity in zeolites[94]. Xylene isomerization has found commercial application. Zeolite ZSM-5 is reported to catalyze the isomerization of cresols, chlorotoluenes, tolunitriles, and toluidines[105]. Isomerization of aniline to 2-methylpyridine, 1, 2 diols to carbonyl compounds, dihydro-5-(hydroxymethyl)-2-furanones to 3, 4-dihydro-2-pyrones and epoxides to aldehydes has been reported[103]. Isomerization of 1, 3 dioxanes to 3 alkoxy propionaldehyde, Bekmann rearrangement of cyclohexanone to ε-caprolactam have also been reported[102,103].

B. Substitution Reactions

Zeolite catalyzed alkylation reactions afford large potential for industrial exploitation. Pentasil zeolites have the ability to direct the alkylation of alkylbenzenes selectively to *para* position[107]. Shape selectivity of modified ZSM-5 catalysts is an important factor in Mobil-Badger process for alkylation aromatics[107]. The most important selective gas phase alkylation of oligocyclic arenes is methylation of napthalene[108]. Alkylation of arenes having functional groups can also be carried out. A broad spectrum of products consisting essentially of cresols, xylenols, and diphenyl ether is obtained when phenol is methylated using zeolites[109]. Gauthier *et al.*[110] have reported acylation of alkylbenzenes on Ce-Y zeolites to aromatic ketones. Zeolites eliminate corrosion and disposal problems in these reactions.

Table 1.2

Commercial processes based on zeolites

Name of the process	Purpose
Selectoforming	Octane boosting
M-forming	Octane boosting
Catalytic cracking	Octane boosting
MDDW	Distillate dewaxing
MLDW	Lube dewaxing
M2-froming, Cyclar	Gas to aromatics
MOGD	Light oefins to gasoline and distillate
MTG	Methanol to gasoline
MTO	Methanol to light olefins
MVPI, MLPI, MHTI	Xylene isomerization
MTDP	Toluene disproportionation
MEB, ALBENE*	Ethylbenzene synthesis
para-Selective reactions	*p*-Xylene synthesis
	p-Ethyl toluene synthesis

Aliphatic nucleophilic substitution reactions studied over zeolite based catalysts include synthesis of amines from alcohols and ammonia, ethers and esters from alcohols, thiols from alcohols and hydrogen sulfide[113,114].

C. Condensation Reactions

Zeolites can be used preferably in condensation of organic molecules which are normally catalyzed by acids and bases. Since the acidity of the zeolites can be easily controlled, it is possible to adjust their catalytic properties in order to suit the desired reaction. Acetone condenses over zeolites to give mesityl oxide, isobutene, phorones, mesitylene and alkyl phenols[103]. Formaldehyde and isobutene condense to give isoprene[115]. Formaldehyde condenses with benzene to give diphenyl methane on large pore zeolites[116]. N-containing heterocyclic compounds can also be synthesized in the presence of ammonia[104]. Cyclic ethers and lactones react with ammonia to give cyclic imines or lactones[102].

D. Oxidation Reactions Using Air

Metal ion exchanged forms of zeolite X are active catalysts for complete oxidation of methane to carbondioxide[117]. Mochida *et.al*[118] reported the oxidation of propene to 2-propanol, acetone and acrolein. Transition metal exchanged zeolites are highly active in oxidation of nitrogen oxides. Steifns and Mars[119] have systematically investigated the behavior of zeolites in oxidation of H_2S to sulphur. Vanadium containing mordenite has been claimed [120] to have very high activity in oxidation of H_2S to SO_2.

E. Oxidation Reactions Using N_2O and H_2O_2

Selective vapor phase hydroxylation of benzene to phenol on medium pore high silica zeolites such as ZSM-5, Fe-ZSM-5 and ferrisilicate molecular sieves using nitrous oxide as oxidant has been reported[111,112]. Titanium silicate molecular sieves were used in selective oxidation of various organic molecules in the presence of dilute hydrogen peroxide[21]. They are active in hydroxylation of benzene, phenol, anisole and toluene. Hydroxylation of phenol is in commercial practice. Oxyfunctionalization of alkanes using titanium and vanadium silicate molecular sieves has recently been reported[121,122].

1.11 MFI and MEL TYPE ZEOLITES

Zeolites ZSM-5 (MFI)[123] and ZSM-11 (MEL)[124] are the two extreme members of a series of "pentasil" zeolites that are based on pentasil building units composed entirely of five membered rings. Kokotailo and Meier proposed the name "pentasil" for the zeolites having five membered ring secondary building units. These are the most used zeolites in the petrochemical processes and organic synthesis. High silica to alumina ratio, absence of cavities inside the pore system, geometrical constraints imposed by 10 membered ring pores have made these zeolites industrially very important. Pure silica analogs of ZSM-5 and ZSM-11 (silicalite-1[125] and silicalite-2[126] respectively) have been reported.

The framework structure of ZSM-5 was described by Kokotailo *et al.*[123]. Olson *et al.*[127] have reported the structure and structure dependent properties. It has twelve crystallographically inequivalent sites.

The structure of ZSM-11 was originally proposed by Kokotailo *et al.*[124] based on X-ray powder diffraction studies and modelling. Tetragonal space group $I\bar{4}m2$ and lattice constants a = b = 20.12 and c = 13.44 which correspond to average values derived from least squares refinement of XRD data have been proposed. Detailed investigation of the zeolite ZSM-11 structure have recently been presented by Fyfe *et al.*[128] using a combination of solid state NMR and synchroton X-ray diffraction techniques. Their study indicated that the structure is temperature dependent and that the high temperature form is tetragonal with space group $I\bar{4}m2$. The tetragonal symmetry implies that there are seven crystallographically inequivalent sites. ZSM-11 structure has been recently investigated using two dimensional ^{29}Si MAS NMR at two different temperatures. It was proposed that the asymmetric unit of the low temperature form has 12 distinct T sites according to 12 resonance lines in the ^{29}Si NMR spectra[68].

In ZSM-5 and ZSM-11 structure groups, the five membered ring secondary building units (Fig.1.2a) are joined along [001] to form chains (Fig.1.2b), which pack laterally along [010]. The ZSM-5 structure is generated when the adjacent [100] planes are sheets (Fig.1.2c) to form are related to one another by inversion ($\bar{1}$) and ZSM-11 structure is formed when the [100] sheets are related to one another by mirror symmetry (σ). Infinite series of intermediate structures may be obtained by applying reflection transformations (σ) to ZSM-5 or inversion transformation ($\bar{1}$) to ZSM-11. Such transformations lead to the channel system. This results in two types of intersecting channels in ZSM-5, with 10 membered ring openings, one with an elliptical cross

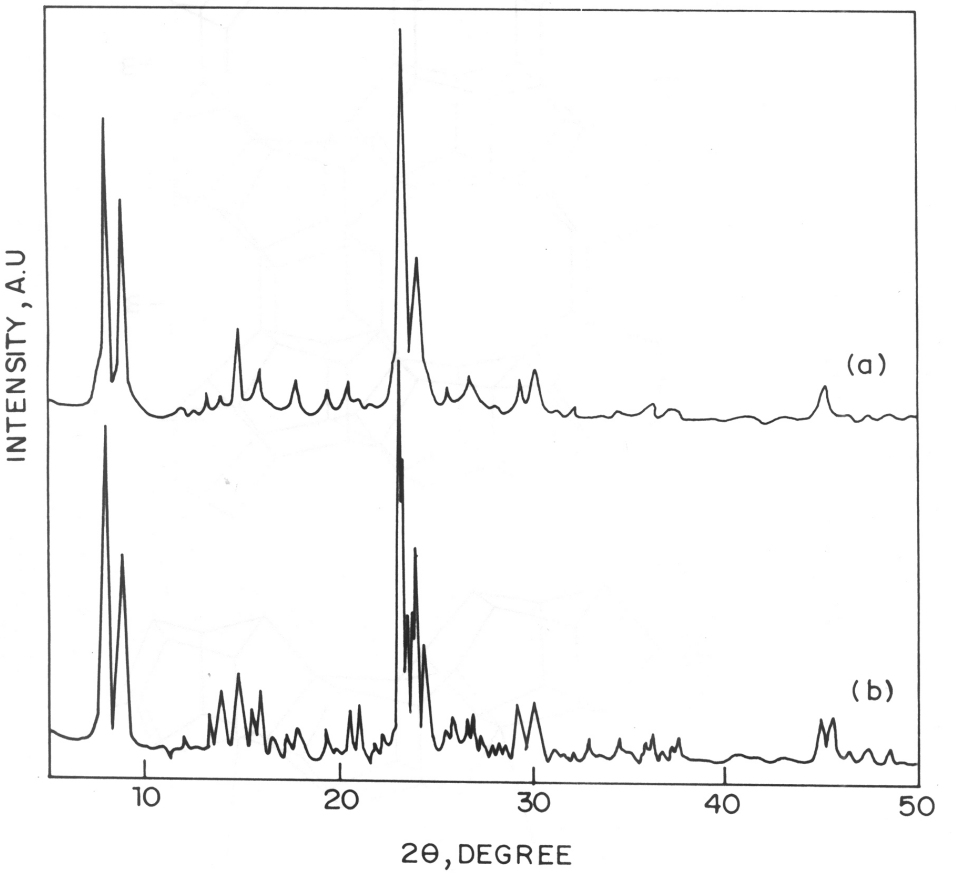

Fig.1.1. X-ray diffraction patterns of Al-MEL (a) and Al-MFI (b) calcined at 823 K.

Fig.1.2. Schematic diagram of the pentasil unit (a), SBU (b) and pentasil layer (c).

Table 1.3

Comparison of crystallographic data of MFI and MEL zeolites

Crystallographic parameters	MFI	MEL
Secondary building units	Complex 5-1	Complex 5-1
Framework density (No. of T-atoms per 1000 ($Å^3$)	17.9(Si + Al)	17.6(Si + Al)
Channels	10 membered ring, intersecting	10 membered ring, intersecting
Fault planes	[100]	[100]
No. of T-atoms per unit cell	96	96
No.of non-equivalent T-atoms	12	7
Space group symmetry	Orthorhombic/P_{nma}	Tetragonal/$I\bar{4}m2$
Unit cell dimensions	a = 20.1 Å, b= 19.9 Å, c= 13.4 Å	a = b = 20.1 Å, c = 13.4 Å

section (0.51 X 0.53 nm), the other one being circular (0.55 nm). In ZSM-11 both the channels are identical (0.51 X 0.55 nm). The cavities formed in ZSM-5 by the intersection of these channels are equivalent, having maximum diameter of 0.9 nm, where as in ZSM-11 two types of intersections exist, one possessing the same volume as those present in ZSM-5 and the other one with larger volume (30 % excess). The calculated channel length of theoretically based on crystallographic data for ZSM-5 and ZSM-11 are 8.8 and 8.0 nm respectively[129,130]. Another important structural difference between ZSM-5 and ZSM-11 is the presence of four 4-MR's per unit cell in ZSM-5 and eight 4-MR's per unit cell in ZSM-11.

The presence of intergrowths of ZSM-5 and ZSM-11 can be detected by various techniques such as high resolution electron microscopy and X-ray powder diffraction[131,132]. Jablonski *et al.*[133] have presented a correlation between the X-ray and electron diffraction patterns for the relative amounts of ZSM-5 and ZSM-11.

The acidity, sorption, catalytic and shape selective properties of ZSM-5 and ZSM-11 have been compared. It has been reported that ZSM-5 contains more number of stronger acid sites compared to ZSM-11[134]. While some reports showed higher sorption capacities for ZSM-5 than ZSM-11, others presented higher sorption capacities for ZSM-11[130,135]. The constraint index (ratio of relative cracking rate constants of 3-methyl pentane and n-hexane) is almost same for ZSM-5 and ZSM-11 (8.3 and 8.7, respectively)[136]. The isomorphous substitution of various tri, tetra and penta valent metal ions such as B, Fe, Ga, Ti and V has been reported in both MFI and MEL framework structures[16,18-24].

1.12 VANADIUM OXIDE CATALYSTS

Vanadium oxides catalysts are industrially very important for a number of catalytic processes such as selective oxidation of hydrocarbons, production of SO_3, ammoxidation of hydrocarbons and reduction of nitric oxide[137-138]. Normally silica, alumina and titania are used as supports. The activity and selectivity of these vanadium oxide catalysts depend on their interaction with the support. Studies on these supported vanadium oxide catalysts were mainly dealing with changes in oxidation state during the chemical processes and the role of the support. Several methods have been proposed for the preparation of both supported and mixed vanadium oxide catalysts to improve their catalytic performance. The development of vanadium oxide catalysts with novel structures and exactly defined state of vanadium is useful to improve their catalytic performance.

1.13 VANADIUM CONTAINING MOLECULAR SIEVES

In 1978 Marosi *et al.*[139] reported the synthesis of vanadium containing ZSM-5. Zeolites containing 0.5 - 3 % vanadium were prepared using sodium silicate and vanadium oxide as starting materials and hexamethylene diamine as templating agent. The resulting zeolite (V-ZSM-5) was claimed to be a useful catalyst in cracking and isomerization reactions. Xu Reren *et al.*[140] showed the possibility of having vanadium in three different oxidation states (V^{3+}, V^{4+} and V^{5+}) in zeolite molecular sieves. The unit cell parameters increased with decrease in the oxidation state of vanadium. The introduction of V^{4+} ions into extra-framework cationic positions by solid state reaction was reported by Kucherov and Slinkin[32]. In 1985, Inui *et al.*[141] had synthesized V-ZSM-5 by introducing vanadium instead of aluminium in the reaction gel. However, the source of silica (*i.e.* sodium silicate) contained aluminum, and hence, they could not obtain pure aluminum free vanadium silicates. They have reported that the V-ZSM-5 is significantly different from its aluminum analog in morphology, acidity and catalytic activity in methanol to gasoline reaction. Miyamoto *et al.*[142] synthesized V-ZSM-5 using different vanadium sources and showed that vanadium acetyl acetonate is a suitable source to prepare V-ZSM-5 with high crystallinity and high BET surface area. The catalytic activity was also in correlation with these physico-chemical properties and the longer catalyst life of V-ZSM-5 was assigned to the accelerated combustion of the coke by the vanadium ions. Miyamoto *et al.*[143] have reported that the activity of their vanadium silicates is 50 time higher than that of bulk V_2O_5 in H_2 oxidation, while considerably lower in NH_3 oxidation. In the reduction of the NO with NH_3, vanadium silicates exhibited higher activity in the absence of oxygen than in the presence of oxygen, a behavior which had never been observed for conventional vanadium oxides. Vanadium silicates are also found to be selective in ammoxidation of xylenes and propane[144,145] and in the oxidation of butadiene to furan[146]. Vanadium silicates are reported to have high catalytic activity and selectivity in the oxidative dehydrogenation of propane to propylene compared to other metallosilicate molecular sieves[147].

Kornatowski *et al.*[22] have reported the synthesis of vanadium silicate with MFI structure. They reported the presence of vanadium at tetrahedral framework positions based on XRD, IR and NMR characterization of their samples. However, a report by Rigutto and van Bekkum[23] postulated that the vanadium ions are strongly bound to framework positions and are located at defect sites. They have reported that V^{4+} ions in the as-synthesized form are penta coordinated, and on calcination V^{5+} ions are in tetrahedral coordination. Fejes *et al.*[79] reported the distorted

square pyramidal coordination from ESR spectroscopic studies for V^{4+} ions in as-synthesized vanadium silicate with MFI structure. Recently, Centi *et al.*[148] have reported that at least two different vanadium species could be identified in vanadium silicates with MFI structure prepared using VCl_3 as the vanadium source.

The earlier reports on vanadium incorporated molecular sieves have focused on some interesting catalytic reactions such as ammoxidation of xylenes and propene, oxidative dehydrogenation of propane and H_2 oxidation. Even though the vanadium was claimed to be well dispersed in zeolite matrix, it was not clear whether vanadium is incorporated in the framework positions or not. Some of the recent reports on vanadium silicates refer to a) the differences in the nature and type of V-species in the samples prepared in the presence and absence of Na^+ ions[149], b) differences between the ion-exhanged V (as VO^{2+}) and V in the framework positions of MFI structure by ESR spectroscopy[79], c) the presence of more than two types of vanadium species in the framework of MFI as inferred from diffuse reflectance, ESR and ^{51}V MAS-NMR studies[148], d) the retention of vanadium on calcination at high temperatures and on treatment with ammonium acetate[148] and e) the valence state of vanadium and its co-ordination in the as-synthesized, dried and calcined forms[23]. Apparently, substantial differences exist among these reports which may be due to differences in the synthesis procedure. **The work presented in this thesis is aimed at preparing well defined and thermally stable vanadium silicates with V in the MEL structure and compare the properties of V-MEL with those of others reported on vanadium silicates.** The approach has been to synthesize vanadium silicates by conventional hydrothermal crystallization methods. Since both bulk V_2O_5 as well as supported V_2O_5 catalysts are good catalysts and used in many oxidation reactions, it would be interesting to see if highly dispersed and isolated V in the framework positions of a molecular sieve would be active in the oxidation of organic substrates. Recently, titanium silicates have been known to possess interesting oxidation activities and also industrially employed. A comparison of vanadium silicates with titanium silicates have been attempted wherever possible in the studies on catalytic oxidations and hydroxylations. Compared to titanium silicates, there are very few reports on the liquid phase oxidation of organic moieties by vanadium silicates in presence of oxidants, such as H_2O_2.

1.13 SCOPE OF THE THESIS

The major objective of the this thesis is to study the synthesis, characterization and catalytic activity of vanadium silicate molecular sieves with MEL structure and wherein vanadium is located framework positions.

Chapter II describes the studies carried out on the synthesis of a new crystalline microporous vanadium silicate with MEL structure. The influence of various synthesis parameters (vanadium source, organic additive, Si/V ratio, water content, effect of temperature) on the kinetics of crystallization is studied. The apparent activation energy for nucleation and crystal growth are evaluated.

Chapter III deals with the results of physico-chemical characterization of vanadium silicates by XRD, spectroscopic (IR/FTIR, ESR, MAS NMR, UV-VIS) studies and sorption studies on isomorphous substitution of vanadium into MEL lattice.

Chapter IV describes the catalytic activity of vanadium silicate molecular sieves in reactions such as 1) Oxyfunctionalization of n-alkanes and cyclohexane, 2) Hydroxylation of benzene and phenol, 3) Oxidation of toluene, 4) Oxidation of aniline and 5) oxidation of sulfides. The influence of various reaction parameters such as Si/V molar ratio, nature of solvent, concentration of the reactants, the catalyst concentration and the reaction temperatures on the activity and selectivity of the catalysts is studied in detail.

Chapter V summarizes the salient features of synthesis, characterization and catalytic properties of vanadium silicate molecular sieves.

1.14 REFERENCES

1. Szostak, R., *Molecular Sieves: Priciples of synthesis and identification* Van Nostrand Rheinhold, New Yark (1989).
2. Loewenstein, W., *Am. Minerals*, **39**, 92 (1954).
3. Breck, D.W., *Zolite Molecular Sieves*, Wiley Pub., New York, (1974).
4. Barrer, R.M., *Hydrothermal Chemistry of Zeolites*, Academic Press, New York, (1982).
5. Meier, W.M. and Olson, D.H., *Atlas of Zeolitic Structure Types*, 2nd Ed. (1987).
6. Bragg, W.L., *The Atomic Structure of Minerals*, Cornell University Press, Ithaca, New York (1937).
7. Meier, W.M., *Molecular Sieves*, Soc. Chem. Ind., London, p. 10 (1968).
8. Sand, L.B., *Ecom. Geol.*, 191 (1967).
9. Flanigen, E.M., *Proc. of 5th Int. Zeolite Conf.*, Ed. L.V.C. Rees, Heydon London, p. 760 (1980).
10. Davis, M.E., Saldarriage, C., Montes, C., Graces, J. and Crowder, C., *Nature*, **331**, 968 (1988).
11. Estermann, M., Me Cusker, L.B., Bacrlocher, Ch., Morrouche, A. and Kessler, H., *Nature*, **352**, 320 (1991).
12. Derouane, E.G., Valyoisik, E.W. and Von Ballmoos, R., E.Pat. Appl. 146384 (1984).
13. Barrer, R.M., *Pure Appl. Chem.*, **51**, 1091 (1979).
14. Reference 1, p. 51
15. Sand L.B., *Pure Appl. Chem.*, **52**, 2105 (1980).
16. Reference 1, p. 209; 212
17. Goldsmith, J.R., *Min. Mag.*, **29**, 952 (1952).
18. Barrer, R.M., Baynham, J.W., Bultitride, F.W. and Meier, W.M., *J.Chem. Soc.*, 195 (1959).
19. Ratnasamy, P. and Kumar, R., *Catal. Today*, **9**, 329 (1991).
20. Chu,C.T.W., Kuehl, G.H., Lago, R.M. and Chang, C.D., *J. Catal.*, **93**, 451 (1985).
21. Notari, B., *Stud. Surf. Sci. Catal.*, **37**, 413 (1988).
22. Kornatowski, J., Sychev, M., Goncharuk, V. and Baur, W.H., *Stud. Surf. Sci. Catal.*, **65**, 581 (1990).
23. Rigutto, M.S. and van Bekkum, H., *Appl. Catal.*, **68**, L1 (1991).
24. Hari Prasad Rao, P.R., Ramaswamy, A.V. and Ratnasamy, P., *J. Catal.*, **137**, 225 (1992).
25. Yamagishi, K., Namba, S. and Yashima, T., *Stud. Surf. Sci. Catal.*, **49 A**, 459 (1989).

26. Reschetilowski, W., Einicke, W.D., Meier, B., Brunner, E. and Ernst, H., *Stud. Surf. Sci. Catal.*, **69** 119 (1991).

27. Hamder, H. and Klinoswski, J., *ACS Symp. Ser.*, **398**, 329 (1988).

28. Yashima, T., Yamagishi, K., Namba, S., Nakata, S. and Asaoka, S., *Stud. Surf. Sci. Catal.*, **37**, 175 (1988).

29. Endoh, A., Nishimiya, K., Tsutsumi, K. and Takaishi, *Stud. Surf. Sci. Catal.*, **46**, 779 (1989).

30. Kraushaar, C. B. and van Hoof, J.H.C., *Catal. Lett.*, **1**, 81 (1988).

31. Whittington, B.I. and Anderson, J.R., *J. Phys. Chem.*, **95**, 3306 (1991).

32. Kucherov, A.V. and Slinkin, A.A., *Zeolites*, **7**, 38, 43 (1987); **8**, 110 (1988).

33. Wilson, S.T., Lok, B.M., Messina, C.A., Cannan, T.R. and Flanigen, E.M., *J. Amer. Chem. Soc.*, **104**, 1146 (1982).

34. Wilson, S.T. and Flanigen, E.M., *ACS Symp. Ser.*, **298**, 329 (1988).

35. Kraushaar, C.B., Hoogervorst, W.G.M., Andrea, R.R., Emeis, C. A. and Stork, W.H.J., *Stud. Surf. Sci. Catal.*, **69**, 231 (1991).

36. Montes, C., Davis, M.E., Murray, B. and Narayana, M., *J. Phys. Chem.*, **94**, 6431 (1990).

37. Lok, B.M., Messina, C.A., Patton, R.L., Gajek, R.T., Cannan, T.R. and Flanigen, E.M., US Pat., 4,440, 870 (1984).

38. Von Ballmooos, R., *Collection of Simulated XRD Powder Patterns for Zeolites*, Buttrworths, London (1984).

39. Reference 1, p. 285.

40. Scherrer, P., *Gottinger Nachichten*, **2**, 98 (1918).

41. Meyers, B.L., Ely, S.R., Kutz, N.A., Kaduk, J.A. and van den Bossche, E., *J. Catal.*, **91**, 352 (1985).

42. Szostak, R., Thomas, T.L., *J. Catal.*, **100**, 555 (1986).

43. Simmons, D.K., Szostak, R., Agrawal, P.K. and Thomas, T.L., *J. Catal.*, **106**, 287 (1987).

44. Perego, G., Bellussi, G., Corno, C., Taramasso, M., Buonomo, F. and Esposito, A., *Stud. Surf. Sci. Catal.*, **28** 129 (1986).

45. Ratnasamy, P., Kotasthane, A.N., Shiralkar, V.P., Thangaraj, A. and Ganapathy, S., in Zeolite Synthesis, *ACS Symp. Ser.*, **398**, 405 (1989).

46. Pluth, J.J., Smith, J.V. and Bennett, J.M., *Acta Crystallog.*, C**42** 283 (1986).

47. Rudolf, P.R., Saldarriaga-Molina, C. and Clearfield, A., *J. Phy. Chem.*, **90**, 6122 (1986).

48. Flanigen, E.M., Khatami, H. and Szymanski, H.A., *Molecular Sieve Zeolite-1*, ACS Monograph, **101**, 201 (1971).

49. Flanigen, E.M., *Zeolite Chemistry and Catalysis*, Ed. Rabo *et al.*, **171**, 80 (1976).

50. Ward, J.W., *Zeolite Chemistry and Catalysis*, Ed. Rabo *et al.*, **171**, 118 (1976).

51. Jacobs, P.A., Beyor, H.K. and Valyon, J., *Zeolites*, **1**, 161 (1981).

52. Coudurier, G., Naccache, C. and Vedrine, J.C., *J. Chem. Soc. Chem. Commun.*, 369 (1984).

53. Kutz, N. A., *Heterogeneous Catalysis-11*, Ed. Sharpiro, B.L., *et al.*, p. 121 (1984).

54. Szostak, R. and Thomas, T.L., *J. Catal.*, **101**, 549 (1986).

55. Barthomeuf, D., *Catalysis by zeolites*, Elsevier, **5**, 55 (1980).

56. Klinowski, J., *Progress in NMR Spectroscopy*, (Ed. Emsley, *et al.*,) Pregamon Press, GB. **17**, 237 (1984).

57. Engelhardt, G. and Michel, D., *High Resolution Solid State NMR of Zeolites and Related Systems*, John Wiley and Sons, London, (1987).

58. Lippmaa, E., Magi, M., Samoson, A., Engelhardt, G. and Grimmer, A.R., *J. Amer. Chem. Soc.*, **102** 4889 (1980); **103**, 4992 (1981).

59. Fyfe, C.A., Gobbi, G.C., Klinowski, J., Thomas, J.S. and Ramdas, S., *Nature*, **296**, 530 (1982).

60. Fyfe, C.A., Gobbi, G.C., Hartman, J.K., Klinowski, J. and Thomas, J.M., *J. Phys. Chem.*, **86**, 1247 (1982).

61. Engelhardt, G., Ohose, U., Lippmaa, E., Tarmak, M. and Magi, M., *Z. Anorg. Allg. Chem.*, **49**, 482 (1981).

62. Mastikhin, V.M. and Zamaraev, K.I., *Z. Phys. Chemie* (Neue Folge) **152**, 59 (1987).

63. Muller, D., Gessner, W., Behrens, H.J. and Scheler, G., *Chem. Phys. Lett.*, **79**, 59 (1981).

64. Thomas, J.M., Fyfe, C.A., Ramdas, S., Klinowski, J. and Gobbi, G.C., *J. Phys. Chem.*, **86**, 3061 (1982).

65. Ramdas, S. and Klinowski, J., *Nature*, **308**, 521 (1984).

66. van Hoof, J.H.C. and Roelofsen, *Stud. Surf. Sci. Catal.*, **58**, 242 (1991).

67. Fyfe, C.A., Grondey, H., Feng, Y. and Kokotailo, G.T., *Chem. Phys. Lett.*, **173**, 211 (1990).

68. Fyfe, C.A., Feng, Y., Grondey, H., Kokotailo, G.T. and Mar, A., *J. Phys. Chem.*, **95**, 3747 (1991).

69. Fyfe, C.A., Feng, Y., Gies, H., Grondey, H. and Kokotailo, G.T., *J. Amer. Chem. Soc.*, **112**, 3264 (1990).

70. Fyfe, C.A., Gies, H. and Feng, Y., *J. Amer. Chem. Soc.*, **111**, 7702 (1989).

71. Kinrade, S.D. and Swaddle, T.W., *J. Amer. Chem. Soc.*, **108**, 7159 (1986).

72. Mc Cormick, A.V., Bell, A.T. and Radke, C.J., *Zeolites*, **7**, 183 (1987).

73. McCormick, A.V., Bell, A.T. and Radke, C.J., *Stud. Surf. Sci. Catal.*, **28**, 247 (1988).

74. van den Berg, J.P., de Jong-Versloot, P.C., Keijsper, J. and Post, M.F.M., *Stud. Surf. Sci. Catal.*, **37**, 85 (1988).

75. Thangaraj, A. and Kumar, R., *Zeolites*, **10**, 117 (1990).

76. Thangaraj, A., Kumar, R. and Ratnasamy, P., *Zeolites*, **11**, 573 (1991).

77. Fraissard, J. and Ito, T., *Zeolites*, **8**, 350 (1988).

78. Pfeifer, H., Freude, D. and Hunger, M., *Zeolites*, **5**, 274 (1985).

79. Fejes, P. Marsi, I., Kirisci, I., Halasz, J., Hannus, I., Rockenbauer, A., Tasi, Gy., Korecz, L. and Schobel, Gy., *Stud. Surf. Sci. Catal.*, **69**, 173 (1991).

80. Vedrine, J.C., *Stud. Surf. Sci. Catal.*, **69**, 25 (1991).

81. Lin, D.H., Coudurier, G. and Vedrine, J.C., *Stud. Surf. Sci. Catal.*, **49**, 1431 (1989).

82. Barrer, R.M., *Proc. Roy. Soc. A*, **167**, 392 (1938).

83. Karger, J. and Rutheven, D.M., *Zeolites*, **9**, 267 (1989).

84. Palekar and Rajadyaksha, R.A., *Catal. Rev. Sci. Eng.*, **28**, 371 (1986).

85. Barrer, R.M., *Pure Appl. Chem.*, **52**, 2143 (1980).

86. Barrer, R.M. and Gibbson, R.M., *Trans. Faradays Soc.*, **59**, 2569 (1963).

87. Vedrine, J.C., Auroux, A. and Coudurier, G., *Catalytic Materials; Relationship between Structure and Reactivity*, Ed. Whyte, Amer. Chem. Soc., Washington, D.C., 253 (1984).

88. Chu, C.T. and Chang, C.D., *J. Phys. Chem.*, **89**, 1569 (1985).

89. Jacobs, P.A. and von Ballmoos, R., *J. Phys. Chem.*, **86**, 3050 (1982).

90. Jacobs, P.A. and Heylen, C.F., *J. Catal.*, **34**, 267 (1974).

91. Jacobs, P.A., Martens, J.A., Weitkamp, J. and Beyer, H.K., Selectivity in Heterogeneous Catalysis, *Far. Disc. Chem. Soc.*, **72**, 351 (1981).

92. Weisz, P.B. and Miale, J.N., *J. Catal.*, **4**, 527 (1965)

93. Kaeding, W.W., Chu, C., Young, L.B. and Butter, S.A., *J. Catal.*, **69**, 392 (1981).

94. Martens, J.A., Tielen, M., Jacobs, P.A. and Weitkamp, J., *Zeolites*, **4**, 98 (1984).

95. Csicsery, S.M., *Zeolites*, **4**, 202 (1984).

96. Magee, J.S. and Blazek, J.J. in *Zeolite Chemistry and Catalysis*, ACS Monograph, **171**, 615 (1976).

97. Weitkamp, J., *Chemie-Technik*, **11**, 707 (1982).

98. Hadden, K., Weitkamp, J., *Chem. Ing. Tech.*, **55**, 907 (1983).

99. Weisz, P.B., *Pure Appl. Chem.*, **52**, 2091 (1980).

100. Chen, N.Y., Maziuk, J., Schwartz, A.B. and Weisz, P.B., *Oil Gas J.*, **66**, 154 (1968).

101. Garwood, W.E., *ACS Symp. Ser.*, **218**, 383 (1983).

102. Venuto, P.B. and Lendis, P.S., *Adv. Catal.*, **18**, 259 (1968).

103. Holderich, W., Hesse, M. and Naumann, F., *Angew, Chemie, Int. Ed. Engl.*, **27**, 226 (1988).

104. van Bekkum, H. and Kouwenhoven, H.W., *Recl. Trav. Chim. Pays-Bas*, **108**, 283 (1989).

105. Weigert, F.J., *J. Org. Chem.*, **52**, 3296 (1987).

106. Parker, D.G., *Appl. Catal.*, **9**, 53 (1984).

107. Lewis, P.J., Dwyer, F.G., *Oil Gas J.*, **75**, 55 (1977).

108. Eichler, K. and Leupold, E., DBP 3 334 084 (1985).

109. Chantal, P.D., Kaliaguine, S. and Maison, G., *Appl. Catal.*, **18**, 133 (1985); *Stud. Surf. Sci. Catal.*, **19**, 93 (1984).

110. Gauthier, C., Chiche, B., Finiels, A. and Geneste, P., *J. Mol. Catal.*, **50**, 219 (1989).

111. Suzuki, E., Nakashiro, K., Ono, Y., *Chem. Lett.*, 953 (1988).

112. Panov, G.I., Sheveleva, G.A., Kharitonov, A.S., Romannikov, V.N. and Vostrikova, L.A., *Appl. Catal. A*, **82**, 31 (1992).

113. Tompsett, A.J., EP 76 034 (1982).

114. Zioolek, M. and Bresinska, I., *Zeolites*, **5**, 245 (1985).

115. Weissermet, K. and Arpe, H.J., *Industrielle Organishe Chemie Verlag Chemie Weinheim*, p.108 (1978).

116. Climent, M.J., Corma, A., Garcia, H. and Primo, J., *J. Catal.*, **130**, 138 (1991).

117. Rudham, R. and Sanders, M.K., *J. Catal.*, **27**, 287 (1972).

118. Mochida, I., Hayata, S., Kato, A., and Seiyama, T., *J. Catal.*, **23**, 23 (1971).

119. Steijns, M. and Mars, P., *Ind. Eng. Chem. Prod. Res. Dev.*, **16**, 35 (1977).

120. US Pat.4 088 743 (1978).

121. Huybrechts, D.R.C., Bruycker, L.D. and Jacobs, P.A., *Nature*, **345**, 240 (1990).

122. Hari Prasad Rao, P.R. and Ramaswamy, A.V., *J. Chem. Soc. Chem. Commun.*, 1245 (1992).

123. Kokotailo, G.T., Lawton, S.L., Olson, D.H. and Meier, W.M., *Nature*, **272**, 437 (1978).

124. Kokotailo, G.T., Chu, P., Lawton, S. L., and Meier, W.M., *Nature*, **275**, 119 (1978).

125. Flanigen, E.M., Bennett, J.M., Grose, R.W., Cohen, J.P., Patton, R.L., Kirchner, R.M., and Smith, J.V., *Nature*, **271**, 512 (1978).

126. Bibby, D.M., Milestone, N.B. and Aldridge, L.B., *Nature*, **280**, 664 (1979).

127. Olson, D.H., Kokotailo, G.T., Lawton, S.L. and Meier, W.M., *J. Phys. Chem.*, **85**, 2238 (1981).

128. Fyfe,C.A., Gies, H., Kokotailo, G.T., Pasztor, C., Strobl, H., Cox, D.E., *J. Amer. Chem. Soc.*, **111**, 2470 (1989).

129. Gabelica, Z., Derouane, E.G. and Blom, M., *ACS Symp. Ser.*, **248**, 219 (1984).

130. Jacobs, P.A., Beyer, H.K. and Valyon, J., *Zeolite*, **1**, 161 (1981).

131. Millward, G.R., Ramdas, S., Thomas, J.M. and Barlow, M.T., *J. Chem. Soc. Farad. Trans II*, **79**, 1075 (1983).

132. Thomas, J.M. and Millward, G.R., *J. Chem. Soc. Chem. Commun.*, 1380 (1982).

133. Jablonski, G.A., Sand, L.B. and Gard, J.A., *Zeolite*, **6**, 396 (1986).

134. Auroux, A., Dexpert, H., Leclercq, C. and Vedrine, J.C., *Appl. Catal.*, **6**, 95 (1983).

135. Harrison, I.D., Leach, H.F. and Whan, D.A., *Zeolites*, **7**, 21 (1987).

136. Frillette, V.J., Haag, W.O. and Lago, R.M., *J. Catal.*, **67**, 218 (1981).

137. Huckneall, D.J., *Selective oxidation of organic compouds,* Academic Press, New York (1974).

138. Dadyburyor, D. B., Jewur, S. S. and Rukenstein, E., *Catal. Rev. Sci. Eng.*, **19**, 293 (1979).

139. Marosi, L., Stabenow, J., Schwarzmann, M., Ger. Pat. 2831631 (1978).

140. Reren, X., Wenguin, P., *Stud. Surf. Sci. Catal.*, **24**, 27 (1985).

141. Inui, T., Medhanavyan, D., Praserthdam, P., Fukuda, K., Ukawa, T., Sakamoto, A. and Miyamoto, A., *Appl. Catal.*, **18**, 311 (1985).

142. Miyamoto, A., Medhanavyan, D. and Inui,T., *Appl. Catal.*, **28**, 89 (1986).

143. Miyamoto, A., Medhanavyan, D. and Inui, T., *Proc. 9th Intern. Congr. Catal.*, (M.J. Philip and M. Ternan, Eds.) pub. Chem. Inst. of Canada, Ontario, vol. **1**, p. 437 (1988).

144. Cavani, F., Trifiro, F., Habersberger, K. and Tvaruzkova, Z., *Zeolites*, **8**, 12 (1988).

145. Miyamoto, A., Iwamoto, Y., Matsuda, H. and Inui, T., *Stud. Surf. Sci. Catal.*, **49 B**, 1233 (1989).

146. Tvaruzkova, Z., Centi, G., Jiru, P. and Trifiro, F., *Appl. Catal.*, **19**, 307 (1985).

147. Zatorski, L.W., Centi, G.,Nieto, J.L., Trifiro, F., Bellussi, G. and Fattore, V., *Stud. Surf. Sci. Catal.*, **49 B**, 1243 (1989).

148. Centi, G., Perathoner, S., Trifiro, F., Aboukais, A., Aissi, C.F., Guelton, M., *J. Phys. Chem.*, **96**, 2617 (1992).

149. Bellusi, G., Maddinelli, G., Carati, A., Gervasani, A., Millini, R., *9th International Zeolite Conference*, Montreal, Canada, July 1992, Absract A8.

CHAPTER 2

SYNTHESIS

2.1 INTRODUCTION

The last decade has witnessed considerable growth in the area of isomorphous substitution of Si or Al by various metal ions in the zeolite framework[1,2]. Replacement of Al by B[3], Fe[4-9], and Ga[8] in the framework of ZSM-5 and ZSM-11 has been reported. Al-free ferrisilicate analogs of Beta[10], ZSM-23[11], EU-11[12], mordenite[13], ZSM-20[14], ZSM-12[15] and Y[14] have been synthesized. Recently, Kumar and Ratnasamy have reviewed the synthesis, characterization and the catalytic properties of various ferrisilicates[16]. Incorporation of Ti into the framework of MFI, MEL and ZSM-48 structures was one of the recent achievements[17-21,35].

Attempts to introduce vanadium into zeolites was made since 1980[22]. Xu Reren *et al.*[23] reported the possibility of isomorphous substitution of vanadium in three (III, IV and V) different oxidation states. Kucherov *et al.*[24] and later Sass[25] introduced V^{4+} ions into framework cationic positions, by solid state interactions. Inui *et al.*[26-28] introduced vanadium compounds instead of Al component into the reaction gel for synthesis of vanadium containing molecular sieve. Kornatowski *et al.*[29], Rigutto *et al.*[30], Fejes *et al.*[31] and Centi *et al.*[32] have reported the incorporation of vanadium into molecular sieves with MFI structure. Recently, we have reported the synthesis of vanadium silicate with MEL structure[33,34].

This Chapter describes the studies carried out to:

a). optimize the synthesis procedure for incorporating vanadium ions into MEL framework and

b). examine the factors influencing the synthesis of vanadium silicates.

2.2 EXPERIMENTAL

2.2.1 HYDROTHERMAL SYNTHESIS

The syntheses runs were carried out using various compositions in stainless steel autoclaves of 80 ml capacity (Fig.2.1) at autogenous pressure and at different temperatures. Different sources of vanadium were tested in order to obtain samples without any extra lattice vanadium. The reactants used for different syntheses are given in Table 2.1.

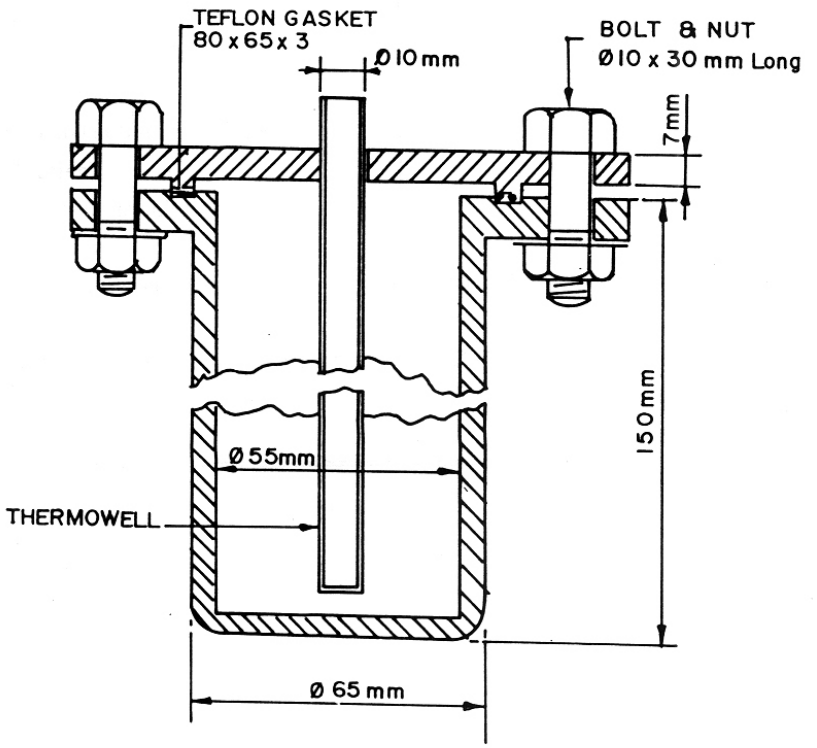

Fig.2.1. Stainless steel (316) autoclave with teflon gasket for hydrothermal synthesis.

Table 2.1

Specification of the reactants used in the synthesis.

S.No.	Chemical Nature	Chemical formula	Purity, %
1.	Teraethylorthosilicate (Fluka AG)	$Si(OC_2H_5)$	98
2.	Vanadyl sulfate trihydrate (Aldrich).	$VOSO_4\ 3H_2O$	100
3.	Vanadium trichloride (Aldrich)	VCl_3	100
4	Ammonium metavenadate (Loba chem)	$NH_4\ VO_3$	98
5.	Tetrabutyl Ammonium hydroxide TBA-OH, (Aldrich)	$(C_4H_9)_4\ NOH$	40 %aq. Solution (diluted to 20 % before use)

A general procedure for the preparation of crystalline vanadium silicate is given below:

To a solution of 25 g of tetraethyl orthosilicate (TEOS), 10 g of tetrabutylammonium hydroxide (TBA-OH) diluted with 10 g of deionized water was added to hydrolyse the TEOS. The mixture was stirred for about 30 min at 298 K. To the above mixture, required quantity of vanadyl sulfate trihydrate ($VOSO_4\ 3H_2O$) in 5 g of deionized water was added slowly. Finally, a solution of 5 g of TBA-OH in 5 g water was added. The clear green solution thus obtained was stirred for 3 h before adding 20 g of water. The resultant liquid was stirred for another 90 minutes. The chemical composition of the initial gel was : SiO_2 : x VO_2 : 0.2 TBA-OH : 30 H_20 (where x = 0.00 to 0.05). Alkali ions are absent in the gel mixture. The crystallization was carried out at 443 K for 48 to 60 h under static conditions. The crystalline material thus obtained was filtered, washed with distilled water and dried at 373 K for 6 h.

It may be pertinent to mention here that using other organic bases such as 1,8 diamino octane and trimethyl benzylammonium hydroxide which are known to produce ZSM-11[40,41], VS-2 (V-MEL) could not be obtained. Under identical synthesis conditions, no crystalline material was observed even after 10 days.

2.2.2 CHARACTERIZATION

2.2.2.1 X-ray Diffraction

The as-synthesized samples were analyzed by X-ray diffraction to study the crystallinity and phase purity, in a Rigaku (model D/MAX III VC, Japan) X-ray diffractometer using Ni filtered Cu-Kα radiation (λ = 1.5404 Å). The samples were scanned from 2 θ = 5 to 50° at a scan rate of 2° min^{-1}. Phase purity of the samples was checked by comparing with the standard X-ray diffraction pattern for MEL structure reported by Fyfe *et al.*[40]. Based on the preliminary experiments, a sample with highest crystallinity was taken as reference sample and was used to check the crystallinity of all the samples. Peak areas were calculated from the collected data, using a semiquantitative software programme provided with the instrument. The degree of crystallinity was calculated from the sum of the areas of the peaks between 2 θ = 21.5 and 25.4°. The degree of crystallinity of the solid product was estimated from the formula given below.

$$\% \textit{ crystallinity} = \frac{\textit{peak area between } 2\theta = 21.5°\text{-}25.4° \textit{ of the product}}{\textit{Peak area between } 2\theta = 21.5°\text{-}25.4° \textit{ of the reference sample}} \times 100$$

2.2.2.2 Infrared Spectroscopy

The infrared spectra of the as-synthesized samples were recorded in an FTIR Perkin Elmer spectrometer in the frequency range of 450 - 1300 cm^{-1} using the Nujol mull technique. KCN was used as the internal standard. The IR crystallinity was determined using the formula:

$$\%\ IR\ crystallinity = \frac{peak\ area\ of\ band\ at\ 550\ cm^{-1}\ of\ the\ product}{Peak\ area\ of\ the\ band\ at\ 550\ cm^{-1}\ of\ the\ reference\ sample} \times 100$$

The absorption band at 550 cm^{-1} is a characteristic peak, observed in pentasil zeolites and is assigned to double five (5 - 5 unit) membered rings.

2.2.2.3 Electron Spin Resonance Spectroscopy

Electron spin resonance spectra were recorded using Bruker ER-200 D spectrometer at 9.7 GHz (X-band) with a rectangular cavity ST 8424. Modulation at 100 KHz with intensity 1.25 GPP and time constant 10^3 m sec. was used. The h.f. power was chosen small enough to prevent any signal saturation. The spectra were recorded at 300 K. A constant weight of 0.1 g of the sample was taken to record the spectra.

2.2.2.4 Thermal analysis

Simultaneous TG-DTA-DTG analyses of as-synthesized and dried vanadium silicate samples were carried out in a TG DTA-92 model (Setaram, France) instrument. A linear rate of 10° min^{-1} in the range from room temperature to 900 °C with an air flow of 30 ml min^{-1} was used, in order to find out the temperature of decomposition of template and hence the calcination temperature required for the samples. A sample volume of about 30 mg was taken with an inert α-alumina as reference. Detailed analysis of weight loss due to decomposition of the template and accompanying heats of decomposition have been calculated from the stored data of each TG-DT analysis, using software programme available with the instrument.

2.2.2.5 Scanning Electron Microscopy

The morphology of MEL samples was investigated using a scanning electron microscope (JEOL, model JSM 5200, Japan). The sample was dusted on alumina and coated with a thin film of gold to prevent surface charging and to protect zeolite material from thermal damage by the electron beam. In all the analyses a uniform thickness of about 0.1 mm was maintained.

2.2.2.6 Chemical analysis

An exact amount of sample was taken in a platinum crucible with a lid and ignited to get the dry weight of the sample. The sample was then cooled in a desiccator and weighed. The difference in weights gave the weight loss on ignition. The anhydrous weight of the sample was noted. Anhydrous sample was then treated with hydroflouric acid (40 wt.%) and evaporated on a hot plate to remove silicon in the form of SiF_4. This treatment was repeated three times and the sample was again ignited, cooled in desiccator and weighed. The loss in the weight of the sample was determined to get the content of silica. The residue was fused with potassium pyrosulfate and dissolved in deionized water. The solution was then analyzed by atomic absorption spectrometer.

2.3 RESULTS AND DISCUSSION

2.3.1 EFFECT OF VANADIUM SOURCE

The source of vanadium used in the synthesis has a marked influence both on the incorporation and catalytic activity of the vanadium silicates. Three different vanadium sources *viz.* NH_4VO_3, $VOSO_4$ and VCl_3 have been used to prepare the vanadium silicate molecular sieves. The gels obtained with NH_4VO_3 and $VOSO_4$ (gel A and gel B, respectively) as vanadium sources are clear solutions, while that with VCl_3 (gel C) was slightly turbid. Gel A was white in color and gels B and C were greenish. The crystallized product from gels A and B was white in color and that from gel C was grayish green. Based on chemical analysis only around 25, 50 and 60 % of input vanadium was retained in the crystallized samples from gels A, B and C, respectively. The samples prepared with the vanadyl sulfate trihydrate as vanadium source were found to have high catalytic activity in the oxidation reactions (subsequently carried out and described in Chapter IV) compared to those prepared from vanadium trichloride and ammonium meta-vanadate and hence detailed studies have been carried out with samples prepared using vanadyl sulfate as vanadium source.

2.3.2 CRYSTALLIZATION KINETICS

2.3.2.1 Effect of temperature

Fig.2.3 shows the influence of the temperature on the nucleation and crystallization of VS-2 at 413, 428, 443 K (curves a, b and c). The curves show that the rate of crystallization of

Table 2.2

Effect of vanadium source on physico-chemical properties of vanadium silicates

Vanadium Source	Si/V Gel	Si/V sample[a]	Yield (%)	Crystal size (μm)	Colour of the samples		
					Gel	As-synthesized	Calcined
VCl_3	40	68	80-85	4.0 - 6.0	green	greenish gray	light yellow
$VOSO_4$	40	78	75-80	1.0 - 2.0	green	white	light yellow
NH_4VO_3	40	182	75-80	1.5 - 2.0	white	white	white

[a] As-synthesized sample

'A'

'B'

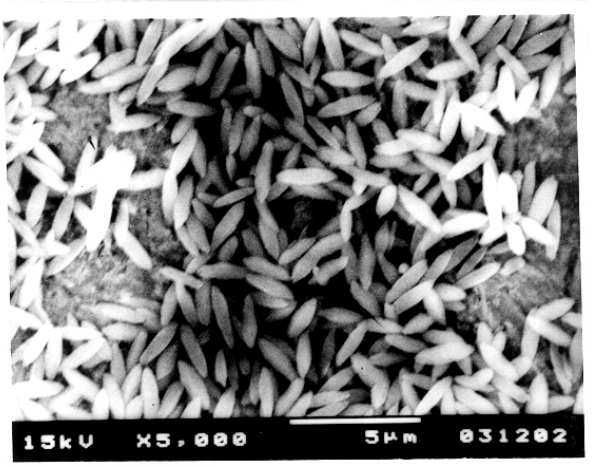

'C'

Fig.2.2. **SEM photographs of VS-2 samples prepared from different vanadium sources.** A : (VCl_3), B : ($VOSO_4$) and C : (NH_4VO_3).

VS-2 significantly depends on the temperature, which strongly influences the crystallization process. Increase in temperature decreased the nucleation period and increased the rate of crystallization considerably. The crystallization rate is faster at 443 K compared to 428 and 413 K. The crystallization curves are characteristic of a process involving two distinct stages *viz.*,

1) an induction period where nuclei are formed and

2) a crystal growth period when the nuclei grow into crystals.

The formation of nuclei during the induction period is an energetically activated process and since nucleation is the rate determining step during the induction period, the apparent activation energy for nucleation (E_n) and crystallization (E_c) can be calculated using the Arrhenius equation. Fig.2.4 illustrates the Arrhenius plots for the rate of nucleation (E_n) and crystallization (E_c) of vanadium silicates. The calculated apparent activation energies for both nucleation (E_n) and crystallization (E_c) are 53.80 and 56.54 $kJ.mol^{-1}$, respectively. The apparent activation energy of E_n and E_c for zeolites mainly depends on the reaction parameters such as the nature and amount of the template, silica source and Si/M ratio.

2.3.2.2 Effect of Si/V molar ratio

The effect of increasing vanadium content in the initial reaction mixture on the crystallization is shown in Fig.2.5. The crystallization becomes faster at higher values of the Si/V molar ratio (Fig.2.5 A). Curves 'a' to 'e' represent crystallization rate from reaction mixtures of Si/V ratio = 20, 40, 60, 80 and 160, respectively. The change in the pH of the gel during crystallization is also plotted against time in Fig.2.5 B. A significant increase in the pH i.e. Δ pH = pH_f-pH_i (where pH_f is the final pH of the mother liquor after crystallization and pH_i is the pH of the initial reaction mixture before crystallization) suggests the formation of a stable and highly crystalline material[36]. Insignificant or negative value of ΔpH indicates either redisolution of less stable phase formed initially or the presence of amorphous material or both[36,37]. In the case of aluminosilicates, while the incorporation of SiO_2 (from solution) into crystalline framework leads to an increase in the pH, the incorporation of AlO_2^- does not influence the pH significantly[36,38]. However, in the case of vanadium silicates and titanium silicates (e.g. TS-2)[37], where trivalent cations and alkali metal cations are absent, the incorporation of both SiO_2 and VO_2 (or TiO_2) may lead to an increase in the pH.

Table 2.3

Physico-chemical properties of vanadium silicates[a]

Si/V Gel	Si/V sample[b]	Si/V sample[c]	Yield (%)	Colour	
				As-synthesized	calcined
20	41	52	75-80	white	light yellow
40	78	79	75-80	white	light yellow
60	116	122	75-80	white	light yellow
80	161	161	65-70	white	light yellow
160	300	302	60-65	white	white

[a] source of vanadium = vanadyl sulfate trihydrate

[b] As-synthesized sample

[c] after treating the calcined sample with 0.5 M ammonium acetate solution at room temperature.

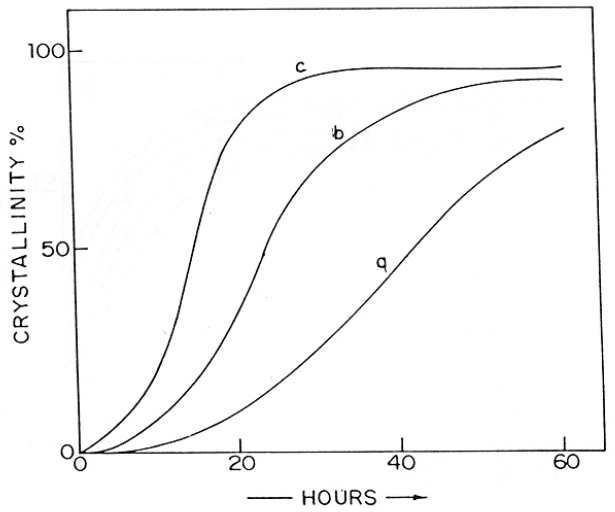

Fig.2.3. **Effect of temperature on the rate of crystallization of VS-2.** Curves 'a' to 'c' represent crystallization at temperatures 413, 428 and 443 K, respectively. Gel composition $SiO_2/VO_2 = 80$, $SiO_2/TBA\text{-}OH = 5$ $H_2O/SiO_2 = 30$. Source of vanadium is $VOSO_4$.

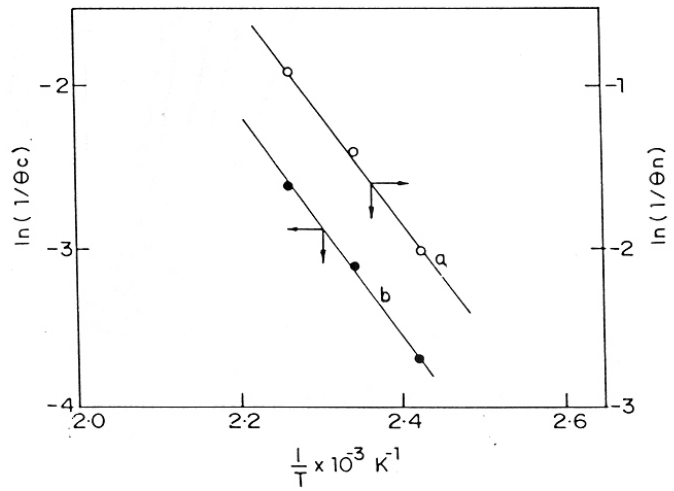

Fig.2.4. **Arrhenius plots for nucleation (curve a) and crystallization (curve b).**

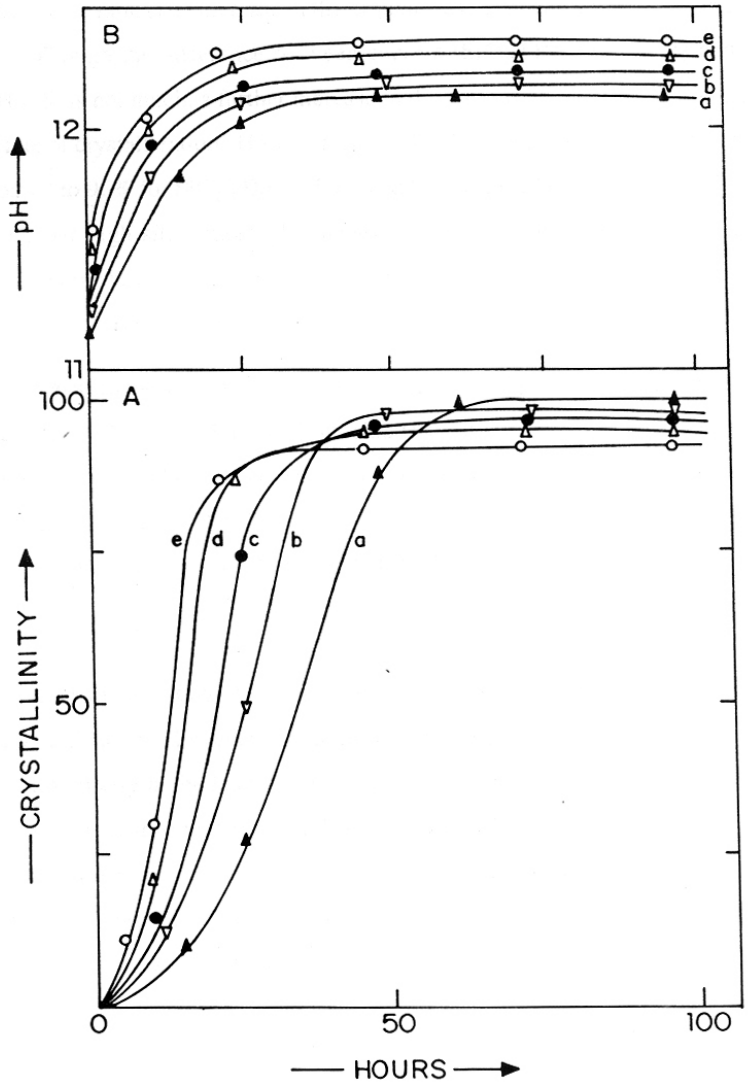

Fig.2.5. **Influence of Si/V mole ratio on the crystallization (A) and on pH (B).** Curves 'a' to 'e' correspond to Si/V mole ratios of 20, 40, 60, 80 and 160, respectively.

2.3.2.3 Effect of template concentration.

In Fig.2.6 A, the influence of SiO_2/TBA-OH molar ratio on the crystallization of VS-2 (V-MEL) is depicted. The corresponding change in pH is also shown in Fig.2.6 B. As expected, with the decrease in the ratio (i.e. increase in the organic base concentration) the crystallization becomes faster. Though the difference between curve a (SiO_2/TBA-OH = 3.3) and curve b (SiO_2/TBA-OH = 5) is not much, a further increase in this ratio (curve c, SiO_2/TBA-OH = 7.5) led to a slower rate of crystallization. However, at a SiO_2/TBA-OH = 3.3, about 90% crystalline material (compared to 96% for SiO_2/TBA-OH = 5 and 100% for SiO_2/TBA-OH = 7.5) has been obtained. Like other high silica molecular sieves, including titanium silicates, an optimum concentration of organic base or template leads to the formation of better crystallization product of vanadium silicate molecular sieve.

With the increase in the TBA-OH concentration, the initial pH of the reaction mixture/gel (pH_i) increases (Fig.2.6 B) because of the high alkalinity of the template. However, a rise in the pH accompanied the crystallization, except in the case of the composition represented by curve c. The maximum value for Δ pH (ca. 1.25 unit) was recorded for the composition having SiO_2/TBAOH = 7.5 and followed by 1.15 for SiO_2/TBAOH = 5 and 0.9 for SiO_2/TBAOH = 3.3.

2.3.2.4 Effect of H_2O/SiO_2 ratio

Fig.2.7 A shows that H_2O/SiO_2 molar ratios in the range of 20-40 do not significantly influence the crystallization. However, the more concentrated systems lead to somewhat faster crystallization, particularly in the later stages of crystallization. The variation in pH of the gel during crystallization is represented in Fig.2.7 B for the three different molar ratios. In this case also, the rise in pH was quite fast following the crystallization, further supporting the results discussed above. The effect of dilution on the crystal morphology was studied with SEM. No significant difference in the size of crystals could be seen.

2.3.2.5 Effect of agitation

Fig.2.8 A demonstrates the effect of the method of crystallization under static conditions (curve b) or under agitation (curve a, rotation at about 70 rpm). The crystallization was accelerated due to agitation (vis-a-vis static), in accordance with the earlier observations on the

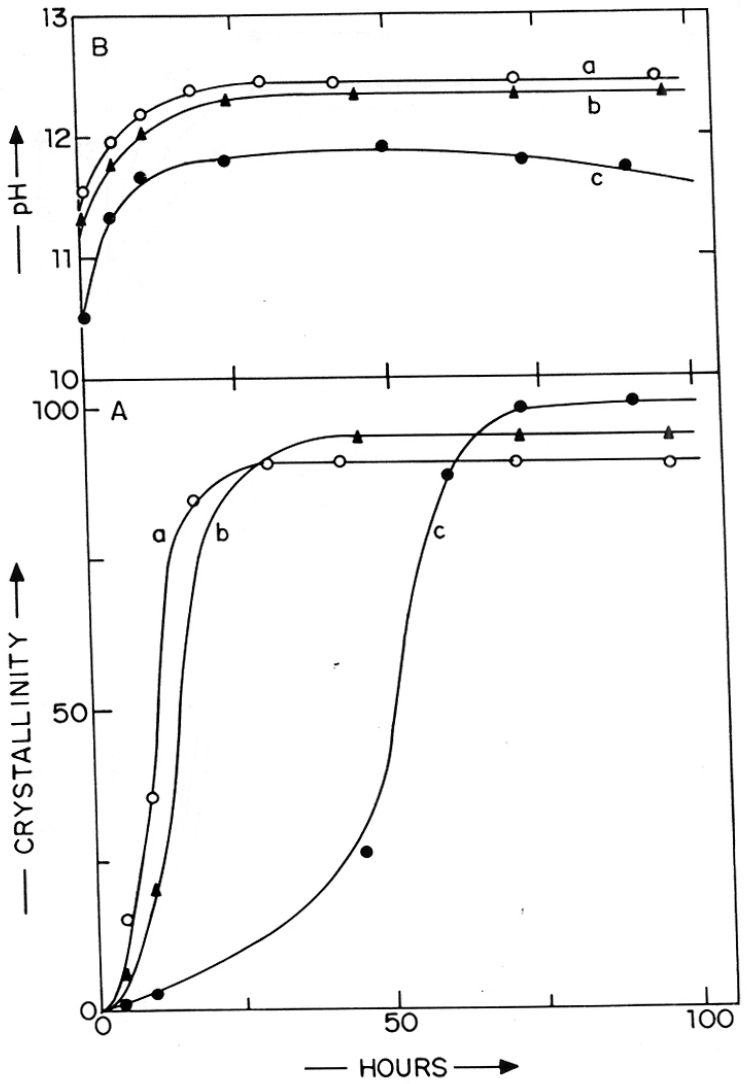

Fig.2.6. **Influence of template concentration on crystallization (A) and on pH (B).** Curves 'a' to 'c' correspond to SiO_2/TBA-OH mole ratios of 3.3, 5 and 7.5, respectively.

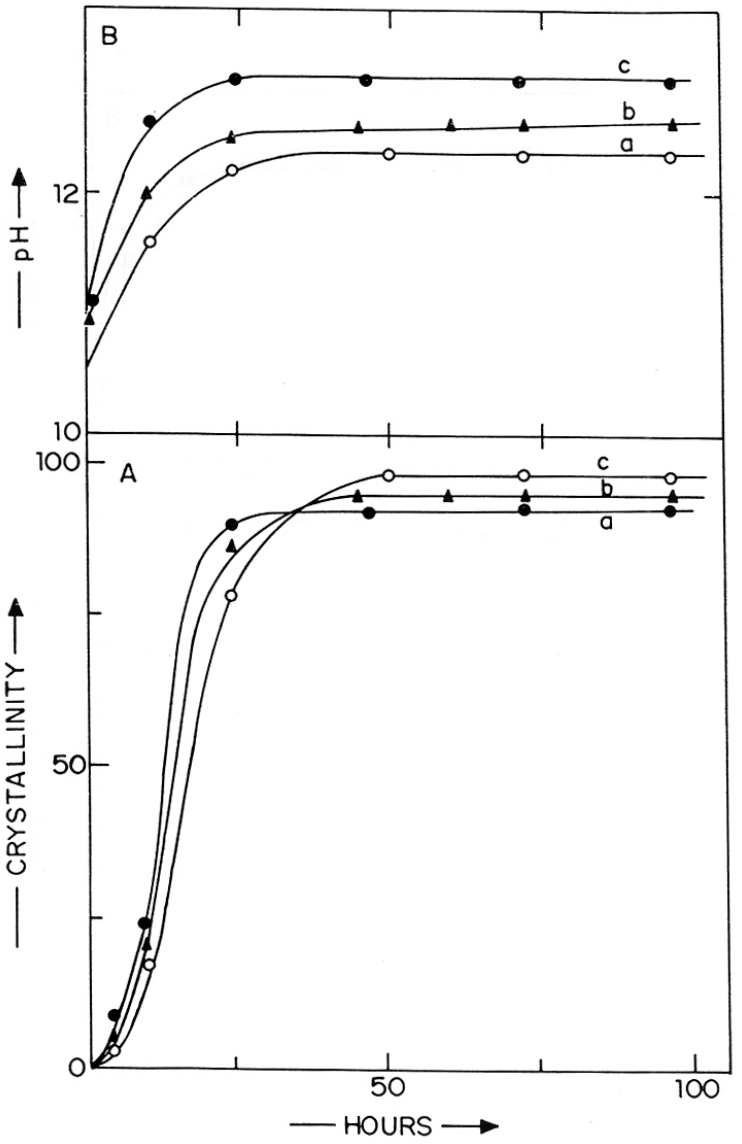

Fig.2.7. **Effect of dilution on the crystallization (A) and on pH (B).**
Curves 'a' to 'c' correspond to H_2O/SiO_2 mole ratios of 20, 30 and 40, respectively.

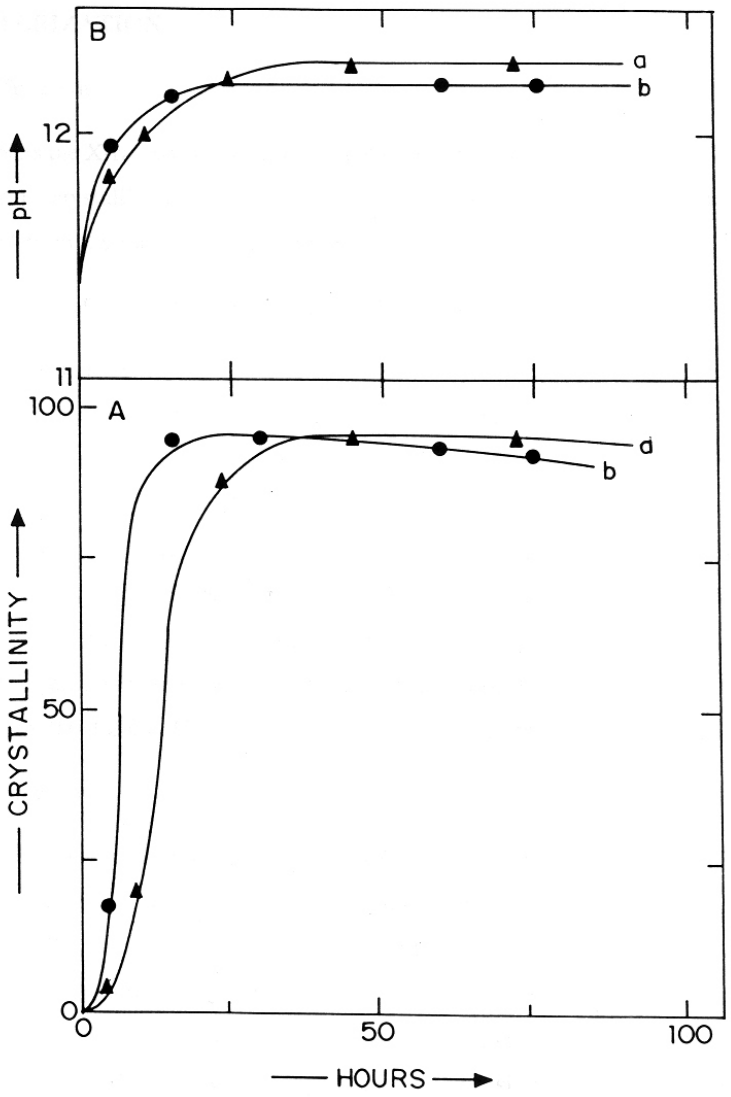

Fig.2.8. Crystallization (A) under static (curve a) and under agitation (curve b) and change in pH (B).

crystallization of high silica zeolites[39]. The pH changes were found to be similar in both the cases (Fig.2.8 B). Under agitation, smaller crystals (0.3 to 0.5 μm size) were formed as expected (Fig.2.9).

2.3.3 CHARACTERIZATION

2.3.3.1 X-ray diffraction

Fig.2.10 depicts the X-ray powder diffraction patterns of the samples removed at different time intervals during crystallization. The figure shows (curves a to e) the development of crystalline material from the initial reaction mixture having the molar composition:

$$Si/V = 80;\ SiO_2/TBA\text{-}OH = 5.0;\ H_2O/SiO_2 = 30$$

Fully crystalline material can be obtained after 48 h at crystallization temperature of 443 K (Fig.2.10, curve e). The X-ray pattern of the crystalline material matched very well with that reported for MEL structures[40]. The crystalline vanadium silicate-2, VS-2 (V-MEL) was found to be free from any MFI type impurity. In the XRD pattern of VS-2, the lines at 2 θ = 9.05 and 24.05° (both these lines are characteristic of MFI structure) are completely absent. Further, a peak at 2 θ = 45° is present as a singlet in MEL, while in MFI it is observed as a clear doublet. In Fig.2.10, curve e clearly demonstrates that XRD pattern of the present sample, VS-2 is consistent with all the criteria mentioned above (viz., absence of peaks at 2θ = 9.05° and 24.05° and presence of a singlet at 2 θ = 45°). Our VS-2 samples are thus free of any MFI impurity.

2.3.3.2 IR Spectroscopy

Fig.2.11 exhibits the framework IR spectra of VS-2 samples, at various stages during the crystallization process (curves a to e), of a gel with Si/V molar ratio of 80. The absorptions characteristic of the MEL structure develop gradually and become narrower. The peak at 550 cm^{-1} exhibited a direct correlation with XRD crystallinity (Fig.2.12) An additional IR absorption peak around 965 cm^{-1} was also observed (Fig.2.11). Kornatowski *et al.*[29] have also observed this IR peak in the case of VS-1 (V-MFI). Crystalline titanium silicate analogs of both MFI (TS-1) and MEL (TS-2) also exhibit such an IR band at around 950-970 cm^{-1} [19-21,42], which was assigned [42,43] on the basis of detailed IR studies, to a stretching mode of a [SiO_4] unit bonded to a Ti^{4+} ion ($O_3Si\text{-}O\text{-}TiO_3$). In the case of vanadium silicate molecular sieves, this peak may

Fig.2.9. **SEM photographs of VS-2 samples crystallized under static (A) and under agitation (B).**

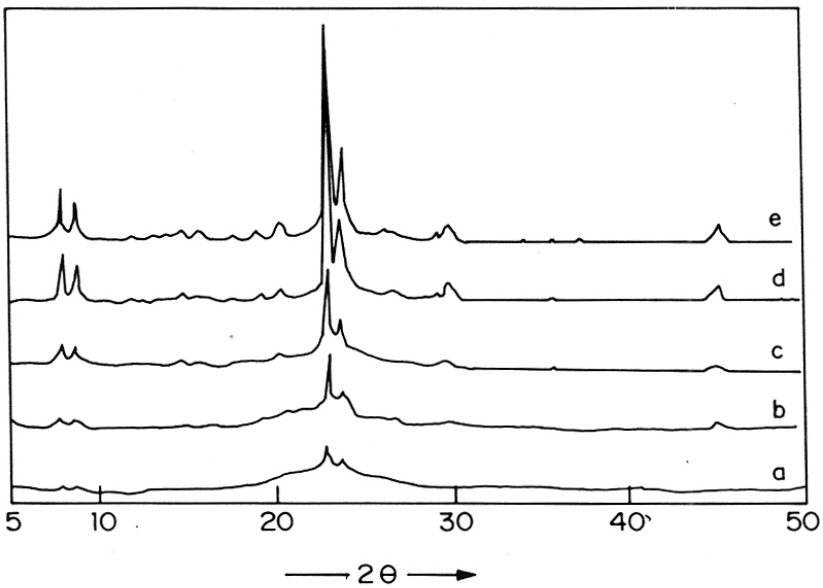

Fig.2.10. **XRD powder paterns of samples derived from a gel composition Si/V = 80, SiO_2/TBA-OH = 5 H_2O/SiO_2 = 30.**
Curves 'a' to 'e' represent samples withdrawn at intervals of 5, 10, 24, 36 and 48 hours, respectively during crystallization.

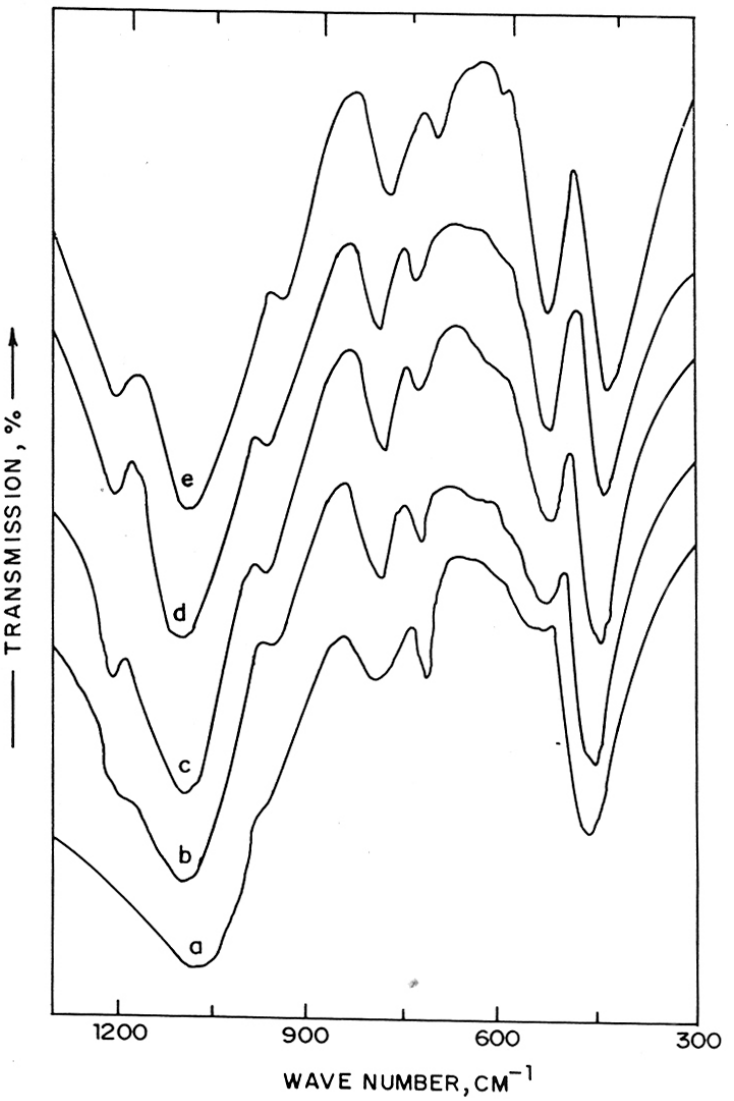

Fig.2.11. **IR spectra of samples crystallized at various time intervals.** Composition and legend as in Fig.2.10.

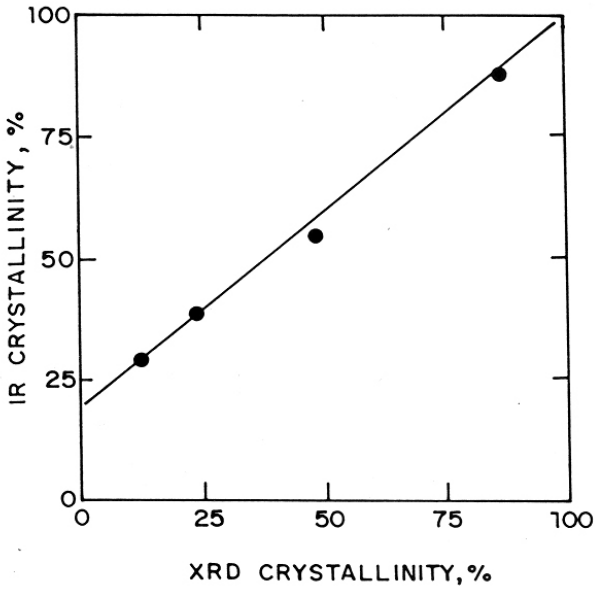

Fig.2.12 Correlation between IR crystallinity and XRD crystallinity.

perhaps be attributed to (O_3Si-O-VO_3) groups. A linear correlation between the vanadium content and the ratio of intensities of 965 to 550 cm^{-1} band in calcined samples indicated the progressive incorporation of vanadium in framework positions of the MEL structure.

2.3.3.3 ESR spectral studies

The ESR spectra of both the as-synthesized and the calcined samples have been recorded at room temperature. In the as-synthesized form, the spectra (Fig.2.13) are characteristic of atomically dispersed and immobile V^{4+} ions. The anisotropic 8-line hyperfine splitting caused by the ^{51}V nucleus is very well resolved in all the cases, without the presence of any superimposed broad singlet. The g-values and hyperfine coupling constants (g_{II}= 1.932; $g_{\perp}$= 1.981; A_{II}= 185 G and $A_{\perp}$ = 72 G, which are notably different from those observed for VO2+ exchanged into ZSM-5 and which are assigned to V^{4+} in framework positions[31]) are typical of vanadyl^{4+} complexes.[30,31,33]. Fig.2.14 represents the spectra of samples synthesized by varying the SiO_2/TBA-OH ratio from 3.3, 5 to 7.5 (curves a, b and c, respectively). At high template concentrations, the concentration of vanadium (V^{4+}) is found to be lower as seen from the ESR signal intensity (curve a). A ratio of 5.0 (of SiO_2/TBA-OH) seems to be optimum for maximum concentration of V^{4+}(probably in lattice positions), as further increase in TBA-OH concentration does not affect the intensity of ESR signals (curves, b and c in Fig.2.14).

The ESR spectra of samples withdrawn at different levels of crystallinity during the synthesis of a vanadium silicate with a gel composition of Si/V = 80 were also recorded. The integrated intensities of V^{4+} signals as a function of crystallization time follow the course given in Fig.2.15. The figure shows that crystallization of MEL and incorporation of V^{4+} in it run closely together during the synthesis. Similarly, the integrated intensities of ESR signals of samples of different Si/V ratios (after completion of the crystallization) were calculated. A linear increase in the ESR signal intensities with increasing vanadium content has been observed. On calcination of the samples at 773 K, no ESR signals were observed either at room temperature or at 77 K indicating the complete oxidation of V^{4+} to V^{5+} state. The oxidation is reversible upon reduction of the sample in H_2, V^{4+} can be regenerated[33]

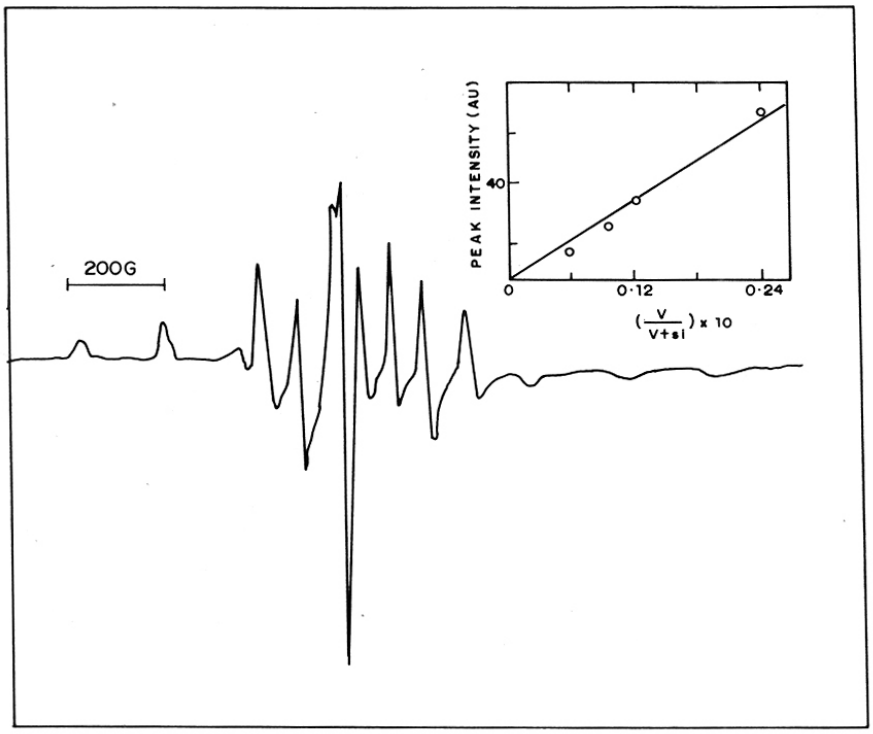

Fig.2.13. ESR spectra of as-synthesized sample Si/V = 161 (gel Si/V = 80). Inset : correlation between ESR peak intensity and vanadium content of the VS-2 samples.

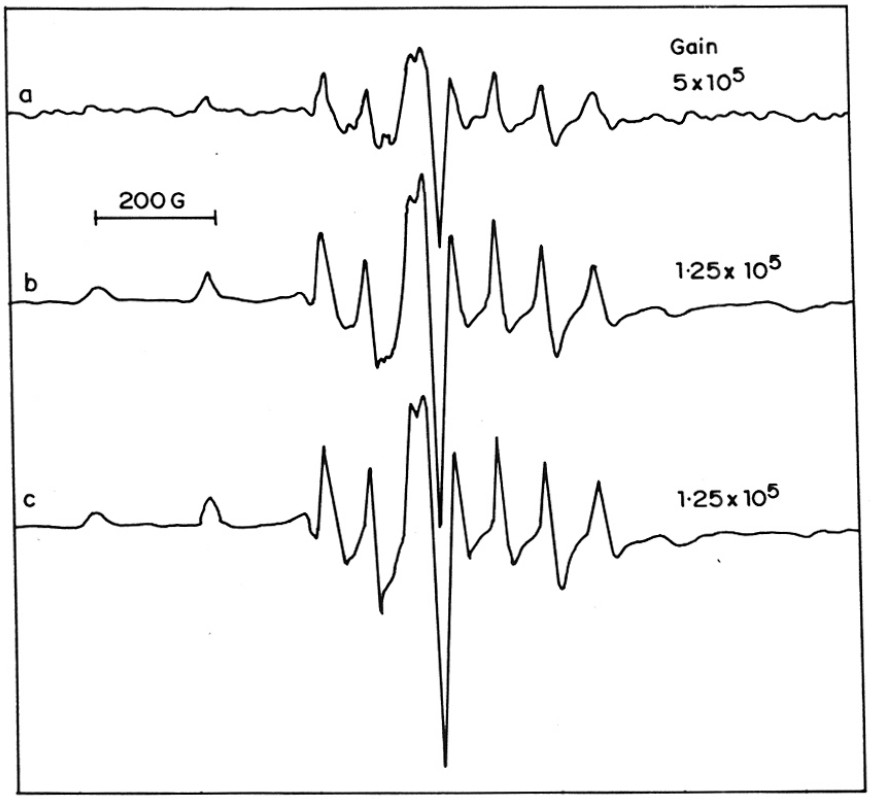

Fig.2.14. ESR spectra of as-synthesized samples of Si/V mole ratio of 161. Influence of template concentration; SiO2/TBA-OH : 3.3 (curve a); 5.0 (curve b) and 7.5 (curve c).

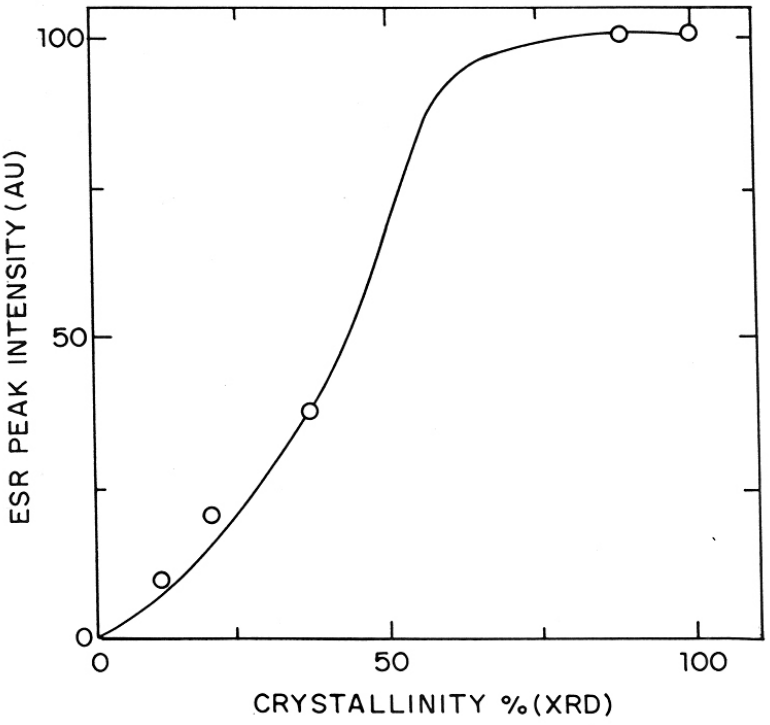

Fig.2.15 **Variation in ESR (V^{4+}) signal intensity with percent crystallinity during synthesis.** Gel composition Si/V = 80, SiO2/TBA-OH = 5 H2O/SiO2 = 30.

2.3.3.4 Thermal Analysis

Simultaneous TG-DTA of samples show (Fig.2.16) that the calcination (in air) of the as-synthesized samples occurs exothermally around 623-633 K, coinciding with a weight loss due to template decomposition. There are shoulders around 548 and 723 K, respectively, on either side of the sharp exotherms.

2.3.3.5 Scanning Electron Microscopy

The scanning electron micrographs of silicalite-2 and VS-2 (Si/V = 41) samples are given in Fig.2.17. All crystals had a distinct "rice grain" like morphology. They were found to be uniform in size and no macroscopic amorphous material was observed in the final samples. The largest crystals were approximately 5 μm in length (size) and < 1 μm in cross section.

2.4 CONCLUSIONS

The following conclusions can be drawn from our studies:

1. Crystalline vanadium silicates having the MEL structure can be synthesized at 443 K using tetrabutylammonium hydroxide as the organic additive. Other organic bases (like 1,8-diamino octane or trimethyl benzylammonium hydroxide) do not produce VS-2. Vanadyl sulfate is found to be a more suitable source than VCl_3 or NH_4VO_3 to synthesize vanadium silicate molecular sieves.

2. An increase in Si/V molar ratio in the reaction mixture enhances the rate of crystallization. There exists an optimum range of values of the SiO_2/TBA-OH ratio outside which the crystallization is too slow.

3. The increase in the pH of the mother liquor (Δ pH) with crystallization is caused by the incorporation of probably both V as well as Si in the framework.

4. The incorporation of V in the framework structure is feasible under optimally controlled reaction conditions. XRD, IR and ESR data support this conclusion. These vanadium silicates were found to be thermally stable.

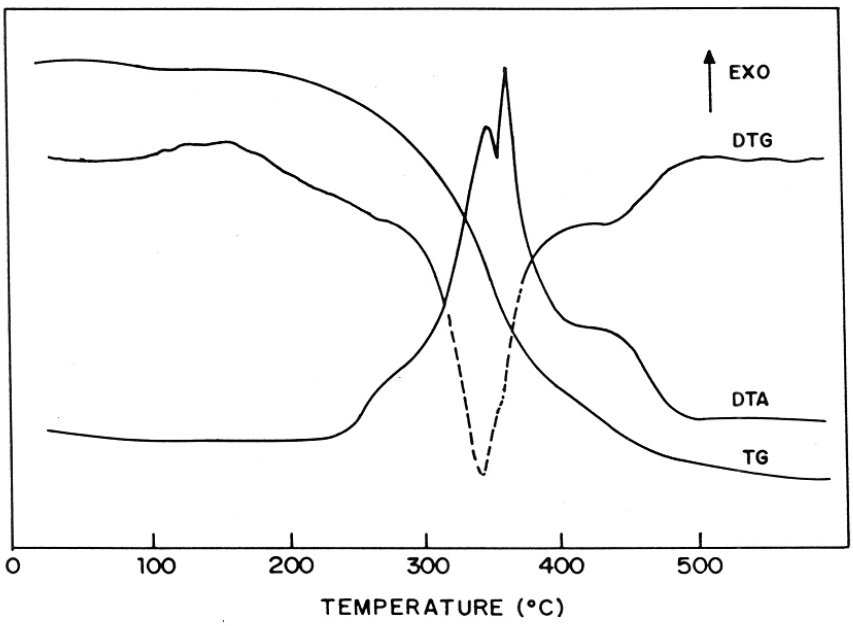

Fig.2.16 Simultaneous TG-DTA of as-synthesized sample of Si/V = 161.

Fig.2.17 SEM photographs of Silicalite-2 (A) and VS-2 (B) (Si/V = 79).

2.5 REFERENCES

1. Barrer, R.M., *Hydrothermal chemistry of zeolites*, Acadamic Press, London, p. 251 (1982).
2. Szostak, R., *Molecular Sieves: Principles of synthesis and identification*, Van Nostrand Reinhold, New York, p. 238 (1989).
3. Chu, C.T.W., Kuchl, G.H., Lago, R.M. and Chang, C.D., *J.Catal.*, **93**, 451 (1985).
4. Ratnasamy, P., Borade, R.B., Sivasanker, S., Shiralkar, V.P. and Hegde, S.G., *Acta Phys. Chem.*, **31**, 137 (1985).
5. Ball, W.J., Dwyer, J., Garforth, A. A. and Smith W.J., *Stud. Surf. Sci. Catal.*, **28**, 137 (1985).
6. Szostak, R.M. and Thomas, T.L., *J. Catal.*, **100**, 555 (1986).
7. Meagher, A., Nair, V. and Szostak, R., *Zeolites*, **8**, 3 (1988).
8. Ione, K.G., Vostrikova, L.A. and Mastikhin, V.M., *J. Mol. Catal.*, **31**, 355 (1985).
9. Reddy J.S., Reddy K.R., Kumar, R. and Ratnasamy, P., *Zeolites,* **11**, 85 (1991).
10. Kumar, R., Thangaraj, A., Bhat R.N. and Ratnasamy, P., *Zeolites*, **10**, 85 (1990).
11. Kumar, R. and Ratnasamy P., *J. Catal.*, **121**, 89 (1990).
12. Kumar, R. and Thangaraj A. in *Zeolites for Ninties* Recent Research Report 8th IZC Amsterdam Eds J.C. Jansen *et. al.*, Amesterdam 1989 p. 53.
13. Chandwarker, A.J., Bhat, R.N. and Ratnasamy, P., *Zeolites*, **11**, 42 (1991).
14. Kotasthane, A.N., Shiralkar, V.P., Thangaraj, A. and Ganapathy, S., *ACS Symp. Ser.*, **398**, 405 (1989).
15. Shizherg, L., Wenyang, X., Tao, D. and Yizhao, Y., *Taiyuam Gogye Daxue Xuebao*, **20**, 329 (1989).
16. Ratnasamy, P. and Kumar, R., *Catal. Today*, **9**, 329 (1991).
17. Taramasso, M., Perego, G. and Notari, B., US Pat. 4,441,501 1983.
18. Prego, G., Bellussi, G., Corno, C., Taramasso, M., Buonomo, F. and Esposito, A., *Stud. Surf. Sci. Catal.*, **28**, 129 (1986).
19. Notari, B., *Stud. Surf. Sci. Catal.*, **37**, 413 (1987).
20. Thangaraj, A., Kumar, R., Mirajkar, S.P. and Ratnasamy, P., *J. Catal.*, **130**, 1 (1991).
21. Reddy, J.S. and Kumar, R., *J. Catal.*, **130**, 440 (1991).

21a. Serrano, D.P., Hong-Xin Li, Davis, M.E., *J. Chem. Soc. Chem. Commun.*, 745 (1992).

22. Marosi, L., Staberow, J., Schwarzmann, M., Ger. Pat. 2831631 (1978).
23. Xu, R. and Pang, W., *Stud. Surf. Sci. Catal.*, **24**, 27 (1985).
24. Kuchrov, A.V. and Slinkin, A.A., *Zeolites,* **6**, 175 (1986).

24a. Kuchrov, A.V. and Slinkin, A.A., *Zeolites,* **7**, 38; 43; 583 (1987).

25. Sass, C.E., Chen, X., Kevan, L., *J. Chem. Soc.,* **86**, 189 (1990).

26. Inui, T., Medhanavyan, D. Praserthdam, P., Fukuda, K., Ukawa, T., Sakamoto, A. and Miyamoto, A., *Appl. Catal.,* **18**, 311 (1985).

27. Miyamoto, A., Medhanavyan, D. and Inui, T., *Appl. Catal.*, **28**, 89 (1986).

28. Miyamoto, A., Medhanavyan, D. and Inui, T., *Proc. 9th Int. Congr. Catal.,* (Ed. Philip, *M.J., et al.*) Pub. Chem. Inst. anada, Ontario, Vol.1 p.12 (1988).

29. Kornatowski, J., Sychev, M., Goncharuk, V. and Baur, W.H., *Stud. Surf. Sci. Catal.*, **65**, 581 (1991).

30. Rigutto, M.S. and Van Bekkum, H., *Appl. Catal.*, **68**, L1 (1991)

31. Fejes, P. *et al. Stud. Surf. Sci. Catal.*, **69**, 173 (1991).

32. Centi, G., Perathoner. S., Trifiro. F., Aboukais. A., Aissi. C.F. and Guelton. M., *J. Phys. Chem.*, **96**, 2617 (1992).

33. Hari Prasad Rao, P.R., Ramaswamy, A.V. and Ratnasamy, P., *J. Catal.* **137**, 225 (1992)

34. Hari Prasad Rao, P.R., Kumar, R., Ramaswamy, A.V. and Ratnasamy, P., *Zeolites*, (Communicated).

35. Thangaraj, A., *Ph. D. Thesis*, University of Poona, 1991.

36. Casci, J,.L. and Lowe, B.M., *Zeolites* **3**, 186 (1983).

37. Reddy, J.S. and Kumar, R., *Zeolites* **12**, 95 (1992).

38. Reference 2, p.71

39. Jacobs, P.A. and Martens, J.A., *Stud. Surf. Sci. Catal.*, **33**, 58 (1987).

40. Fype, C.A., Gies, H., Kokotailo, G.T., Pasztor, C., Strobl, H. and Cox, D.E., *J. Amer. Chem. Soc.*, **111**, 2470 (1989).

41. Jacobs, P.A. and Martens, J.A., *Stud. Surf. Sci. Catal.*, **33**, 177 (1987).

42. Zecchina, A., Spoto, G., Bordiga, S., Padovan, M., Leofanti, G. and Petrini, G., *Stud. Surf. Sci. Catal.*, **65**, 671 (1991).

43. Boccuti, M.R., Rao K.M., Zacchina, A., Leofarti, G. and Petrini, G., *Stud. Surf. Sci. Catal.*, **48**, 133 (1989).

CHAPTER 3

PHYSICO-CHEMICAL CHARACTERIZATION

3.1 INTRODUCTION

Several researchers have studied the introduction of vanadium into the zeolites[1-15], and aluminophosphate molecular sieves[16-20]. Reports have appeared recently on the synthesis of vanadium containing zeolites with MFI structure and their interesting catalytic properties[21-24]. The location and the state of vanadium in these zeolites are, however, still ambiguous. Recently, Rigutto *et al.* and Fejes *et al.* have reported synthesis and characterization of vanadium containing silicalite with MFI structure[22,23]. It was postulated that vanadium ions are located at defect sites. Earlier Kornatowskii *et al.* had also reported synthesis of vanadium silicate with MFI structure[21]. In a recent report, Centi *et al.* have identified more than three different vanadium species, which contained extractable and occluded vanadium in the pore structure[24]. V-silicalite and V-ZSM-5 samples have also been prepared recently by chemical vapor deposition of $VOCl_3$ on silicalite and HZSM-5[25]. High temperature interaction of V_2O_5 with ZSM-5 zeolite[26] leads to the formation of VO^{2+} species which replaced both strong acid protons and terminal Si-OH groups located on the surface. Fejes *et al.*[23] have proposed a square pyramid ligand field symmetry in dehydrated vanadium oxide-zeolite mixture and square bipyramid coordination after adsorption of water or ammonia.

This Chapter describes the detailed characterization of vanadium silicates with MEL structure. Evidence for the incorporation of vanadium ions into the zeolite framework has been obtained from X-ray diffraction (XRD), Infra-red (IR and FT-IR), electron spin resonance (ESR), and NMR techniques. Additional support is obtained from surface area and sorption studies. The catalytic activity in various oxidation reactions (which will be discussed in the next chapter) also confirm the presence of vanadium at framework positions.

3.2 EXPERIMENTAL

3.2.1 X-RAY DIFFRACTION

The samples were analyzed by X-ray diffraction to study the crystallinity and phase purity. Rigaku (model D/MAX III VC, Japan) X-ray diffractometer, with Ni filtered Cu-Kα radiation (λ = 1.5404 Å) was used to record powder diffraction profile. The samples were scanned from 2 θ, 5 to 50° at a scan rate of 2° min^{-1}. Phase purity of the samples was worked out from the X-ray diffraction pattern reported by Fyfe *et al.*[27] for MEL structure. Based on the preliminary

experiments, a sample with highest crystallinity was taken as reference sample and was used to check phase purity and crystallinity. Peak areas were calculated from the collected data, using a semiquantitative software programme provided with the instrument.

Silicon was used as internal standard for calibrating the 2 θ values. The unit cell parameters were calculated for calcined samples from x-ray diffraction pattern scanned at a rate of 0.25° min^{-1}.

3.2.2 INFRARED SPECTROSCOPY

The infrared spectra of the as-synthesized samples were recorded in FT-IR Perkin Elmer spectrometer in the frequency range of 450 - 1400 cm^{-1} using the Nujol mull technique. KCN was used as the internal standard.

The spectra in the range of 4000- 1300 cm^{-1}, were recorded in a Nicolet 60 SXB FT-IR spectrometer using self supported wafers. For in-situ studies, a cell in which the temperature can be varied from liquid nitrogen temperature to 773 K was fabricated and used. This cell was connected to a volumetric adsorption apparatus (Micromeritics, USA, Model: Accusorb-2000 E).

The cell was basically a DEWAR flask with a modification as shown in Fig.3.1. The sample was pressed under pressure of 5 ton/$inch^2$ into a thin pellet (5-6 mg/cm^2) and mounted in the sample holder (SH). It was then placed inside the heating compartment of the cell (HC) and aligned with the IR beam. The cell was sealed at both the ends by potassium bromide windows (KW) with the help of elastometer "O" rings. A thermocouple is placed in close vicinity of the sample to measure the temperature of the sample. The side tube at the top of the cell was connected to the vacuum system. Cold water was constantly circulated through the cooling coil provided near the KBr windows. The sample was heated to 673 K with a heating rate of 5 K min^{-1}, under vacuum The spectra were recorded by averaging more than 100 scans with 2 cm^{-1} resolution. Vapors of ammonia, pyridine and benzene were admitted to the sample through the adsorption manifold of the system.

3.2.3 ELECTRON SPIN RESONANCE SPECTROSCOPY

Electron spin resonance spectra were recorded using Bruker ER-200 D spectrometer at 9.7 GHz (X-band) with a rectangular cavity ST_{8424}. Modulation at 100 KHz with intensity 1.25

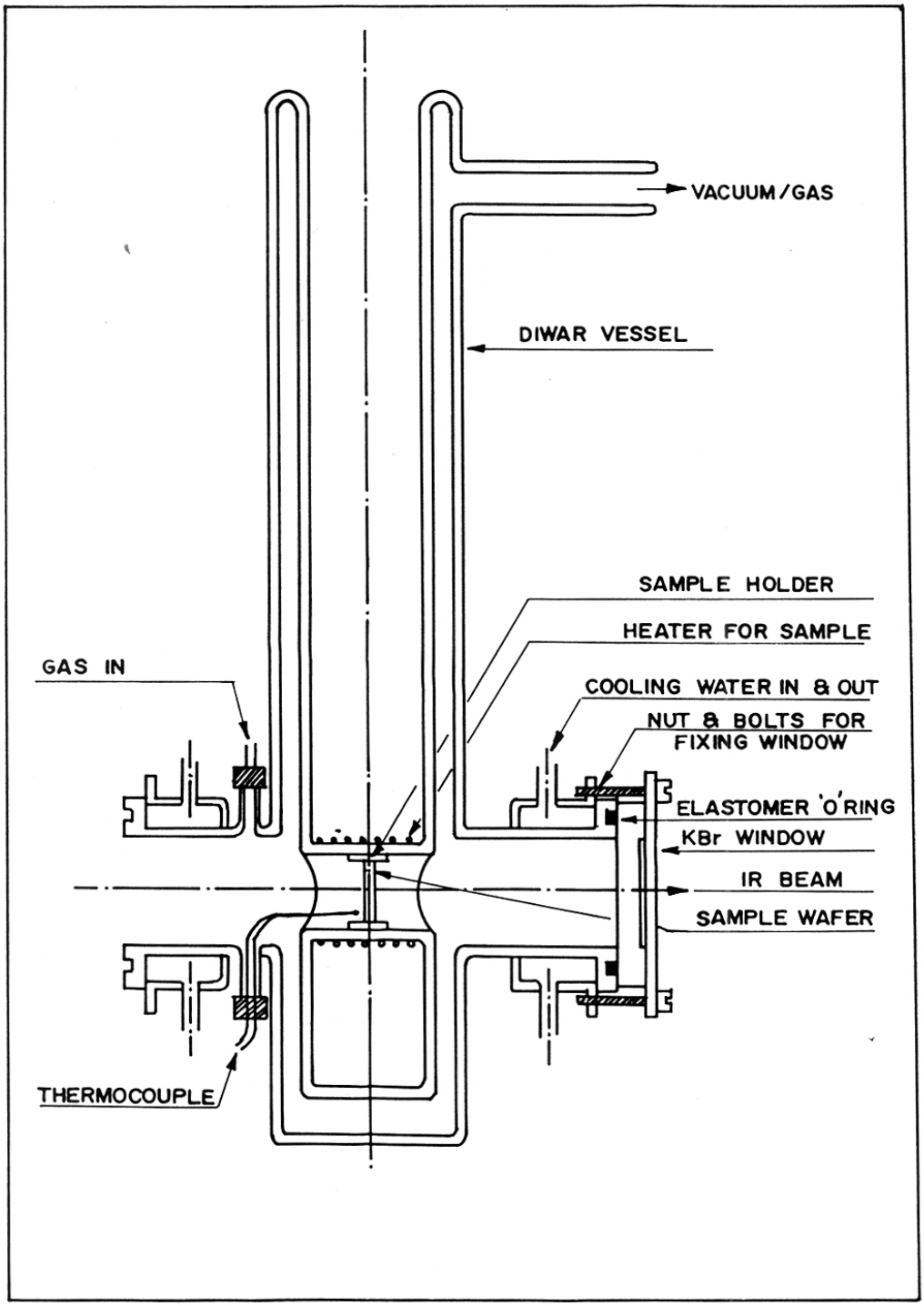

Fig.3.1 FT-IR transmittance cell.

GPP and time constant 10^3 m sec. was used. The h.f. power was chosen small enough to prevent any signal saturation. The spectra were recorded at 300 K. A constant weight of 0.1 g of the sample was taken to record the spectra.

3.2.4 ^{51}V MAS-NMR SPECTROSCOPY

The wide-line solid state ^{51}V MAS NMR measurements of vanadium silicate samples were recorded on a Bruker MSL-400 FT-NMR spectrometer at 105 MHz. The spectral width was 2.5 MHz and 200 m.sec repetition time was used. The spectra were from accumulation of 10,000 to 20,000 transients. Liquid $VOCl_3$ was chosen as reference to measure the chemical shift.

3.2.5 THERMAL ANALYSIS

Simultaneous TG-DTA-DTG analyses of as-synthesized and dried vanadium silicate samples were carried out in a computer controlled thermal analyzer instrument (Setaram, France TG-DTA92). A linear rate of heating of 10° min^{-1} in the range from room temperature to 900 °C in air flow at a rate of 30 ml min^{-1} was used to find out the temperature of decomposition of template and hence the calcination temperature required for the samples. A sample volume of about 30 mg was taken with an inert α-alumina as a reference. Detailed analysis of weight loss due to decomposition of template and accompanying heats of decomposition have been calculated from stored data of each TG-DT analysis using software programme available with the instrument.

3.2.6 UV-VIS SPECTROSCOPY

The UV-VIS diffuse reflectance spectra of the sample were recorded in a Pye Unichem SP-8-100 UV-Visible spectrometer.

3.2.7 ION-EXCHANGE STUDIES

The calcined samples were treated with 0.05 N NaCl for 3 h at 323 K to exchange protons with Na. The Na form was exchanged with 0.05 N KCl for 3 h at 323 K. The solid was filtered, washed thoroughly with deionized water and dried at 373 K for 10 h. The resultant material was analyzed for K^+ and vanadium ions.

3.2.8 ADSORPTION STUDIES

The sorption measurements for water, cyclohexane and n- hexane were carried out gravimetrically in a recording electromicrobalance (Model: Cahn-2000 G). The calcined sample of about 60 mg was pressed into a pellet and weighed into an aluminium bucket which was attached to the balance. The system was evacuated down to pressure of 10^{-6} torr at 673 K. After two hours, the temperature was lowered to the desired value. The sorbate was admitted into the sample at a constant pressure and temperature and the weight gain was recorded as a function of time. After adsorption was over, the catalyst was heated to 673 K under vacuum in the order of 10^{-6} torr and used for the next measurement.

3.2.9 SUSRFACE AREA MEASUREMENTS

Omnisorb 100 CX (supplied by COULTER Corporation, USA) unit was used for the measurement of nitrogen adsorption to determine apparent surface area. The samples were activated at 673 K for 2 h in high vacuum (10^{-5} mm). After the treatment, the anhydrous weight of the sample was taken. The samples were then cooled to 94 K using liquid nitrogen. After cooling, the sample was allowed to adsorb nitrogen gas. From the adsorption isotherm the micropore area (by BET method) and mesopore area (by t-method) were calculated.

3.2.10 STEAMING EXPERIMENTS

The zeolite samples were treated in a muffle furnace to the desired temperature at a heating rate of 2.5 K min^{-1}. Then the samples were cooled to room temperature and kept in a desiccator over saturated ammonium chloride solution. The hydrothermal treatment was carried out in a tubular furnace with steam (100 %) at atmospheric pressure.

3.3 RESULTS AND DISCUSSION

3.3.1 X-RAY DIFFRACTION

The X-ray diffraction patterns of vanadium silicates (VS-2) sample were similar to that of silicalite-2[27,28] (Fig.3.2). The structure belonged to tetragonal space group $I\bar{4}m2$ [119]. The crystalline VS-2 was found to be free from any MFI type impurity. In the XRD pattern of VS-2, the lines at $2\theta = 9.05°$ and $24.05°$ (both these lines are characteristic of MFI structure) are completely absent. Further, a peak at $2\theta = 45°$ is present as a singlet.

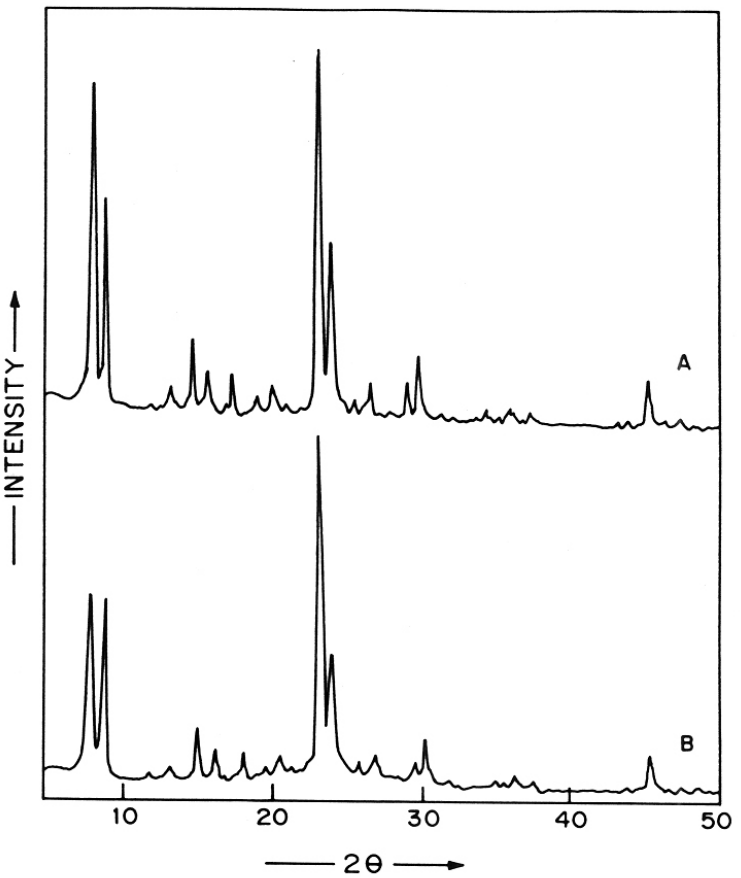

Fig.3.2. X-ray powder paterns of Silicalilte-2 (A) and VS-2 (B) calcined at 823 K.

The unit cell parameters increased uniformly and regularly with the vanadium content in the sample (Table 3.1 and Fig.3.3 A-C curve 1) suggesting the incorporation of vanadium in the framework of the MEL structure. On steaming the samples at 873 K for 2 h, all the vanadium silicates exhibited a reduction in the unit cell parameters to values typical of silicalite-2 (Fig.3.3 A-C curve 2), evidently due to the removal of vanadium from the framework to non-framework positions. Silicalite-2 itself did not show any decrease in the unit cell parameters after similar steam treatment. The results of steaming experiments thus suggest that in the VS-2 samples the vanadium ions are in the framework positions.

3.3.2 INFRARED SPECTROSCOPY

Additional support for the location of vanadium is suggested by the observation of an absorption band at around 965 cm^{-1} in the IR spectra of VS-2 samples[29,30] (Fig.3.4). Bands in this region are characteristic of metal oxygen stretching vibrations. Titanium silicates (both TS-1 and TS-2) containing titanium in the lattice positions and vanadium silicate with MFI structure also exhibit this band around 960 cm^{-1} due to Si-O-Ti linkages[21,31-33]. This band is absent in the IR spectra of pure silicalite-2 as well as silicalite-2 impregnated with oxides of vanadium (or titanium[31-35]). The intensity of this IR band increased linearly with vanadium content in VS-2. The ratio of 965 to 550 cm^{-1} band also increases with unit cell parameters (Fig.3.3 D). The band at 550 cm^{-1} is characteristic of the MEL framework structure. IR spectroscopic results, thus, lend additional support to the presence of vanadium in framework positions.

Fig.3.5 illustrates the IR spectra of the calcined samples in the hydroxyl stretching region (4000 - 2800 cm^{-1}) after outgassing in vacuum at 673 K. A sharp band at 3728 cm^{-1} and a broad band at 3532 cm^{-1} can be seen. The former is due to terminal silanol groups and the latter is assigned to H- bonded hydroxyl groups[36]. The sharp peak due to isolated silanols, probably located on the external surface, is present in pure silicalite-2 also (Fig.3.5 curve d) The broad band at 3532 cm^{-1} is found in all vanadium silicate samples, their intensity increasing with the vanadium content. Centi *et al.*[24] have in addition reported a band at 3682 cm^{-1}, attributed to less thermally stable -OH groups. This band is also present but as a shoulder in our samples (Fig.3.5) The band ascribable to V-OH vibration, however, is not clearly distinguished due probably to the broad nature of the 3532 cm^{-1} band and the low vanadium content in the samples. It was earlier suggested that the vanadium ions are probably at surface defect sites where the Si-OH

Table 3.1

Physico-chemical properties of vanadium silicates

Catalyst	Si/V sample[a]	Si/V sample[b]	Na/V[c]	Surface area (m^2/g)	Unit cell volume[d]	ESR signal intensity[e]	Sorption capacity, (wt. %)		
							n-hexane	cyclohexane	water
VS-2	41	52	0.61	539	5391.3	68	8.4	13.6	6.1
VS-2	78	79	0.56	550	5373.2	33	8.2	12.8	6.0
VS-2	116	122	0.51	506	5367.5	24	8.0	13.0	5.8
VS-2	161	161	0.53	554	5362.5	14	8.1	12.9	4.6
VS-2	300	302	0.48	542	5358.2	8	8.2	13.0	3.2
S-2		-	-	548	5354.4	-	8.0	12.8	2.1

[a] as-synthesized sample

[b] after treating the calcined sample with 0.5 M ammonium acetate solution at room temperature

[c] after treating the calcined sample with 0.05 M NaCl solution at room temperature

[d] Unit cell volume of the calcined samples (in $Å^3$) calculated from XRD parameters.

[e] ESR signal intensity (arbitrary units) due to V^{4+} ions in the as-synthesized samples.

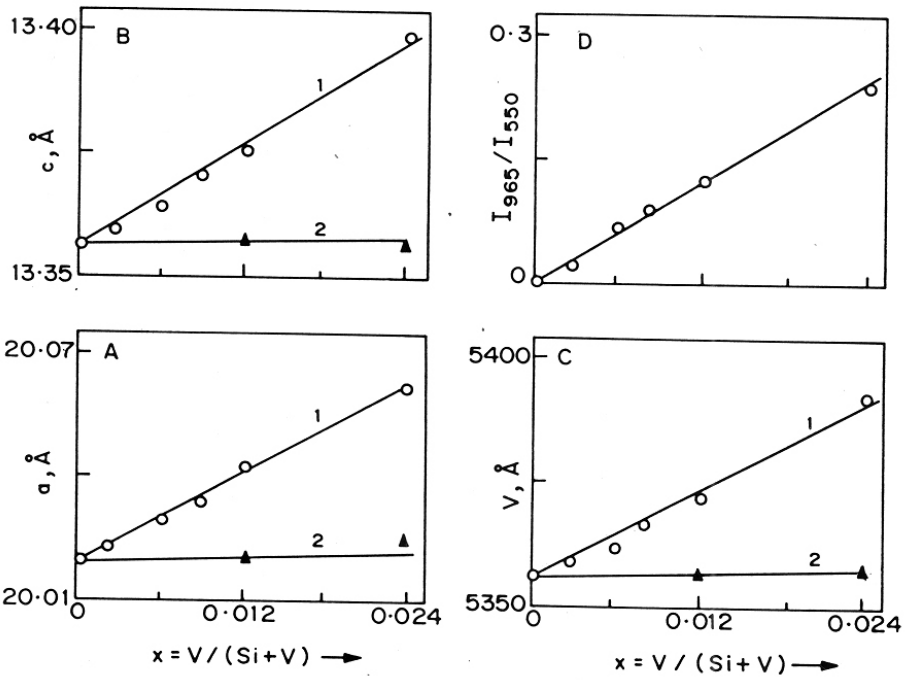

Fig.3.3. **The unit cell parameters a = b (A), c (B) and volume, v (C) and ratio of intensities of 965/550 cm^{-1} IR bands vs mole fraction of vanadium (x) (D) in various VS-2 samples.**

Curve 1, calcined samples in air at 753 K and curve 2, after steaming the calcined samples at 873 K for 1 hr in 100 % steam.

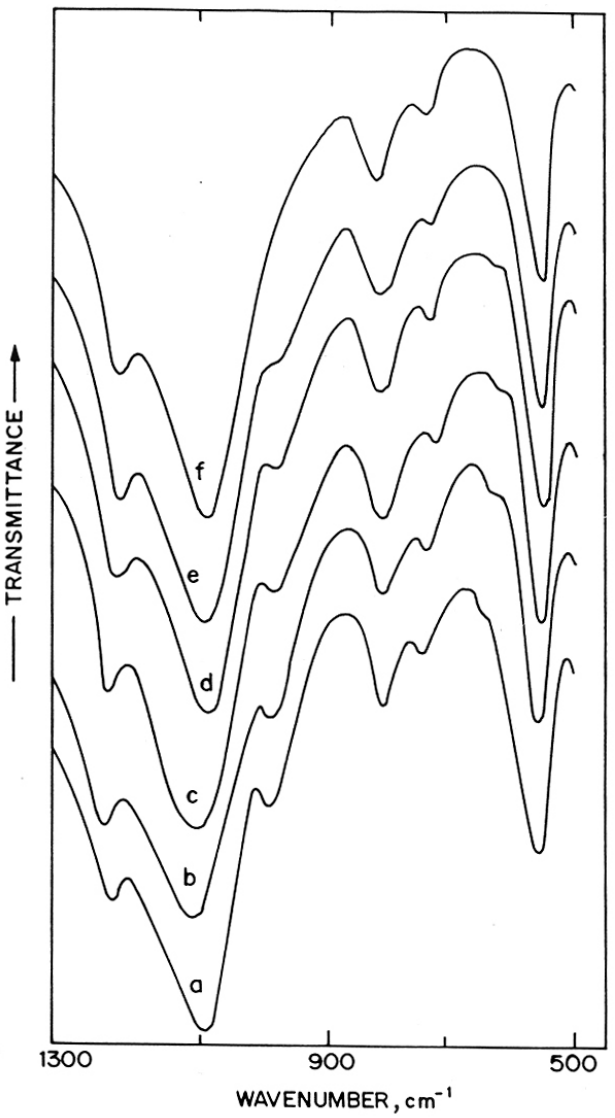

Fig.3.4. Framework IR spectra of VS-2 samples (calcined 753 K).
Curves 'a' to 'e' represent samples with Si/V 41, 79, 122, 161 and 302, respectively and silicalite-2 (curve f).

concentration is likely to be high[22,24,29]. That the formation of such sites could be enhanced by the presence of vanadium during the hydrothermal synthesis is indicated by the linear increase in the total integrated intensity of the absorption in the region 3850 to 3150 cm^{-1} with the vanadium content in the three samples, (inset in Fig.3.5). Irrespective of the differences in the preparation of vanadium silicates, this correlation supports the model proposed for V-MEL[29] and V-MFI[22,24] molecular sieves for the possible environment of vanadium in the pentasil structure.

In order to study the surface acidity of the above samples, adsorption of ammonia was performed on vanadium silicate (Si/V = 79). The spectra on desorption of ammonia from the calcined sample at various temperatures are shown in Fig.3.6. Two bands at 1680 cm^{-1} and 1450 cm^{-1} due to ammonium ions (δ_s and δ_{as} of NH_4^+, respectively) indicate the presence of Brönsted acid sites[37-39]. The intensity of these bands decreased drastically on evacuation even at 373 K indicating the presence of only weak Brönsted acid sites. At 373 K when most of the bands due to Brönsted acidic sites have disappeared, a distinct band at 1620 cm^{-1} is seen clearly. This band is due to ammonia coordinatively bonded to Lewis acid sites[37]. Brönsted acid sites, were not observed in pure silicalite. These observations are in broad agreement with the recent report of Centi *et al.*[24] on vanadium silicate (Si/V = 262) with MFI structure. However, the presence of a distinct band at 1620 cm^{-1} after evacuation at 373 K had not been observed earlier.

The spectra of the adsorbed pyridine after evacuation at 323 K for the three vanadium silicates and pure silicalite-2 are presented in Fig.3.7 (curves a to d, respectively). Fig.3.8 illustrates the spectra of adsorbed pyridine on vanadium silicate (Si/V = 79) after evacuation at 323, 373 and 423 K (curves a, b and c), respectively. A weak band at 1581 cm^{-1} observed in the spectra supports the presence of H-bonded pyridine[37,40]. In addition, a weak band at 1547 cm^{-1} due to Brönsted acid sites (due to the formation of pyridinium ions) is seen in the vanadium silicate samples. This The 1547 cm^{-1} band is absent in pure silicalite-2 and . The intensity of this band increases with the vanadium content. The pyridinium ions on vanadium silicates are unstable on evacuation at 423 K (Fig.3.8). Hence, only weak Brönsted acid sites are present in the vanadium silicates. They are probably related to V-OH species. This is in agreement with the sodium ion-exchange behavior of the samples reported earlier (Table 3.1)[22,24,29].

Centi *et al.*[24] using adsorption probe molecules such as ammonia, pyridine, duterated acetonitrile and *tert*-butylcyanide reported the presence of stronger Brönsted acid sites in the

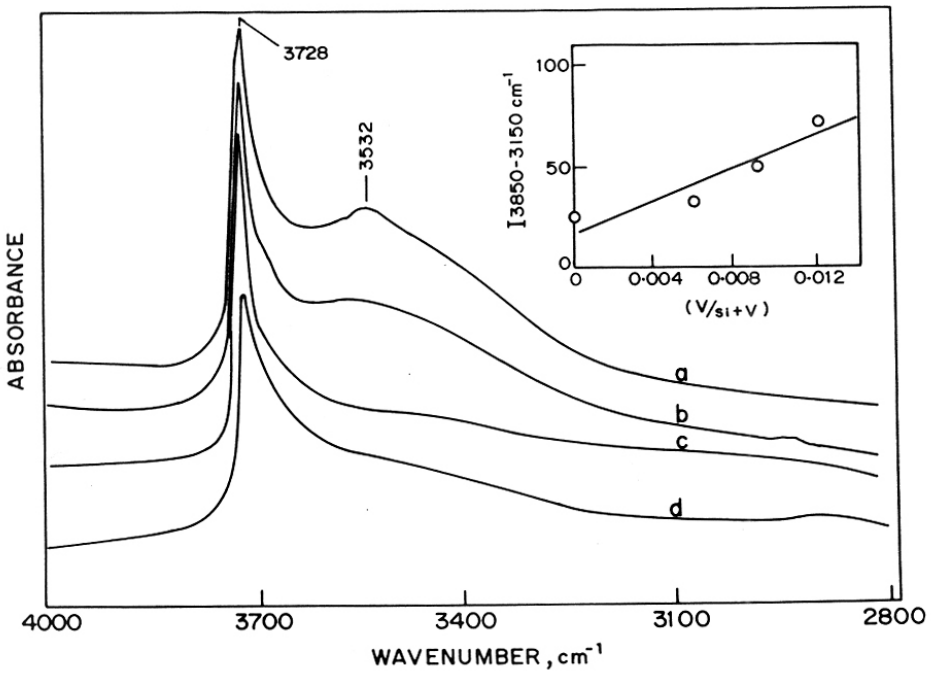

Fig.3.5. FT-IR spectra of vanadium silicate-2 and silicalite-2 samples.
Curves 'a' to 'c' refer to VS-2 samples with Si/V mole ratios of 79, 122 and 161, respectively and curve d for silicalite-2.
Inset : correlation between integrated intensity of IR absorbance in the range 3850-3150 cm^{-1} and mole fraction of vanadium in various VS-2 samples.

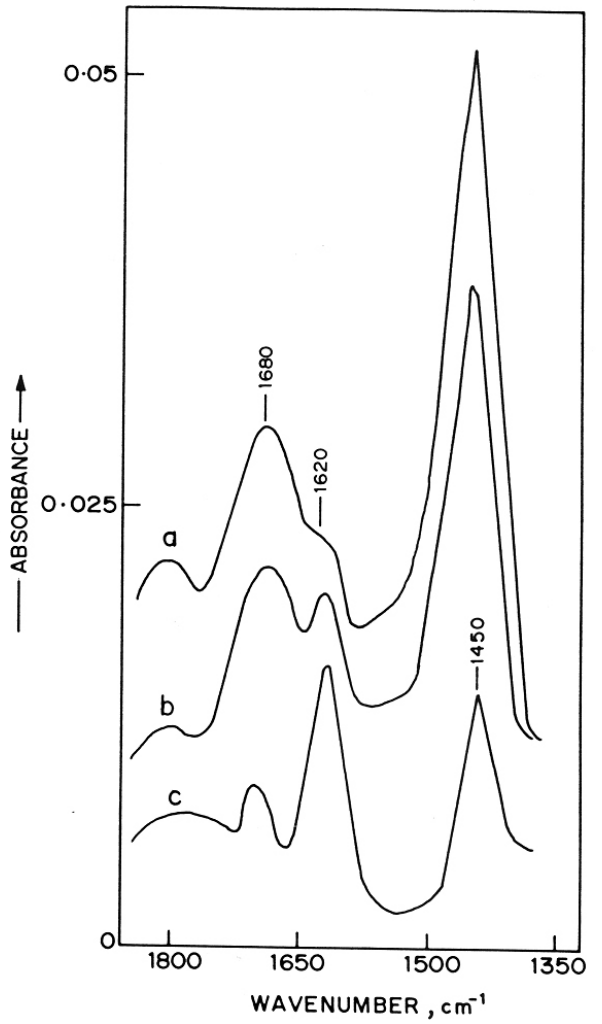

Fig.3.6. FT-IR specrta of VS-2 (Si/V = 79) sample after adsorption of ammonia at 303 K and evacuation at 303, 323 and 373 K (curves 'a' to 'c' respectively).

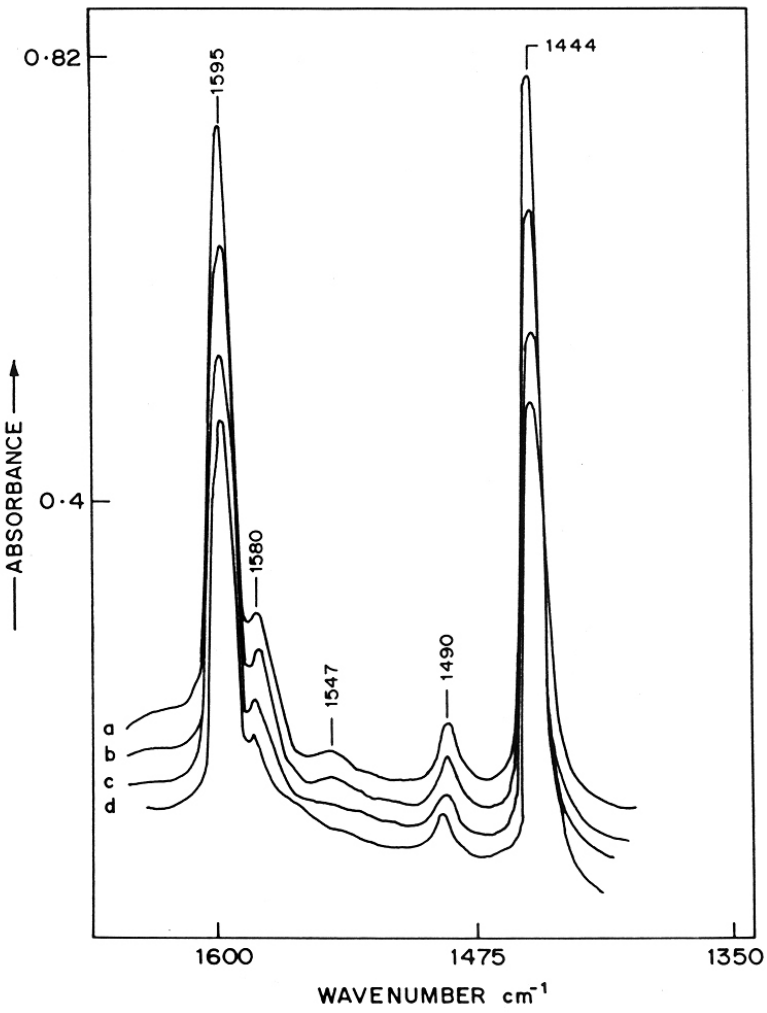

Fig.3.7. FT-IR spectra after adsorption of pyridine at 303 K and evacuation at 323 K. Curves 'a' to 'c' refer to VS-2 samples with Si/V = 79, 122 and 161, respectively and curve d for silicalite-2.

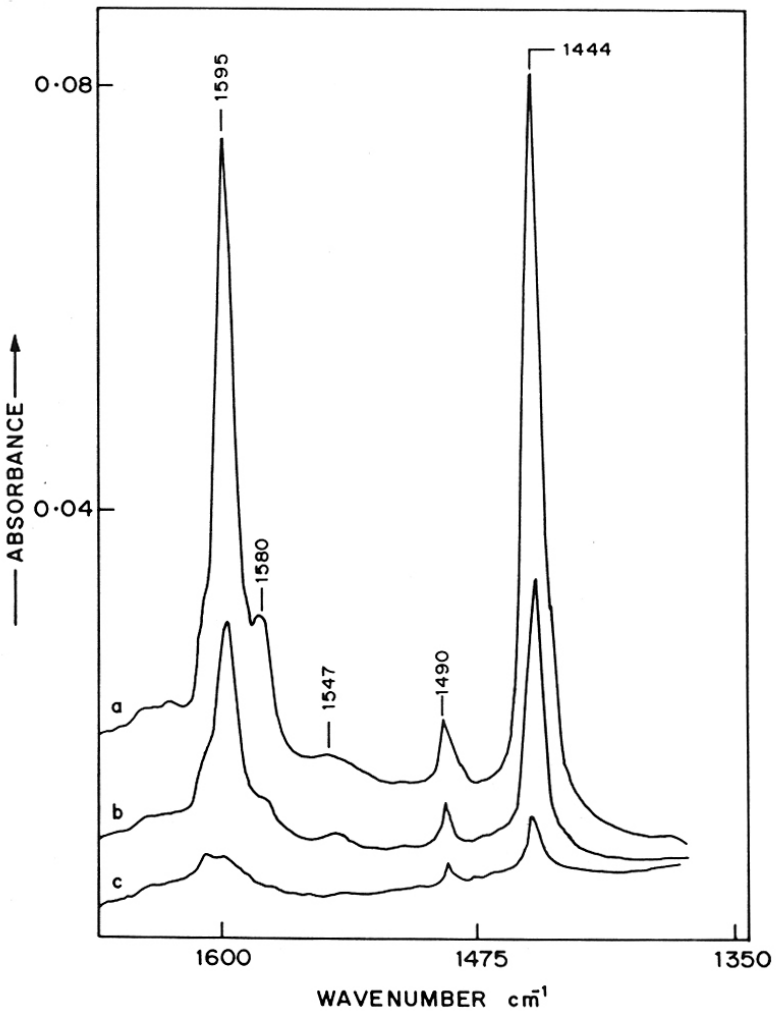

Fig.3.8. FT-IR spectra of VS-2 (Si/V = 79) sample after adsorption of pyridine at 303 K and evacuation at 323, 373 and 423 K (curves 'a' to 'c' respectively).

vanadium silicate-1 (V-MFI) compared to pure silicalite-1. They have also reported that very weak Lewis acids are present on the external surface of both VS-1 and pure silicalite, but additional stronger Lewis site are present inside the zeolite channels in VS-1. Our results on vanadium silicate with MEL structure are in agreement with those proposed for vanadium silicate for MFI structure[24].

3.3.3 ELECTRON SPIN RESONANCE SPECTROSCOPY

The ESR spectra of both the as-synthesized and the calcined samples have been recorded at room temperature. In the as-synthesized form, the spectra (Fig.3.9) are characteristic of atomically dispersed and immobile V^{4+} ions. The anisotropic 8-line hyperfine splitting caused by the ^{51}V nucleus is very well resolved in all the cases, without the presence of any superimposed broad singlet. The g-values and hyperfine coupling constants ($g_{\parallel}$= 1.932; $g_{\perp}$= 1.981; $A_{\parallel}$= 185 G and $A_{\perp}$= 72 G), are notably different from those observed for VO2+ exchanged into ZSM-5. They are assigned to V^{4+} in framework positions[23]. The latter are typical of vanadyl^{4+} complexes[18-20,23,24].

Similarly, the integrated intensities of ESR signals of samples of different Si/V ratios (after completion of the crystallization) were calculated. A linear increase in the ESR signal intensities with increasing vanadium content in the samples and a corresponding parallel increase in the unit cell volume (calculated from the XRD data) of the synthesized samples, as presented in Fig.3.10 A, strongly suggest that V^{4+} ions are incorporated at framework positions.

Identical spectra were obtained at 298 K and 77 K indicating that V^{4+} ions are not in tetrahedral symmetry positions (Fig.3.9 curve a). On calcination of the samples in air at 753 K, the samples did not exhibit any ESR spectra either at 298 or at 77 K (Fig.3.9 curve b). The V^{4+} ions are probably oxidized to the V^{5+} (d^0) state on calcination. The complete oxidation of V^{4+} to V^{5+} indicates the absence of any polymeric vanadium clusters. On reducing the calcined samples at 673 K in H_2, the typical spectrum of V^{4+} reappeared (Fig.3.9 curve c) indicating the reversibility of the V^{4+} <--> V^{5+} transition. This is further confirmed by the observation of V^{4+} ESR signals for the sample after catalytic reaction with hydrocarbons (Fig.3.9 curve d). Table 3.2 compares the 'g' values and hyperfine coupling constants ('A') observed in VS-2 with those observed in other but similar matrices. In the closely related vanadium silicalite-1 (VS-1) system, Rigutto and van Bekkum[22] concluded that vanadium is five coordinate (square pyramidal), probably at defect sites. The different ESR signal response with the magnetic field for samples

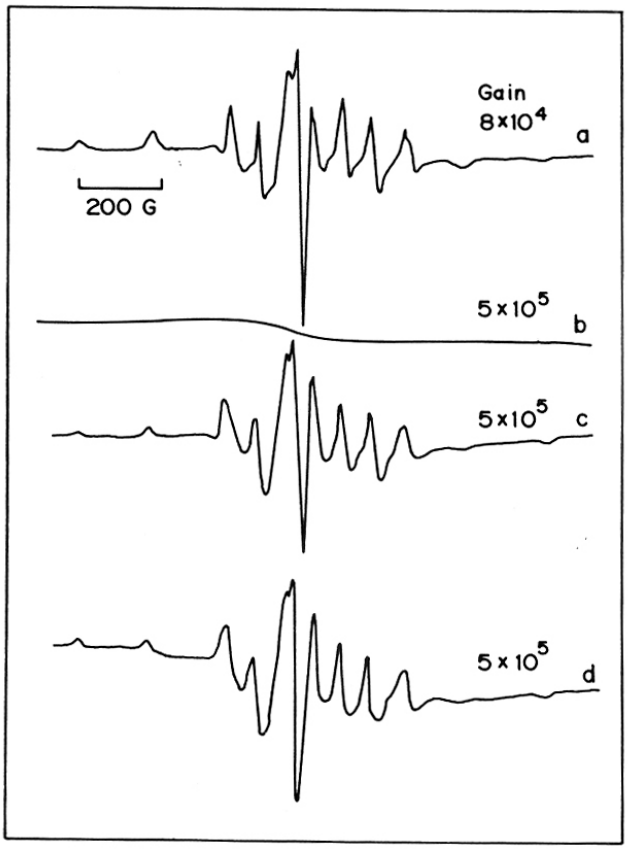

Fig.3.9. **ESR spectra of as-synthesized vanadium silicalite-2 (a), calcined (b), calcined and reduced (c) and after use in catalytic reaction (d).**

with VO^{2+} in ion-exchanged positions and V^{4+} in the framework positions of ZSM-5 has recently been discussed by Fejes *et al.*[23]. In their study, notable differences were observed in the parallel component of the 'g' tensor and the elements on the main diagonals of the hyperfine coupling tensors of VO^{2+}(ex)-ZSM-5 (vanadium at exchangeable cation positions) and V^{4+}(f)-ZSM-5 (vanadium at framework positions) zeolites, due to a displacement of the V^{4+}(f)-ZSM-5 spectrum to higher fields as shown in Fig.3.10 B. The shift of the first parallel lines was 51.9 gauss which diminished to 15.5 gauss for the 8th line, due to the greater width of VO^{2+}(ex)-ZSM-5 spectrum. The observed 'g' values in our samples are consistent with the argument that the V^{4+} ions are in the framework positions in addition to being well dispersed and immobile. In the case of VAPO-5 system, Montes *et al.*[20] proposed that vanadium in as-synthesized VAPO-5 is V^{4+} in a vanadyl like environment and that upon calcination in O_2 at 773 K most of the vanadyl species were converted to V^{5+} in framework positions. This transition was found to be reversible on reduction.

The calcined samples at higher temperatures are white in color. However, in contact with water vapor they turn yellow in color. At higher temperatures, the net positive charge of the framework caused by the presence of V^{5+} ions can be compensated by O^{2-} ions only (Fejes *et al.*[23] reported ESR signal due to O_2^- ion radical with g = 2.0027 for incompletely oxidized samples, in contact with oxygen, confirming the interaction of framework elements with gaseous oxygen). In contact with water vapor they undergo hydration causing the change in color from white to yellow. This indicates that the yellow color is caused by the hydration and not by the oxidation state of vanadium ions[23].

$$\{V^{4+}O_2\} + O_2 \text{ ---> } \{V^{5+}O_2\}^+ O_2^-.$$

$$[2\{V^{5+}O_2\}]O^{2-} + H_2O \text{ ----> } 2\{V^{5+}O_2\}^+.OH^-$$

The H^+ ion of these V-OH groups can be exchanged with Na^+ ions. Based on the adsorption studies of ammonia and pyridine described earlier, they are weakly acidic in nature.

3.3.4 ^{51}V MAS-NMR SPECTROSCOPY

The ^{51}V NMR spectrum of a vanadium silicate sample (Si/V = 79) is shown in Fig.3.11 a. The spectrum is quite complex due to simultaneous line-broadening effects arising from second order quadrupolar and chemical shift anisotropy interactions. The spectrum shows a main signal at -573 ppm (relative to $VOCl_3$). The observed line width at half-height (approximately 50 ppm) is much narrower than that reported (around 250 ppm) for other supported

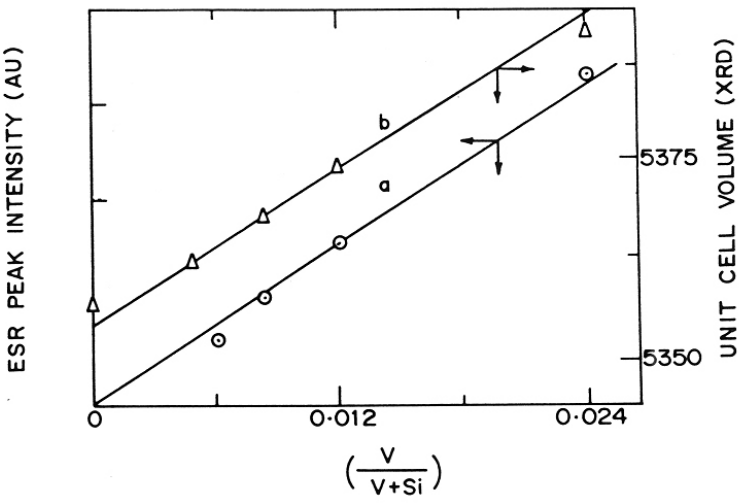

Fig.3.10 A. Correlation between vanadium content and integrated ESR signal intensities (a) and the corresponding unit cell volumes (b).

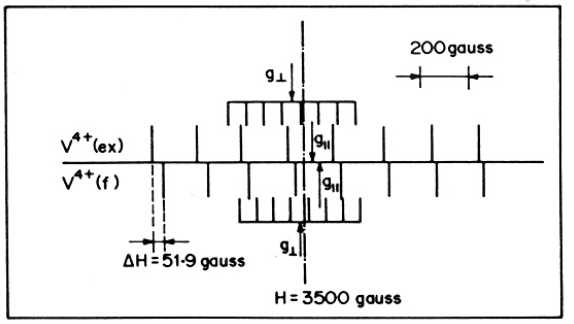

Fig.3.10 B. Term scheme for VO_2(ex) and V^{4+}(f). (Ref. 23)

Table 3.2

Principal Values of **g** and **A** for V^{4+} in some host matrices.

S.No.	Sample	Temp. (K)	$g_{\parallel}$	$g_{\perp}$	$A_{\parallel}$	$A_{\perp}$	ref.
1.	VS-2 As-synthesized	298	1.932	1.981	185	72	29, 30
		77	1.935	1.981	185	70	
	Reduced in Hydrogen	298	1.933	1.972	185	71	
		77	1.929	1.975	185	69	
2.	VS-1 As-sinthesized	298	1.935	1.994	183	69	22
	Reduced in benzene	298	1.935	1.996	179	65	
3.	V^{4+} (f) - ZSM-5 As-synthesized		1.949	1.990	185.8	72.5	23
	VO^{2+} (ex)-ZSM-5		1.963	2.007	190.8	75.4	
4.	VAPO-5 As-synthesized	300	1.932	1.983	198	78	20
		77	1.932	1.983	198		
5.	V-$ThGeO_4$ (V^{4+} in T_d)	77	1.831	1.980	166	32	50
6.	$Ga_2NaMg_2V_3O_{12}$ (V^{4+} in T_d)	4.7	1.855	1.980	152	30	51

vanadium oxide catalysts[41-44]. The ^{51}V NMR spectrum of a vanadium silicate prepared using VCl_3 as the source of vanadium (instead of $VOSO_4$) is shown in Fig.3.11 b. The main signal is around -513 ppm, with a line width of about 60 ppm. Monomeric orthovanadates such as Na_3VO_4 and $Mg_3(VO_4)_2$ contain isolated tetrahedrally coordinated vanadium ions in a nearly symmetrical environment and show characteristic ^{51}V NMR spectrum of narrow symmetrical lines centered around -550 ppm[45,46]. The wide line ^{51}V NMR spectrum of V_2O_5, which has a square pyramidal geometry around V is, on other hand, dominated by a central line around -300 ppm[42,45]. The absence of an absorption band around -300 ppm shows that no V_2O_5-like phase is present in our samples.

Rigutto *et al.*[22] have reported a main signal at -500 ppm for their samples (with MFI structure) prepared using vanadyl sulfate. For vanadium silicates (MFI) prepared using VCl_3 as the vanadium source, Centi *et al.*[24], on the other hand, reported a symmetrical spectrum with a line centered at - 480 ppm and ascribed the line shape to the presence of V^{5+} sites in a nearly symmetrical tetrahedral environment. The considerable shift in the line position from that normally observed for orthovanadates (-520 to -590 ppm) was attributed by them to the presence of a slightly shorter V-O bond length. For a ZSM-5 (Si/Al = 30) sample treated with VCl_3 at 600°C for 48 h., Fejes *et al.* observed the ^{51}V NMR signal at -512 ppm[47]. In the same study, vanadium silicate prepared using $VO(COO)_2$ in the synthesis mixture exhibited two signals at - 567 ppm (10 %) and - 575 ppm (90%), respectively They concluded that at least two different V^{5+} species both in the framework positions of MFI are present in their samples. These results clearly show the difference in the environment of the vanadium in samples synthesized using different vanadium sources and synthesis procedures. The single signal for ^{51}V observed in our studies (Fig.3.11) indicates that vanadium ions are located in a single structural environment. The value of the chemical shift (-573 ppm) and linewidth (50 ppm) in the sample prepared using vanadyl sulfate as the raw material suggests that the vanadium ions in these samples are located in framework positions with, perhaps, distorted tetrahedral symmetry. More detailed studies using samples prepared under well defined conditions are needed for a definitive assignment of NMR signals of ^{51}V in vanadium silicates.

3.3.5 UV-VIS SPECTROSCOPY

The optical absorption spectra of VS-2 samples are presented in Fig.3.12. The bands below 400 nm arise from O --> V charge transfer transitions. No significant absorption was

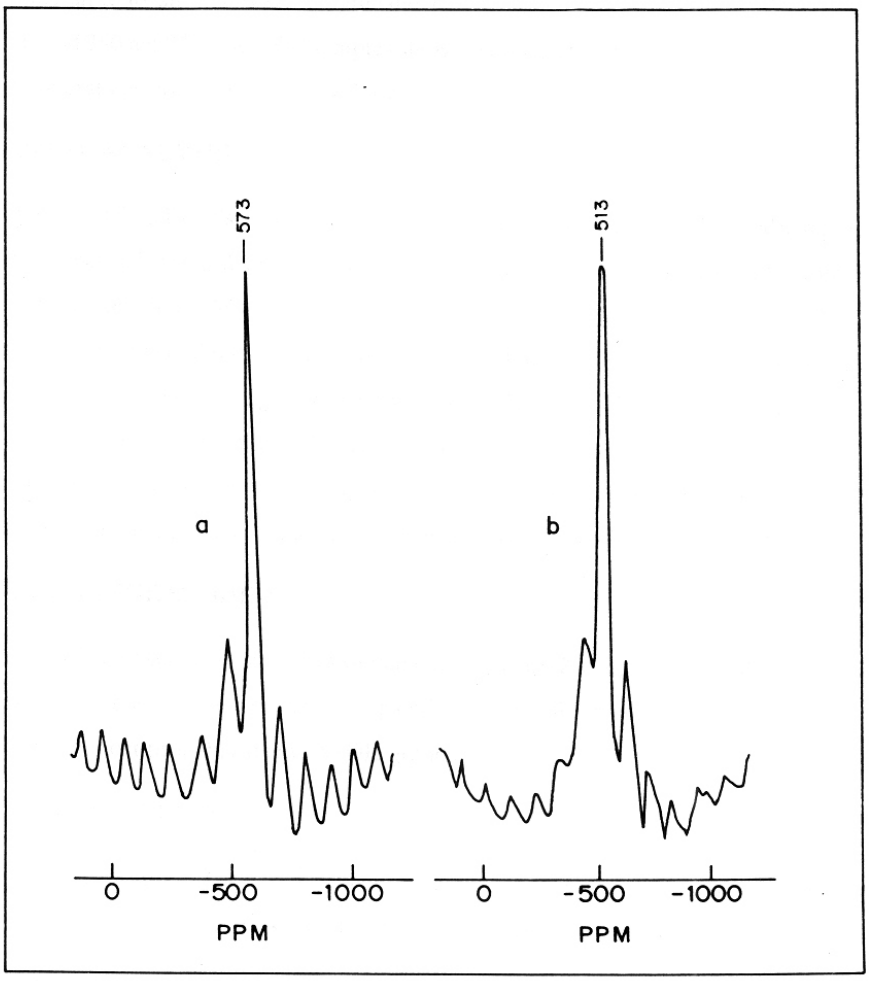

Fig.3.11. ^{51}V MAS-NMR spectra of VS-2 samples prepared using $VOSO_4$ (Si/V = 79, spectrum a) and VCl_3 (Si/V = 68, spectrum b) as source of vanadium.

observed in the 400 - 800 nm region (consistent with the white color of the material). The absence of any absorption above 550 nm shows that no V^{4+} ions in tetrahedral coordination are present[19,48]. The electron charge transfer energy is strongly influenced by the number of ligands on the central ion and gives information on the coordination of the vanadium in the clusters[48,49]. It has been reported that when the number of the ligands on vanadium decreases from 6 to 4, the absorptions shift to shorter wave length and that tetrahedrally coordinated V^{5+} shows absorption around 350 nm[48,49]. The VS-2 samples show absorption at 310 nm which may indicate distorted tetrahedral environment around V^{5+} ion.

3.3.6 THERMAL ANALYSIS

Simultaneous TG-DTA of samples show that the calcination of the as-synthesized samples in air occurs exothermally (Fig.2.16). The decomposition around 623-633 K, coincides with a weight loss due to template decomposition. There are shoulders around 548 and 723 K, respectively, on either side of the sharp exotherms. The template removal and weight loss occurs endothermally in the presence of argon (Fig.3.13) between 523 and 773 K. The well-resolved exotherms in the presence of air and endotherms in the presence of argon point to diffusional hindrances for the template removal. In argon, a first weight loss occurs between 373 K and 523 K, which corresponds to water removal and is accompanied by a broad DTA endotherm.

3.3.7 ION-EXCHANGE STUDIES

The cation (Na^+) exchange capacities of vanadium silicate-2 samples with different Si/V ratios are given in Table 3.1. Ion exchange capacities indicate the presence of exchangeable protons. These are most probably due to V-OH groups.

3.3.8 ADSORPTION STUDIES

The sorption capacities of water, n-hexane, cyclohexane (at $p/p_o = 0.5$ and $T = 298$ K) on vanadium silicates with different Si/V ratios and silicalite-2 are given in the Table 3.1.

The values in Table 3.1 are comparable to those reported for silicalite-2 and metallosilicate analogs with MEL structure[32]. The adsorption capacities for n-hexane and cyclohexane do not vary with of Si/V ratio. However the sorption capacities of water decrease with increase in Si/V ratio. Sorption capacity of water is indicative of the relative hydrophobicity/ hydrophilicity of the molecular sieves and is dependent on Si/V ratios. The equilibrium sorption capacities for the larger molecules of cyclohexane are lower than for the linear n-hexane.

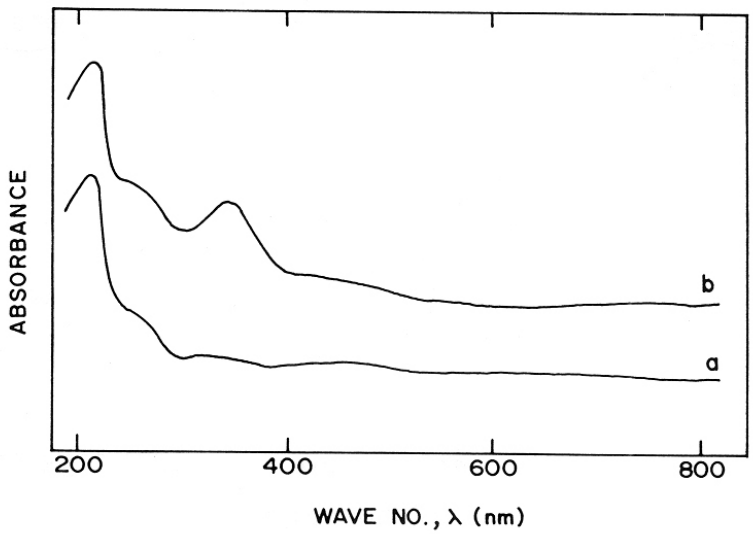

Fig.3.12. Diffuse reflectance UV-VIS spectra of VS-2 samples. Curve 'a' Si/V = 41 and Curve 'b' Si/V = 161

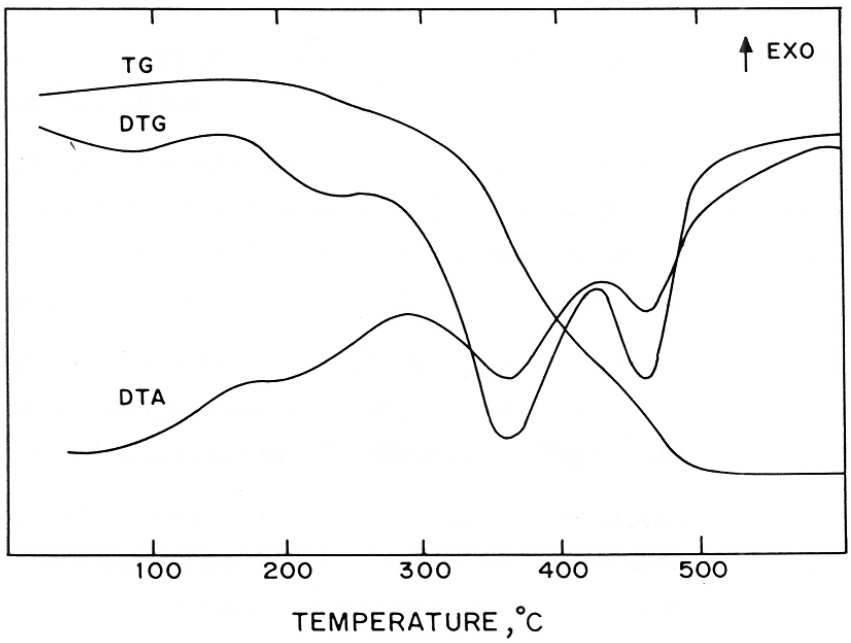

Fig.3.13. Simultaneous TG-DTA of as-synthesized sample with Si/V = 79 in argon

3.3.9 SURFACE AREA MEASUREMENTS

The low pressure ($p/p_o = 0.001$) nitrogen adsorption isotherm at liquid nitrogen temperature is typical of microporous material. The apparent surface area of the vanadium silicates with different Si/V ratios are given in Table 3.1. In VS-2 samples, a high surface area of the order 500 - 550 m^2/g and a t area (due to mesoporous impurities) of only 20 - 40 m^2/g, indicate that the content of amorphous phase in the samples is very small.

3.4 CONCLUSIONS

The results bearing on the structural identity of the vanadium in the VS-2 samples may be summarized as follows :

1. There is a linear and progressive increase in unit cell parameters (from X-ray diffraction) of the MEL lattice with increase in vanadium content. On hydrothermal treatment the unit cell parameters decrease to values characteristic of vanadium-free silicalite-2, presumably due to exit of vanadium from MEL framework positions.

2. The intensity of the framework IR adsorption band around 965 cm^{-1} (probably due to Si-O-V linkages) also increases linearly with the vanadium content and the crystalline unit cell volume of the vanadium silicate material (Fig.3.3 and 3.4).

3. There is a correlation between the vanadium content and the concentration of H-bonded hydroxyl groups (Fig.3.5). It is possible that a) the presence of V ions during the hydrothermal synthesis enhances the concentration of such hydroxyl groups and that b) the hydroxyl groups once formed bind the vanadium ions in a coordinative manner to generate VS-2. This observation supports the model for vanadium silicate proposed earlier[22,24,29].

4. There are weak Brönsted and Lewis acid sites on VS-2 as may be seen from the spectra of adsorbed ammonia and pyridine at various temperatures (Fig.3.6 - 3.8). They originate from the modification induced by vanadium in the silicalite structure.

5. The ^{51}V NMR spectra of VS-2 reveal that the nature of the vanadium species depends strongly on the source of vanadium used in the synthesis. Samples prepared from $VOSO_4$ contain only one vanadium species with a chemical shift parameter of -573 ppm and

signal linewidth of 50 ppm, similar to those observed in monomeric orthovanadates and contain isolated vanadium ions in distorted tetrahedral coordination. Clusters of vanadium as well as V_2O_5-like phases are absent.

6. ESR experiments indicate that in the as-synthesized samples, the vanadium occurs as atomically dispersed V^{4+} ions. On calcination in air the spectra disappear indicating the complete oxidation of V^{4+} to V^{5+} species. Reduction in H_2 restored the original spectra. The vanadium ions are, hence, accessible to gas molecules and the V^{4+} <--> V^{5+} transition is reversible. The complete oxidation of V^{4+} to V^{5+} upon calcination indicates the absence of any clustered vanadium.

7. The observed 'g' values and hyperfine coupling constants ($g_{\parallel}$ = 1.932; $g_{\perp}$ = 1.981; $A_{\parallel}$= 185 G and $A_{\perp}$= 72 G) are notably different from those observed for VO^{2+} exchanged into ZSM-5 and are assigned to V^{4+} in framework positions. A linear increase in the integrated intensities of ESR signals and the unit cell volume of the samples with vanadium content (Fig.3.10) suggest that the atomically dispersed vanadium ions observed by ESR spectroscopy are located in the MEL lattice framework positions.

8. Adsorption experiments indicate that the pore volume is free of occluded oxides of vanadium.

9. Vanadium silicate samples have exchangeable protons, as indicated by Na^+ ion exchange capacity and adsorption of probe molecules.

A possible structure and environment of the vanadium in VS-2 consistent with our results and those of others[22-24] (for other systems like VS-1 and VAPO-5[20]) may be envisaged as shown in Fig.3.14. The proton of the OH group attached to the vanadium can be exchanged for Na^+ ions (as indeed observed).

The vanadium ions are probably coordinated at defect sites wherein the concentration of SiOH groups is likely to be high. This tentative model is consistent with several of the above observations. During the preparation of pure silicalite, only some silanol groups are present on the external surface due to defects or crystal faults. It is quite possible that specific defects are created by the presence of vanadium during hydrothermal synthesis and that these are associated

with the stabilization of vanadium in the silicalite structure. The linear increase in the integrated intensity of the IR band (3550 cm^{-1}) with the vanadium content of the sample supports this hypothesis.

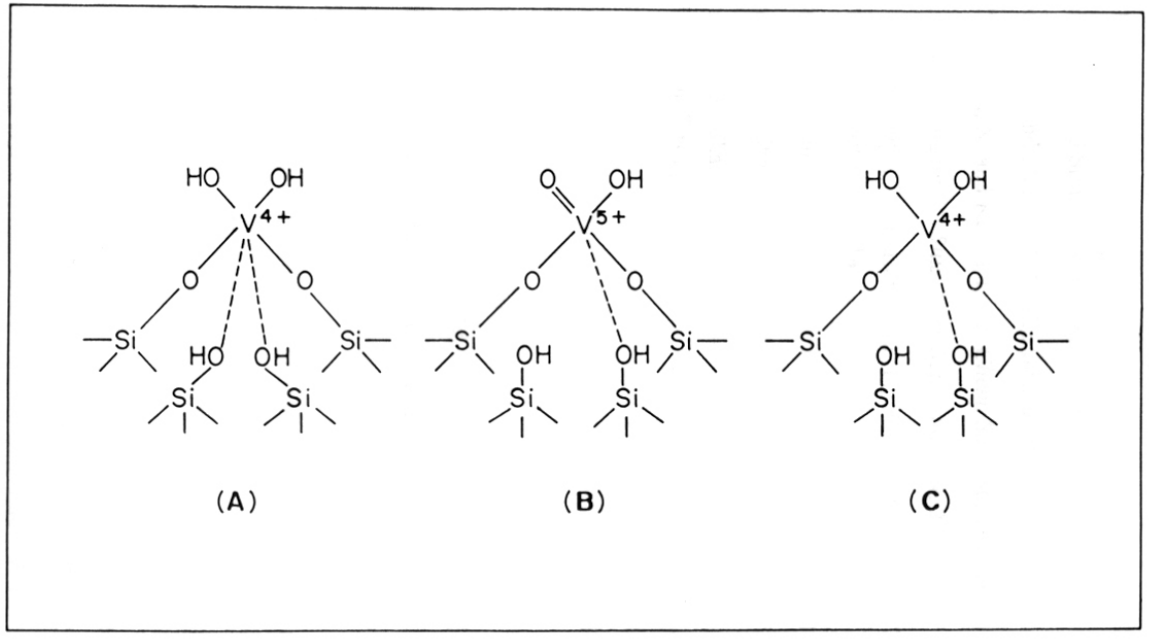

Fig.3.14. Possible environment of vanadium in VS-2, in as-synthesized (A), calcined (B) and calcined and reduced (C) forms.

3.5 REFERENCES

1. Marosi, L., Stabenow, J., Schwarzamann, M., Ger. pat. 2831631 1978, (abstr. **93**, 10354 (1980)).
2. Kucherov, A.V. and Slinkin, A.A., *Zeolites*, **6**, 175 (1986).
3. Kucherov, A.V. and Slinkin, A.A., *Zeolites*, **7**, 38; 43; 583 (1987).
4. Sass, C.E., Chen, X. and Kevan, L., *J. Chem. Soc.*, **86**, 189 (1990).
5. Ruren, X. and Wenguin, P., *Stud. Surf. Sci. Catal.*, **24**, 27 (1985).
6. Inui, T., Medhanavyn, D., Praserthdam, P., Fukuda, K., Ukawa, T., Sakamoto, A. and Miyamoto, A., *Appl. Catal.*, **18**, 311 (1985).
7. Miyamoto, A. Medhanavyn, D. and Inui, T., *Appl. Catal.*, **28**, 89 (1986).
8. Miyamoto, A. Medhanavyn, D. and Inui, T., *Chem. Express*, **1**, 559 (1986).
9. Miyamoto, A. Medhanavyn, D. and Inui, T., *Proc. 9th Intern. Congr. Catal.*, (M.J. Philip and M. Ternan, Eds.) pub. Chem. Inst. of Canada, Ontario, vol. **1**, p. 437 (1988).
10. Cavani, F., Trifiro, F., Habersberger, K. and Tvaruzkova, Z., *Zeolites*, **8**, 12 (1988).
11. Zatorski, L.W., Centi, G., Nieto, J.L., Trifiro, F., Bellussi, G. and Fattore, V., *Stud. Surf. Sci. Catal.*, **49 B**, 1243 (1989).
12. Trifiro, F. and Jiru, P., *Catal. Today*, **3**, 519 (1988).
13. Centi, G., Jiru, P. and Trifiro, F., *Stud. Surf. Sci. Catal.*, **44**, 247 (1988).
14. Tvaruzkova, Z., Centi, G., Jiru, P. and Trifiro, F., *Appl. Catal.*, **19**, 307 (1985).
15. Habersberger, K., Jiru, P., Tvaruzkova, Z., Centi, G., and Trifiro, F., *React. Kinet. Catal. Lett.*, **39**, 95 (1989).
16. Flanigen, E.M., Lok, B.M., Patton,R.L.and Wilson, S.T. Eur.Pat., 0158976 (1985).
17. Pyke, D.R., Whitney, P. and Houghton, H., *Appl. Catal.*, **18**, 173 (1985).
18. Miyamoto, A. Iwamoto, I., Matsuda, H.and Inui, T., *Stud. Surf. Sci. Catal.*, **49B**, 1233 (1989).
19. Jhung, S.H., Sun Uh, Y. and Chon, H., *Appl. Catal.*, **62**, 61 (1990).
20. Montes, C., Davis , M.E., Murray, B. and Narayana, M., *J. Phys. Chem.* **94**, 6431 (1990).
21. Kornatowski, J., Sychev, M., Goncharuk, V. and Baur, W.H., *Stud. Surf. Sci. Catal.*, **65**, 581 (1991).
22. Rigutto, M.S. and Van Bekkum, H., *Appl. Catal.*, **68**, L1 (1991).
23. Fejes, P., Marsi, I., Kiricsi, I., Halasz, J., Hannus, I., Rockenbauer, A., Tasi, G., Korecz, L. and Schobel, G., *Stud. Surf. Sci. Catal.*, **69**, 173 (1991).
24. Centi, G., Perathoner. S., Trifiro. F., Aboukais. A., Aissi. C.F. and Guelton. M., *J. Phys. Chem.*, **96**, 2617 (1992).

25. Whittington, B.I. and and Anderson, J.R., *J. Phys. Chem.*, **95**, 3306 (1991).

26. Petras, M. and Wichterlova, B., *J. Phys. Chem.*, **96**, 1805 (1992).

27. Fyfe C.A., Gies, H., Kokotailo, G.T., Pasztor, C., Strobl, H. and Cox, D.E., *J. Amer. Chem. Soc.*, **111**, 2470 (1989).

28. Jacobs, P.A. and Martens, J.A., *Stud. Surf. Sci. Catal.*, **33**, 177 (1987).

29. Hari Prasad Rao, P.R., Ramaswamy, A. V. and Ratnasamy, P. *J. Catal.*, **137**, 225 (1992).

30. Hari Prasad Rao, P.R., Ramaswamy, A. V., Kumar, R. and Ratnasamy, P. *Zeolites*, (Communicated).

31. Perego, G., Bellussi, G., Corno, C., Taramasso, M., Buonomo, F. and Esposito A., *Stud. Surf. Sci. Catal.*, **28**, 129 (1986).

32. Reddy, J.S. and Kumar, R. *J. Catal.*, **130**, 440 (1991).

33. Notari, B. *Stud. Surf. Sci. Catal.*, **37**, 413 (1987).

34. Bellussi, G. and Fattor, V., *Stud. Surf. Sci. Catal.*, **69**, 79 (1991).

35. Thangaraj, A., Kumar, R., Mirajkar, S.P. and Ratnasamy, P., *J. Catal.*, **130**, 1 (1991).

36. Woolery, G.L., Alemany, L.B., Dessau, R.M. and Chester, A.M., *Zeolites*, **6**, 14 (1986)

37. Kung, M.C. and Kung, H.H., *Catal. Rev. Sci. Eng.*, **27**, 425 (1985).

38. Tsyganenko, A.A. Pozdnyakov, D.V. and Filimonov, V.N., *J. Mol. Struct.*, **29**, 299 (1975).

39. Jobson, E., Baiker, A. and Wokaum, A., *J. Chem. Soc. Faraday*, **86**, 1131 (1990).

40. Knozinger, H., *Adv. Catal.*, **25**, 184 (1976).

41. Le Costoumer, L.R., Taouk, B., Le Meur, M., Payen, E., Guelton, M. and Grimblot, J., *J. Phys. Chem.*, **92**, 1230 (1988).

42. Taouk, B., Guelton, M. Grimblot, J. and Bonnelle, J.P., *J. Phys. Chem.*, **92**, 6700 (1988).

43. Eckert, H. and Wachs I.E., *J. Phys. Chem.*, **93**, 6796 (1989).

44. Sobalik, Z., Markvart, M., Stopka, P., Lapina, O.B. and Mastikhin, V.M., *J. Mol. Catal.*, **71**, 69 (1992).

44a. Chary, K.V.R., Venkat Rao V. and Mastikhin, *J. Chem. Soc. Chem. Commun.*, 202 (1989).

45. Centi, G., Lena, V., Trifiro, F. Ghoussoub, D., Aissi C.F., Guelton, M. and Bonnelle, J.P., *J.Chem. Soc. Faraday Trans.*, **86**, 2775 (1990).

46. Lapina, O.B., Simakov, A.V., Mastinkhin, V.M. Veniaminov, S.A. and Shibin, A.A., *J. Mol. Catal.*, **50**, 55 (1989).

47. Fejes, P. and Nagy, J.B., to be published.

48. Lischke, G., Hanke, W., Jerschkewitz, H.G. and Ohlmann, *J. Catal.*, **91**, 54 (1985).

49. Hanke, W., Bienert, R. and Jerschkewitz, H.G., *Z. Anorg. Allg. Chem.*, **414**, 109 (1975).

50. Grejorio, S.D., Greenblatt, M., Pifer, J.H. and Sturge, M.D., *J. Chem. Phys.*, **76** 2931 (1982).

51. Fritsch, E., Babonneau, F., Sanchez, C.and Calas, G., *J. Non Cryst. Sol.*, **92**, 282 (1987).

CHAPTER 4

CATALYTIC OXIDATION REACTIONS

4.1 INTRODUCTION

The presence of transition metal sites in a molecular sieve has potential for generating oxidation catalysts with shape selective properties. Unlike the conventional aluminosilicate zeolites, the titanium analogs, TS-1 and TS-2 (with MFI[1-3] and MEL[4] structures, respectively) are effective in oxidation reactions such as hydroxylation of aromatics[5-7], oxidation of alkanes[8,9], ammoximation of cyclohexanone[10,11], selective oxidation of alcohols[5,6], epoxidation of olefins[6,12] with aqueous hydrogen peroxide as oxidant and oxidative dehydrogenation of ethanol to acetaldehyde in presence of molecular oxygen[13]. The first commercial process using titanium silicate (TS-1) as catalyst was the hydroxylation of phenol to hydroquinone and catechol introduced by Enichem, Italy. Vanadium incorporated molecular sieves are also expected to have interesting properties in various oxidation reactions particularly, since V^{5+} <---> V^{4+} transition is possible for the lattice vanadium. They are found to catalyze various oxidation reactions in presence of aqueous hydrogen peroxide[14-17].

Vanadium containing molecular sieves are reported to be active in the conversion of methanol to hydrocarbons[18,19], reduction of nitrogen oxides and ammoxidation of xylenes[20-23], oxidation of butadiene to furan[24-26], ammoxidation of propane to acrylonitrile[27], oxidative dehydrogenation of propane to propylene[28] and aqueous ethanol to acetaldehyde in the presence of molecular oxygen[29].

This Chapter presents the studies carried out on the catalytic properties of vanadium silicates in the following reactions:

1. Oxyfunctionalization of alkanes
2. Hydroxylation of benzene and phenol
3. Oxidation of alkyl aromatics
4. Oxidation of aniline and
5. Oxidation of sulfides

4.2 EXPERIMENTAL

4.2.1 PREPARATION OF CATALYSTS

Details of the synthesis of vanadium silicates of different Si/V ratios and their characterization were presented in Chapters II and III. The calcined vanadium silicate samples were treated with 1N ammonium acetate and recalcined at 753 K in air for 6 h before use in catalytic

reactions. For comparison, vanadium impregnated silicalite-2, silicalite-2, ZSM-11 and titanium silicates (TS-1 and TS-2), have also been investigated in the oxidation reactions. They were prepared following the procedures reported in the literature[4,7,30-32]. Vanadyl sulfate was used to prepare vanadium impregnated silicalite-2 samples.

4.2.2 CATALYTIC REACTIONS

4.2.2.1 Alkane oxidation

The oxidation of alkanes was carried out in a stirred autoclave (Parr Instrument, USA) of 300 ml capacity at 373 K under autogenous pressure. Typically, 0.1 g of the catalyst, 2.53 g of 26 % (by wt.) aqueous H_2O_2 (alkane/H_2O_2 = 3 moles) and 5 g of alkane were mixed in 25 ml of acetonitrile (solvent) and the reaction was carried out for 8 h. After the completion of the reaction, 25 ml of acetone was added to the products, which were then separated from the catalyst by filtration and analyzed by GC (HP 5880) using a capillary (crosslinked methylsilicone gum) column and flame ionization detector. The identity of the products was confirmed by GC mass spectroscopy (Shimadzu GCMS-QP 2000A) using standard compounds.

Oxidation of cyclohexane was carried out in a similar way except that the amount of catalyst used was 0.5 g.

4.2.2.1 Oxidation of aromatics, substituted aromatics and sulfides

The oxidation of benzene, phenol, toluene, and aniline as well as the oxidation of sulfides were carried out in batch reactors. In a typical reaction, 100mg of catalyst was dispersed in a solution containing 1 g of reactant and 10 g of solvent. The mixture was vigorously stirred and H_2O_2 was then added. After completion of the reaction, the products were separated from the catalyst and analyzed by GC (HP 5880) using a capillary (crosslinked methylsilicone gum) column and flame ionization detector (FID).

4.3 RESULTS AND DISCUSSION

4.3.1 OXYFUNCTIONALIZATION OF ALKANES

The introduction of oxygen containing functional groups in alkanes proceeds with low selectivities over most homogeneous and heterogeneous catalysts. The catalysts used in alkene oxidation are ineffective for alkanes[33,34]. Many transition metal complexes, on the other hand, are very effective in C-C bond cleavage leading to complete oxidation to respective acids[34].

Oxyfunctionalization with high selectivities was reported on natural and synthetic metallo-porphyrin systems[35,36] and on vanadium (V) oxo peroxo complexes[38]. The use of zeolites and molecular sieve-based catalysts in the oxidation reactions has been reported in recent times. Titanium silicates exhibiting a pentasil structure (both TS-1 and TS-2) have been found to catalyze the oxidation of a variety of organic substrates with an aqueous solution of H_2O_2[14] and are selective in the oxidation of alkanes[8,9].

Vanadium silicate molecular sieves can oxidize unactivated alkanes under mild conditions with aqueous hydrogen peroxide. Unlike titanium silicates, vanadium analogs are able to oxidize also the primary carbon atoms of alkanes as well to corresponding primary alcohols and aldehydes[16,17].

A. Activity of different catalysts

A comparison of the activity of VS-2, silicalite-2, Al-ZSM-11, vanadium-impregnated silicalite-2 and titanium silicate (TS-2) (all crystalline samples with MEL structure) in the oxidation of *n*-hexane is given in Table 1. The major products of the reaction are 2- and 3-hexanols and hexanones. In addition, 1-hexanol and 1-hexanal were also detected on VS-2. Small quantities of other products with more than one functional group (*e.g.* dihydroxyalkanes) and lactones were also detected but were not analyzed in detail. The results show that the most active catalysts are TS-2 and VS-2 (*n*-hexane conversions 15.9 and 14.6 mole % respectively), which are also the most selective for the formation of monofunctional compounds. On all the other samples (not containing V or Ti in framework positions), including the vanadium impregnated silicalite-2 sample, both the activity and the selectivity are very low (hexane conversions 2.8 - 3.6 mole %). Between TS-2 and VS-2, the oxyfunctionalization of the primary carbon atoms leading to the formation of primary alcohols and aldehydes is observed only with the vanadium silicate. It has also been observed that in addition to VS-2, other vanadium silicates such as VS-1 (with MFI structure) and V-NCL-1 (the vanadium silicate analogue of NCL-1, a novel large pore molecular sieve[17]) also exhibit this unique catalytic property of oxyfunctionalizing the primary carbon atom in alkanes and in the side chain alkyl groups of aromatics. Toluene, for example, yields benzyl alcohol and benzaldehyde in addition to cresols[14,16].

An examination of the product distribution shows that the activation of the carbon atom at the second position is preferred to others and the activation follows the order, 2 > 3 > 1 on vanadium silicates. Investigation of the oxidation kinetics revealed that the ratio of (aldehyde

Table 1

Oxidation of n-hexane on different molecular sieve catalysts[a]

Catalyst[b]	conversion (mole %)	H_2O_2 selectivity[c]	Product distribution (mole %)[d]							Product selectivity[f]
			1-ol	2-ol	3-ol	1-al	2-one	3-one	Others[e]	
VS-2	14.6	57.1	3.7	9.2	8.2	7.2	26.3	25.0.	21.4	79.5
S-2	3.6	4.4	-	9.5	9.5	-	4.7	7.1	69.2	30.8
ZSM-11	2.8	5.2	-	3.8	4.7	-	14.4	13.9	63.2	36.8
V-imp-S-2	3.5	3.6	-	8.0	12.0	-	4.0	4.0	72.0	28.0
TS-2	15.9	58.6	-	19.1	17.6	-	23.7	23.0	16.6	83.4

[a] Reaction conditions: catalyst (g) = 0.1; n-hexane (g) = 5; temperature (K) = 373; n-hexane/H_2O_2 (mole ratio) = 3; solvent = acetonitrile; reaction duration = 8 h.

[b] VS-2: Si/V = 79; S-2: Si/Al = >2000; ZSM-11: Si/Al = 82; V-imp S-2 : Si/V = 80; TS-2: Si/Ti = 77.

[c] H_2O_2 utilized for monofunctional product formation.

[d] 1-ol = 1-hexanol; 2-ol and 3-ol = 2 and 3 hexanol; 1-al = hexanaldehyde; 2-one and 3-one = 2 and 3 hexanone.

[e] Oxygenates with more than one functional group and lactones, methyl cyclopentane and unidentified oligomeric material

[f] (alcohols, aldehyde and ketones/alkane reacted)X 100, mole/mole

+ ketones) to alcohol increased with time as shown in Fig.4.1. This suggests that the aldehydes and ketones are secondary products from the corresponding primary and secondary alcohols. After 8 h, the product distribution levelled off. A higher (aldehyde + ketone) to alcohol ratio in the product distribution in the case of VS-2 compared to TS-2 (2.77 and 1.27, respectively, Table 1) indicates a greater oxidation ability of the vanadium silicates compared to titanium silicates in the secondary oxidation reaction.

B. Oxidation of *n*-heptane, *n*-octane and cyclohexane.

In addition to *n*-hexane, the oxidation of *n*-heptane, *n*-octane and cyclohexane has been studied on a VS-2 sample, with Si/V = 79 at 373 K (Table 2). The results are similar to those observed in the case of *n*-hexane. The oxyfunctionalization of the secondary carbon atom is preferred eventhough significant quantities of primary alcohols and aldehydes are formed with both C_7 and C_8 substrates. The product distribution is in the order, 2C > 3C > 4C > 1C. No regio selectivity has been observed in these cases. Oxidation of cyclohexane, on the other hand, leads to cyclohexanol and cyclohexanone with very small concentration of oxygenates with more than one functional group. The product selectivity is, therefore, considerably higher than observed in the oxidation of *n*-alkanes. However, the oxidative conversions and the H_2O_2 selectivities decreased in the order *n*-C_6 > *n*-C_7 > *n*-C_8 > cyclohexane (Table 2). This order is consistent with the observed large decrease in the diffusivity of these alkanes in zeolites with increasing chain length and molecular size[37].

C. Influence of solvent

The effect of solvent on the oxidation of *n*-hexane in the presence of VS-2 (Si/V = 79) has been studied by employing other less-polar solvents than acetonitrile. In methanol and acetone, the conversions are lower *i.e.* 9.1 and 5.4 mole %, respectively (Table 3). Acetonitrile is found to be the most effective solvent with the highest selectivity to monosubstituted products. The activity and H_2O_2 selectivity seems to be related to the polarity of the solvent and decreased in the order, acetonitrile > methanol > acetone. The product distribution, however, in both methanol and acetone is similar to that in acetonitrile. A change of solvent from the non-polar acetone to mixtures of acetone and acetonitrile and then finally to the more polar acetonitrile increases both the conversion and H_2O_2 selectivity (Table 3). On titanium silicate, on the other hand, the rates are not influenced by the polarity of the solvents[9a]. Indeed, in non-polar solvents

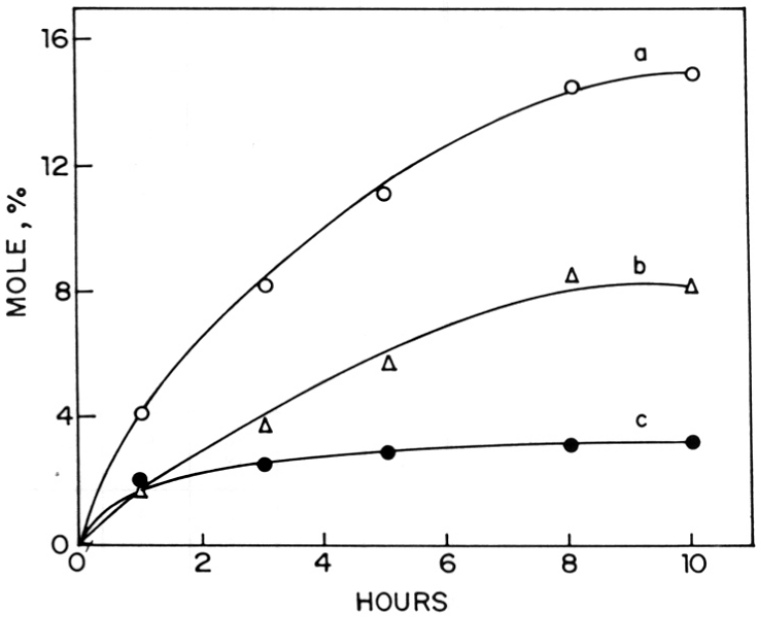

Fig.4.1. Oxidation of n-hexane over VS-2 (Si/V = 79) at 373 K in the presence of aqueous acetone. Other conditions as given in Table 4.1. Curves a to c represent, hexane conversion, ketones + aldehydes and alcohols, respectively.

Table 2

Oxidation of alkanes over vanadium silicate molecular sieves[a]

Reactant	Conversion (mole %)[b]	H_2O_2 selectivity[c]	Product distribution (mole %)[d]									Product selectivity[f]
			1-ol	2-ol	3-ol	4-ol	1-al	2-one	3-one	4-one	Others[e]	
n-Hexane	14.6	57.1	3.7	9.2	8.2	-	7.2	26.3	25.0.	-	21.4	79.5
n-Heptane	14.3	50.1	3.1	6.8	5.8	2.1	4.2	25.1	21.7	7.0	24.2	75.8
n-Octane	12.8	43.4	4.6	5.9	4.6	3.8	3.2	21.7	18.0	13.8	24.4	75.6
Cyclohexane	8.4	32.7	33.3[g]				60.7[h]				6.0	94.0

[a] Reaction conditions: catalyst (g) = 0.1 (Si/V = 79); alkane (g) = 5; temperature (K) = 373; alkane/H_2O_2 (mole ratio) = 3; solvent = acetonitrile; reaction duration = 8 h.

[b] Moles of alkane converted/total no. of moles of alkane X 100

[c] H_2O_2 utilized for monofunctional product formation.

[d] 1-ol = 1-alcohol; 2-ol = 2-alcohol; 3-ol = 3-alcohol; 4-ol = 4-alcohol; 1-al = 1-aldehyde; 2-one = 2-ketone; 3-one = 3-ketone and 4-one = 4- ketone of corresponding alkanes.

[e] Mostly oxygenates with more than one functional group and lactones

[f] (alcohols, aldehyde and ketones/alkane reacted)X 100, mole/mole

[g] Cyclohexanol and [h] Cyclohexanone.

Table 3

Influence of solvent on n-hexane oxidation over vanadium silicate molecular sieves[a]

Solvent	conversion (mole %)[b]	H_2O_2 selectivity[c]	Product distribution (mole %)[d]							Product selectivity[f]
			1-ol	2-ol	3-ol	1-al	2-one	3-one	Others[e]	
Acetonitrile	14.6	57.1	3.7	9.2	8.2	7.2	26.3	25.0.	21.4	79.5
Methanol	9.1	30.3	3.0	11.9	10.9	4.9	18.8	18.8	31.7	68.3
Acetone	5.4	18.9	1.8	9.3	9.3	1.9	22.2	24.1	31.4	68.6
Aetonitile + Acetone (1:1)	8.4	29.1	3.6	8.3	8.3	3.7	21.4	22.6	32.1	67.9
Aetonitile + Acetone (4:1)	11.8	42.6	4.2	8.5	9.3	3.4	22.9	22.9	28.8	71.2

[a] Reaction conditions: catalyst (g) = 0.1 (Si/V = 79); n-hexane(g) = 5; temperature (K) = 373; alkane/H_2O_2 (mole ratio) = 3; reaction duration = 8 h.

[b] Moles of hexane converted/total no. of moles of hexane X 100

[c] H_2O_2 utilized for monofunctional product formation.

[d] 1-ol = 1-hexanol; 2-ol and 3-ol = 2 and 3 hexanol; 1-al = hexanaldehyde; 2-one and 3-one = 2 and 3 hexanone.

[e] Mostly oxygenates with more than one functional group and lactones

[f] (alcohols, aldehyde and ketones/alkane reacted)X 100, mole/mole

such as acetone, fairly high conversions (of the order of 20 to 25 mole %) and high H_2O_2 selectivities have been reported both on TS-1 and TS-2 samples[9]. Moreover, a changeover to more polar solvents retarded the rate of oxidation on titanium silicates[9a].

D. Influence of vanadium content

The oxidation of *n*-hexane was carried out over three VS-2 samples with different vanadium contents (Si/V = 79, 122 and 161, respectively) under identical conditions. The results are given in Table 4. As expected, the conversion and selectivity of the samples increased with vanadium content. However, the increase in the activity is not linearly proportional to the vanadium content of the samples. The alcohol to (aldehyde + ketone) ratio is higher on the two low vanadium containing samples showing that the secondary oxidation from alcohol to aldehydes and ketones is slower on these samples. The higher vanadium in the sample with Si/V = 79 leads to a more extensive secondary oxidation. Interestingly, the oxyfunctionalization of the primary carbon atom is enhanced at higher vanadium content as seen from increasing concentration of (1-ol and 1-al) in the product with increasing vanadium content in the catalyst.

E. Influence of *n*-hexane to H_2O_2 ratio

While maintaining the concentration of *n*-hexane constant (0.058 moles), the concentration of hydrogen peroxide in the reaction mixture was varied during the oxidation of *n*-hexane. The results are given in Table 5. Conversion, as expected, increases with increasing H_2O_2 content. The selectivity for alcohols, ketones and aldehydes decreases marginally (80.4 to 75.7 %) due to the formation of polyoxygenated products. The H_2O_2 selectivity also decreases at higher H_2O_2 concentrations due to the formation of polyoxygenated compounds and greater loss of H_2O_2 by decomposition into $H_2O + O_2$.

F. Influence of temperature

Conversion increases with temperature. On a given VS-2 sample (Si/V = 79), the observed conversions of *n*-hexane at 353, 373 and 393 K are 9.0, 14.6 and 16.8 mole %, respectively (Table 6). Beyond 373 K, the selectivity for monoxoygenated products decreases. A marginal decrease in H_2O_2 selectivity was also observed. In the product distribution, the 2/3 ratio (2-substituted/ 3- substituted products) decreased from 1.4 to 1.0 with increase in reaction temperature.

Table 4

Influence of vanadium content on oxidation of n-hexane over vanadium silicate molecular sieves[a]

Si/V ratio	Conversion (mole %)[b]	H_2O_2 selectivity[c]	Product distribution (mole %)[d]							Product selectivity[f]
			1-ol	2-ol	3-ol	1-al	2-one	3-one	Others[e]	
79	14.6	57.1	3.7	9.2	8.2	7.2	26.3	25.0.	21.4	79.5
122	10.0	36.6	5.0	10.0	11.1	3.0	21.1	24.1	25.7	74.3
161	7.0	24.6	4.2	8.6	10.1	2.8	20.0	24.3	30.0	70.0

[a] Reaction conditions: catalyst (g) = 0.1; n-hexane (g) = 5; temperature (K) = 373; solvent = acetonitrile; reaction duration = 8 h.

[b] Moles of hexane converted/total no. of moles of hexane X 100

[c] H_2O_2 utilized for monofunctional product formation.

[d] 1-ol = 1-hexanol; 2-ol and 3-ol = 2 and 3 hexanol; 1-al = hexanaldehyde; 2-one and 3-one = 2 and 3 hexanone.

[e] Mostly oxygenates with more than one functional group and lactones

[f] (alcohols, aldehyde and ketones/alkane reacted)X 100, mole/mole

Table 5

Effect of H_2O_2 concentration on oxidation of n-hexane over vanadium silicate molecular sieves[a]

Hexane/H_2O_2 mole ratio	Conversion (mole %)[b]	H_2O_2 selectivity[c]	Product distribution (mole %)[d]							Product selectivity[f]
			1-ol	2-ol	3-ol	1-al	2-one	3-one	Others[e]	
1.5	23.0	42.2	3.4	7.5	6.2	8.4	26.7	23.0.	24.3	75.7
3.0	14.6	57.1	3.7	9.2	8.2	7.2	26.3	25.0.	21.4	79.5
4.5	10.2	61.7	5.9	9.8	10.8	4.9	25.5	23.5	19.6	80.4

[a] Reaction conditions: catalyst (g) = 0.1 (Si/V = 79); n-hexane (g) = 5; solvent = acetonitrile; reaction duration = 8 h.

[b] Moles of hexane converted/total no. of moles of hexane X 100

[c] H_2O_2 utilized for monofunctional product formation.

[d] 1-ol = 1-hexanol; 2-ol and 3-ol = 2 and 3 hexanol; 1-al = hexanaldehyde; 2-one and 3-one = 2 and 3 hexanone.

[e] Mostly oxygenates with more than one functional group and lactones

[f] (alcohols, aldehyde and ketones/alkane reacted)X 100, mole/mole

Table 6

Effect of temperature on oxidation of n-hexane over vanadium silicate molecular sieves[a]

Temperature	Conversion (mole %)[b]	H_2O_2 selectivity[c]	Product distribution (mole %)[d]							Product selectivity[f]
			1-ol	2-ol	3-ol	1-al	2-one	3-one	Others[e]	
353	9.0	35.8	2.3	8.3	7.2	2.2	32.2	22.2.	25.6	74.3
373	14.6	57.1	3.7	9.2	8.2	7.2	26.3	25.0.	21.4	79.5
393	16.8	56.4	6.0	11.3	11.3	3.5	19.0	19.1	29.7	70.3

[a] Reaction conditions: catalyst (g) = 0.1 (Si/V = 79); n-hexane (g) = 5; alkane/H_2O_2 (mole ratio) = 3; solvent = acetonitrile; reaction duration = 8 h.

[b] Moles of hexane converted/total no. of moles of hexane X 100

[c] H_2O_2 utilized for monofunctional product formation.

[d] 1-ol = 1-hexanol; 2-ol and 3-ol = 2 and 3 hexanol; 1-al = hexanaldehyde; 2-one and 3-one = 2 and 3 hexanone.

[e] Mostly oxygenates with more than one functional group and lactones

[f] (alcohols, aldehyde and ketones/alkane reacted)X 100 mole/mole

G. Mechanism of Oxidation

Vanadium(V) peroxo complexes in non-protic solvents are effective oxidants of olefins (to epoxides), aromatics (to phenols) and alkanes (to alcohols and ketones)[38]. This reactivity was attributed to a peroxo radical V^{4+}-O-O· species generated from peracid-like forms, which adds to double bonds or aromatic nuclei and abstracts hydrogen from alkanes to give a carbon radical intermediate[38]. The peroxo complexes are derived from the reaction of the V=O groups with H_2O_2 and may be represented as :

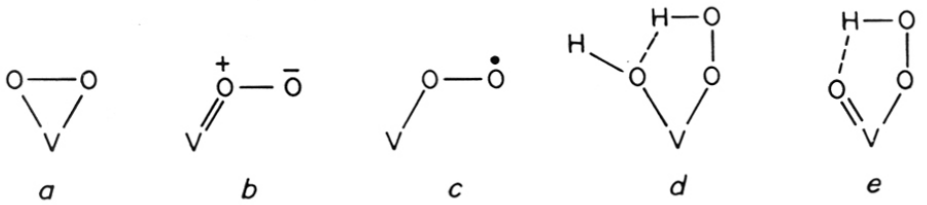

In the homogeneous medium, the oxidation is usually carried out in non-protic solvents such as CH_3CN, the reaction rate being retarded in protic solvents like CH_3OH. Protic solvents probably inhibit the formation of intramolecular hydrogen-bonds. The formation of the peroxo radical was detected (an ESR signal with g = 1.987), when VS-2 was added to a mixture of *n*-octane and H_2O_2. This signal was not observed in the absence of VS-2. The intensity of the signal increased upto 30 min and then decreased. The formation of the radical and its subsequent decay by reaction with the alkane molecules may be envisaged to proceed as given below :

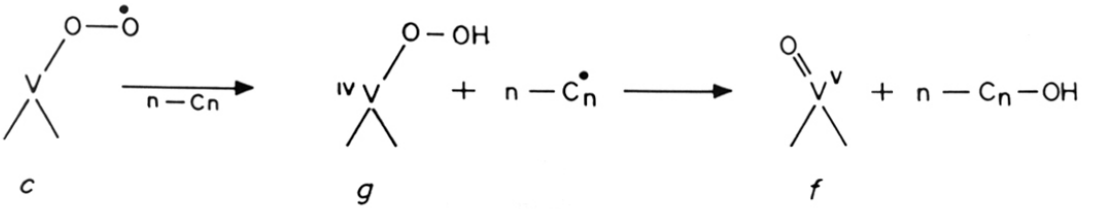

In this scheme, a hydrogen atom of the alkane is abstracted by the diradical, *c* to give an intermediate carbon radical. The latter combines with a hydroxyl radical coming from V^{4+}-O-O-H (species *f*) to give an alcohol molecule and the V^{5+}oxo complex (*g*). Peroxo species like *c* may be generated by the rearrangement of the intramolecularly hydrogen-bonded oxo-hydroperoxide species like *e*[38]. Only isolated V^{5+} species are probably involved in the formation of such peroxo moieties and hence, it is not surprising that the vanadium impregnated silicalite sample (which probably contains vanadium clusters) are inactive in this reaction.

4.3.2 OXYFUNCTIONALIZATION OF CYCLOHEXANE

Among the alkane oxidation reactions, the conversion of cyclohexane to cyclohexanol and cyclohexanone is industrially important. At present, oxidation of cyclohexane is carried out over transitional metal catalysts[39]. In a recent report, titanium silicate-2 (TS-2) was found to be selective for this reaction[40].

Table 7 illustrates the oxidation of cyclohexane using aqueous hydrogen peroxide on vanadium silicate, VS-2. In all the experiments, the major products were cyclohexanol and cyclohexanone. Small amounts of compounds with more than one functional group were also detected. Increasing temperatures also favour the formation of cyclohexanone. Increase in the content of H_2O_2 favours the formation of higher amounts of cyclohexanol with an increases in the cyclohexane conversion. Hydrogen peroxide selectivity, however, decreases.

The activity and selectivity of H_2O_2 increases with vanadium content suggesting that the vanadium ions are active centers. Conversion of cyclohexane on three catalysts with different Si/V ratios of 79, 122, 161, are 13.0, 8.6 and 7.0 mole %, respectively. Increase in the amount of catalyst also increases the cyclohexane conversion.

4.3.3 HYDROXYLATION OF BENZENE

The hydroxylation of benzene to phenol in the liquid phase using many metallic systems such as Fenton's reagent (Fe^{2+}-H_2O_2)[41], the Udenfriend system (Fe^{2+}-EDTA-ascorbic acid-O_2 or H_2O_2)[42] and Hamilton's reagent (Fe^{3+}-catechol-H_2O_2)[43] was well studied. Kinoshita *et al.*[44] reported that benzene was hydroxylated by air under ambient conditions in the presence of cuprous chloride. Orita *et al.*[45] oxidized benzene with the cuprous-chloride-dioxygen catalytic

Table 7

Oxidation of cyclohexane over vanadium silicate molecular sieves[a]

Si/V	Amount of Catalyst (g)	Moles of H_2O_2	Conversion[b] (mole, %)	H_2O_2 Selectivity[c]	Product distribution (mole %)			Product selectivity[e]
					Cyclohexanol	Cyclohexanone	Others[d]	
79	1.0	0.0198	14.0	52.2	52.9	35.7	11.4	88.6
79	0.5	0.0198	13.0	48.6	47.7	38.5	13.2	86.2
79	0.25	0.0198	8.1	32.4	46.9	43.2	8.9	90.1
79	0.1	0.0198	7.1	28.5	43.6	45.0	11.3	88.7
122	0.5	0.0198	8.6	35.1	50.0	43.0	7.0	93.0
161	0.5	0.0198	7.0	27.6	48.6	41.4	10.0	90.0
79	0.5	0.0397	19.2	36.9	40.4	43.8	15.8	84.2
79	0.5	0.0132	8.5	47.8	60.7	32.1	7.2	92.8

[a] Reaction conditions: cyclohexane (g) = 5; temperature (K) = 373; solvent = acetonitrile; reaction duration = 5 h.

[b] $$\text{Conversion} = \frac{\text{No. of moles of cyclohexane converted}}{\text{Total no. of moles of cyclohexane}} \times 100$$

[c] H_2O_2 utilized for cyclohexanol and cyclohexanone formation

[d] Mostly oxygenates with more than one functional group and lactones

[e] (cyclohexanol + cyclohexanone/cyclohexane reacted)X 100 mole/mole

system. Vapor phase hydroxylation of benzene using nitrous oxide on acidic zeolites such as ZSM-5, FeZSM-5[46,47] has been reported. A direct catalytic hydroxylation of benzene efficiently using titanium silicate (TS-1) has recently been reported[7].

Table 8 compares the activities of VS-2, Silicalite-2, V impregnated silicalite-2, V_2O_5, and TS-2 in the hydroxylation of benzene. The active catalysts for hydroxylation of benzene are vanadium and titanium silicates. Apart from phenol, the presence of secondary oxidation products such as *para* -benzoquinone was also observed in the products. No hydroxylated products were observed in this reaction on pure silicalite-2, on vanadium impregnated silicalite-2, or on vanadium pentoxide and in blank experiments. This shows that as in the case of ~~titanium~~ silicates only those vanadium ions, which are probably in the framework positions, are able to catalyze the hydroxylation of benzene. However, the selectivity of H_2O_2 on vanadium silicates is lower compared to titanium silicates. This may be due to the faster decomposition of H_2O_2 on the active vanadium centers compared to titanium ions.

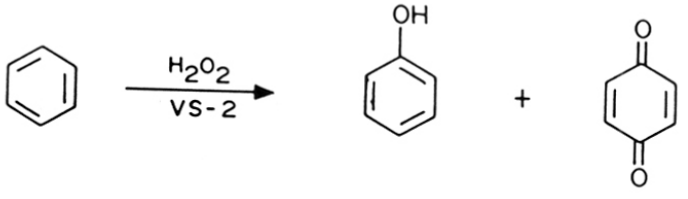

Table 9 illustrates the influence of various solvents on the catalytic activity of the vanadium silicates in the hydroxylation of benzene in presence of aqueous hydrogen peroxide. The activity of the vanadium silicates increases with increase in polarity of the solvent. The activity in the hydroxylation reaction decreases in the following order :

acetonitrile> methanol> acetone

It was reported that the hydroxylation of benzene over titanium silicate proceeds with the formation of an appreciable amount of *para*-benzoquinone as secondary oxidation product[7], while only phenol was the product on pure acidic zeolites (Al-ZSM-5 and Fe-ZSM-5) when reaction was carried out at room temperature in the absence of the solvent. In the case of

Table 8

Hydroxylation of benzene on different catalysts[a]

Catalyst[b]	Conversion[c] (mole, %)	H_2O_2 selectivity[d]	Product distribution (mole, %)		
			Phenol	PBQ[e]	Others
VS-2	7.2	18.2	90.3	6.9	2.8
S-2	0	-	-	-	-
V-imp-S-2	0	-	-	-	-
V_2O_5	-	-	-	-	-
TS-2	17.1	42.2	88.2	9.4	2.4

[a] Reaction conditions : benzene/catalyst (wt. ratio) = 10; benzene/H_2O_2 (mole ratio) = 3; temperature (K) = 333; reaction duration (h) = 8

[b] VS-2 : Si/V = 79; S-2 : Si/Al = > 2000; V-imp-S-2 (vanadium impregnated silicalite-2): Si/V = 80; TS-2 : Si/Ti = 77.

[c] $$\text{Conversion} = \frac{\text{No. of moles benzene converted}}{\text{Total no. of moles of aniline in reaction mixture}} \times 100$$

[d] H_2O_2 utilized for the formation phenol and *para*-benzeoquinone

[e] PBQ = *para*-benzoquinone

Table 9

Hydroxylation of benzene on vanadium silicate molecular sieves[a]

Solvent	Conversion	H_2O_2 selectivity	Product distribution (mole, %)		
			Phenol	PBQ	Others
Acetonitrile	7.2	18.2	90.3	6.9	2.8
Methanol	4.2	10.1	81.0	10.5	8.5
Acetone	3.6	9.3	88.9	8.3	2.8

[a] Reaction conditions : catalyst = VS-2, Si/V = 79; benzene/catalyst (wt. ratio) = 10; benzene/H_2O_2 (mole) = 3; temperature (K) = 333; reaction duration (h) = 8.

[b] $$\text{Conversion} = \frac{\text{No. of moles benzene converted}}{\text{Total no. of moles of aniline in reaction mixture}} \times 100$$

[c] H_2O_2 utilized for the formation phenol and *para*-benzeoquinone

[d] PBQ = *para*-benzoquinone

vanadium silicate molecular sieves also *p*-benzoquinone is formed during the reaction. A similar type of oxidation mechanism is probably involved, both on vanadium and titanium silicate molecular sieves.

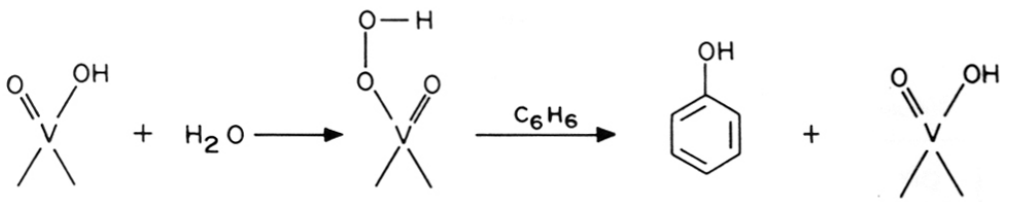

A free radical mechanism involving hydroxycyclohexadienyl radical intermediates was proposed for metal ion catalyzed hydroxylation of benzene with hydrogen peroxide[48]. Olah and Onishi[49] have suggested an ionic mechanism in the case of super acid catalyzed hydroxylation of benzene with hydrogen peroxide. The hydroxylation of benzene and phenol over TS-1 has been postulated to occur by the formation of titanium peroxo species which facilitate the direct insertion of the oxygen into the aromatic ring[6]. On vanadium silicates a similar mechanism to that on titanium silicates with the formation of vanadium peroxo species may be involved in the hydroxylation of aromatics.

4.3.4 HYDROXYLATION OF PHENOL

The direct catalytic hydroxylation of phenol is an industrially important reaction, catalyzed by strong mineral acids such as $HClO_4$. Titanium silicate molecular sieves, (TS-1 and TS-2)[6,7] are effective in catalytic hydroxylation of phenol to hydroquinone and catechol. The first commercial process utilizing titanium silicate (TS-1) as a catalyst was the hydroxylation of phenol, introduced by Enichem, Italy[2,5,6]. Several reports have since appeared on the influence of the various parameters, such as titanium content, feed ratio, influence of solvent, *etc.* on the conversion and product distribution[7,52-55]. This reaction is frequently used as a test reaction to show the presence or absence of titanium ions at framework positions[52]. The vanadium analog of ZSM-11, namely VS-2 also possesses such catalytic activity in the hydroxlation of phenol to catechol and hydroquinone[15]. It is postulated that as in the case of titanium silicate molecular sieves only those vanadium ions which are in the framework catalyze this reaction.

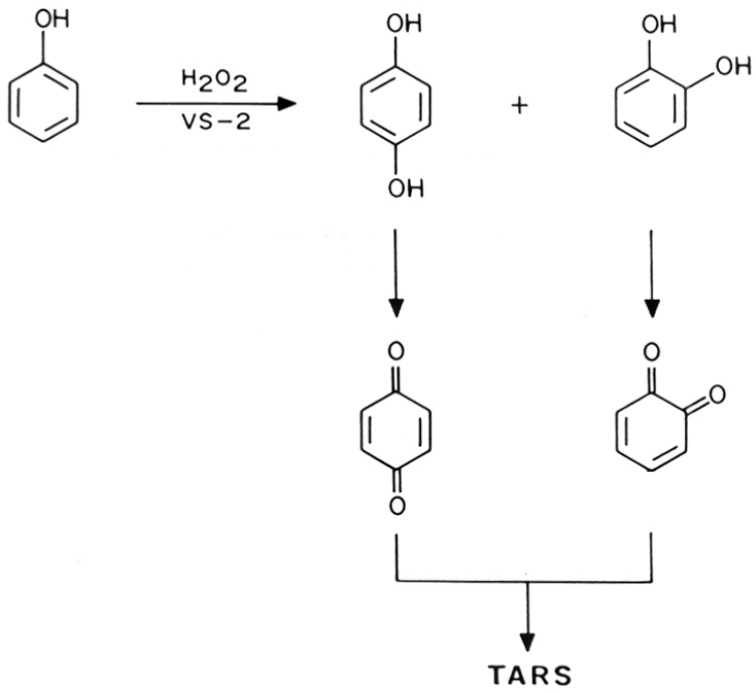

A. Influence of vanadium content

Hydroxylation of phenol did not take place in the absence of catalyst. Neither pure silicalite nor silicalite-2 impregnated with vanadium was active in the reaction. The introduction of vanadium even at a very low concentration in the silicalite lattice made the catalysts active in the hydroxylation of phenol. This is similar to the observation made on titanium silicates, where hydroxylation of phenol and benzene has frequently been used as a test reaction to characterize the presence or absence of Ti^{4+} ions in the framework positions[52]. Table 10 reports the catalytic activity of vanadium silicates (VS-2) with different Si/V mole ratios in the hydroxylation of phenol using water as solvent. Phenol conversion marginally increased upto 27.8 mole % on increasing the catalyst concentration. Large amounts of *para*-benzoquinone (PBQ) are present at a catalyst concentration of 0.01 - 0.02 g in the reaction mixture. Depending upon the concentration of the catalyst in the reaction mixture, the amount of the quinones decreased with time. For a given duration of the run (8 h) the decrease was found to be rapid, when the catalyst

Table 10

Influence of vanadium content/catalyst concentration on hydroxylation of phenol over vanadium silicates[a]

Si/V	Catalyst amount (g)	Conversion[b] (mole, %)	H_2O_2 Sel[c]. (%)	Product distribution (mole,%)[d]		
				HQ	CAT	PBQ
79	0.01	13.4	19.0	13.6	46.4	40.0
79	0.02	18.7	34.5	21.8	56.2	22.0
79	0.05	24.2	53.9	41.0	53.6	5.4
79	0.010	25.8	58.7	42.2	55.5	2.3
79	0.020	27.8	62.9	44.3	52.0	3.7
122	0.010	25.0	58.0	41.1	58.1	0.8
161	0.010	24.1	55.3	36.7	61.5	1.8

[a] Reaction conditions: catalyst = VS-2; phenol (g) = 1; solvent = water (10 ml); temperature (K) = 353; phenol/H_2O_2 (mole ratio) = 3; reaction duration (h) = 8.

[b] $$\text{Conversion} = \frac{\text{No. of moles of phenol converted}}{\text{Total no. of moles of phenol in the raction mixture}} \times 100$$

[c] $$H_2O_2 \text{ selectivity} = \frac{\text{No. of moles of } H_2O_2 \text{ consumed in the formation of dihydroxy benzenes}}{\text{Total no. of moles of } H_2O_2 \text{ added}} \times 100$$

consumption for quinones and tars excluded

[d] Break-up (in mole %) of products excluding tars. HQ = hydroquinone; CAT = catechol; PBQ = *para*-benzoquinone.

concentration was greater than 5 % in the reaction mixture *i.e.* > 0.05 g for 1 g of phenol. Irrespective of the catalyst concentration in the reaction mixture, all the H_2O_2 initially taken is transformed and no H_2O_2 was detected after completion of the reaction.

B. Influence of Solvent

The solvent used in this reaction is known to have a profound influence on the phenol conversion, H_2O_2 selectivity and the ratio of catechol to hydroquinone over both vanadium and titanium silicates[5,15,57]. The influence of various solvents on vanadium silicate-2 (VS-2) is illustrated in Table 11. Phenol conversion increases with increase in the polarity of the solvent (7.0, 13.9 and 24.3 mole % in acetone, acetonitrile and water, respectively) with a corresponding increase in the efficiency of H_2O_2 utilization. Under identical conditions, maximum phenol conversion is observed in water. Interestingly, no hydroxylation products were obtained in methanol. Even an increase in the temperature upto 353 K or a higher concentration of the catalyst in the reaction mixture did not lead to the formation of any dihydroxylated product from phenol. Similarly no oxidation products are formed from aniline when methanol is the solvent. However, vanadium silicates are active in the oxidation of alkanes, benzene and toluene even when methanol is used as solvent. This observation is in contrast to that observed with titanium analogs. In case of the latter, high H_2O_2 selectivity (of the order of 80 %) has been observed in methanol solvent[57].

The influence of the solvent on the product distribution is more complex. *Para*-benzoquinone is obtained (4 to 5 %) in all the three solvents (acetone, acetonitrile and water). Surprisingly only hydroquinone is observed when acetone was used as the solvent. The products of hydroxylation of phenol on titanium silicates, on the other hand consist almost of equimolar mixture of catechol and hydroquinone[2,56]. Tuel *et al.*[57] have recently reported enhanced yields of catechol in this reaction over TS-1, on changing the solvent from methanol to acetone.

C. Influence of phenol to H_2O_2 ratio.

The results of the influence of concentration of hydrogen peroxide on the phenol conversion and utilization of H_2O_2 are presented in Table 12. As expected, the efficiency of utilization of H_2O_2 increases at higher phenol to H_2O_2 molar ratios. A H_2O_2 selectivity of 71.5 % was observed at a ratio of phenol/H_2O_2 of 10 using water as solvent. The ratio of hydroquinone to catechol shifted marginally in favour of hydroquinone with an increase in phenol to H_2O_2 ratio.

Table 11

Influence of solvent on the hydroxylation of phenol over vanadium silicates[a]

Solvent	Conversion[b] (mole, %)	H_2O_2 Sel.[c] (%)	Product distribution (mole, %)[d]		
			HQ	CAT	PBQ
water	24.3	55.7	44.1	52.0	3.9
Acetonirile	13.9	29.7	55.4	39.8	4.8
Acetone	7.0	12.7	95.1	0.0	4.9
Methanol	0.0	0.0	-	-	-
Acetone + water (1:1)	12.5	27.8	53.6	43.9	4.5
Acetone + water (1:3)	18.8	42.1	51.4	42.6	4.0

[a] Reaction conditions: Catalyst = VS-2 (Si/V = 79); temperature (K) = 333; phenol/VS-2 (wt. ratio) = 10; phenol/H_2O_2 (mole ratio) = 3; reaction duration (h) = 8.

[b] $$\text{Conversion} = \frac{\text{No. of moles of phenol converted}}{\text{Total no. of moles of phenol in the raction mixture}} \times 100$$

[c] $$H_2O_2 \text{ selectivity} = \frac{\text{No. of moles of } H_2O_2 \text{ consumed in the formation of dihydroxy benzenes}}{\text{Total no. of moles of } H_2O_2 \text{ added}} \times 100$$

consumption for quinones and tars excluded

[d] Break-up (in mole %) of products excluding tars. HQ = hydroquinone; CAT = catechol; PBQ = *Para*-benzoquinone.

Table 12

Influence of H_2O_2 concentration on the hydroxylation of phenol over vanadium silicates[a]

Phenol/H_2O_2 (moles)	Conversion[b] (mole, %)	H_2O_2 Sel.[c] (%)	Product distribution (mole,%)[d]		
			HQ	CAT	PBQ
3	25.8	58.7	42.2	55.5	2.3
5	17.4	65.7	45.0	53.4	1.6
10	9.5	71.5	49.6	48.7	1.7

[a] Reaction conditions: catalyst = VS-2 (Si/V = 79); phenol/VS-2 (wt. ratio) = 10; temperature (K) = 353; reaction duration (h) = 8; solvent (10 ml) = water

[b] $$\text{Conversion} = \frac{\text{No. of moles of phenol converted}}{\text{Total no. of moles of phenol in the reaction mixture}} \times 100$$

[c] $$H_2O_2 \text{ selectivity} = \frac{\text{No. of moles of } H_2O_2 \text{ consumed in the formation of dihydroxy benzenes}}{\text{Total no. of moles of } H_2O_2 \text{ added}} \times 100$$

consumption for quinones and tars excluded

[d] Break-up (in mole %) of products excluding tars. HQ = hydroquinone; CAT = catechol; PBQ = *para*-benzoquinone.

D. Comparison with titanium silicates

A comparison of the activities of VS-2 and titanium silicates, TS-1 and TS-2 in hydroxylation of phenol under similar operating conditions has been made. The phenol conversion, H_2O_2 selectivity and product distribution as a function of time on VS-2, TS-2 and TS-1 are presented in Fig.4.2. A, B and C respectively. The reactions were carried out using water as solvent at 353 K and phenol to H_2O_2 mole ratio of 3.0. 100 mg of each of three catalyst having almost similar Si/M ratios was used in the batch reaction. At the end of a 8 h run, the phenol conversions are 25.8, 26.7 and 30.1 mole % with H_2O_2 selectivities of 58.7 62.3 and 72.2 % for VS-2, TS-2, and TS-1 respectively. A fairly large difference observed in phenol conversions on VS-2 on the one hand and the titanium silicates on the other, in solvent acetone is not discernible when the reactions were carried out in protic solvent such as water. Fig.4.2 shows that the initial activity of VS-2 is much lower compared to those of TS-1 and TS-2. The rates follow the order, TS-1> TS-2> VS-2. The difference in the product distributions at the end of the run on three catalysts is seen from the catechol to hydroquinone ratios, which are 1.3, 1.1 and 0.9 for VS-2, TS-2 and TS-1, respectively.

4.3.5 OXIDATION OF ALKYL AROMATICS

The common reaction of aromatic derivatives with H_2O_2 in the liquid phase in presence of metals[33], super acid catalysts[49], or pyridinium polyhydrogen fluoride[58] catalyst is the hydroxylation of the aromatic ring. Insertion of oxygen atom in the alkyl group was achieved either by autoxidation in the presence of metal catalyst, typically in a polar solvent[59], or by application of stoichiometric oxidants (*e.g.* cerium sulfate[60], cerium ammonium nitrate[61]) or peroxy sulfate[62]. Oxidation of side chain alkyl group was also reported using H_2O_2-manganese phoryrin-imidazole system and Ru(III) complex[63].

Oxidation of toluene to benzaldehyde was well studied both in liquid phase using hydrogen peroxide and in vapor phase oxidation using air as oxidant. Oxidation of toluene to benzaldehyde was reported on (acetylacetonato) oxovanadium catalyst with H_2O_2 in CF_3COOH[64]. Ru(III) complex[65] also catalyzed this reaction. Titanium silicates both TS-1 and TS-2 catalyze hydroxylation of toluene to cresols and are inactive in the oxidation of the alkyl substituent. Vanadium silicates are active in both the hydroxylation of the aromatic nucleus and the oxidation of the alkyl substituent.

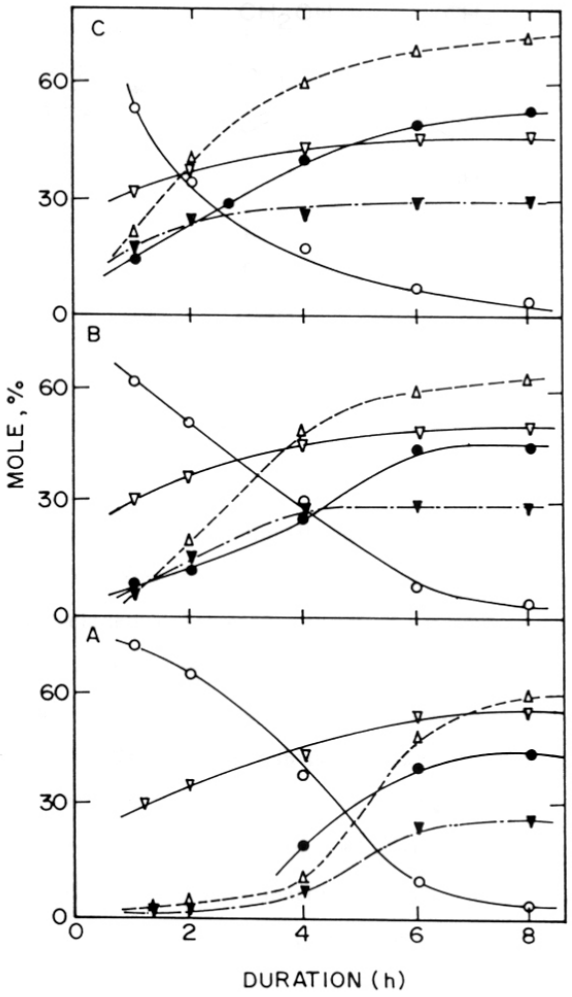

Fig.4.2. Comparison of hydroxylation of phenol over VS-2 (A), TS-2 (B) and TS-1 (C) catalysts. Solvent = water, temperature (K) = 353, phenol/H_2O_2 (mole ratio) = 3. (▼) : phenol conversion, (▲) : H_2O_2 selectivity, (○) : *para* benzoquinone, (▽) : catechol, (●) : hydroquinone.

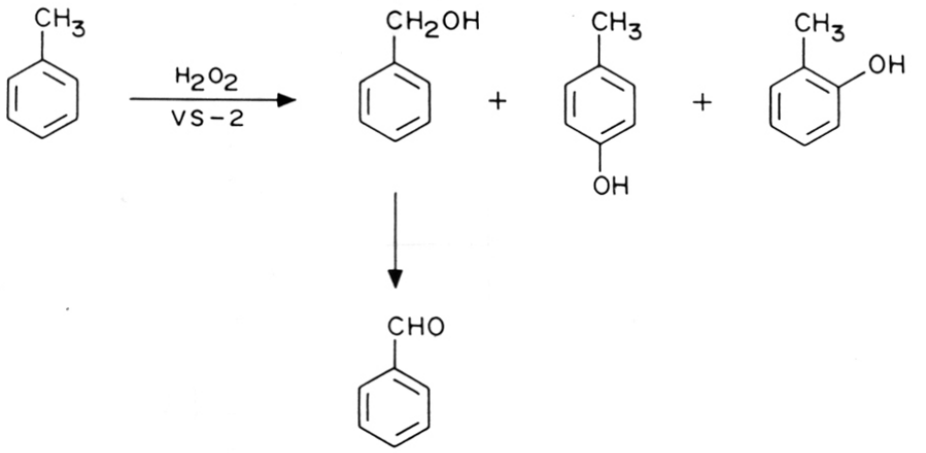

The oxidation of toluene over vanadium silicate samples is illustrated in Table 13. For comparison the activities of V-free silicalite-2, vanadium impregnated silicalite and titanium silicate (TS-2) are also included in Table 13. The products of the oxidation of toluene on vanadium silicates are mainly benzyl alcohol, benzaldehyde (formed by the secondary oxidation of benzyl alcohol), *o*- and *p*-cresol. The formation of benzaldehyde as the major product in the product distribution indicates that vanadium silicates are more effective in the oxidation of the side chain alkyl group. The formation of significant quantities of benzyl alcohol and benzaldehyde is in contrast to the observation on titanium silicates wherein the products are only *o*- and *p*-cresols. Silicalite-2 is completely inactive in the oxidation of toluene either to benzaldehyde or to cresols. It may be also mentioned that vanadium impregnated silicalite-2 showed negligible activity in the above oxidation reaction.

Table 14 illustrates the activity of the vanadium silicates with different Si/V ratios. Both the conversion and the hydrogen peroxide selectivity increased with the content of the vanadium. For the samples with Si/V ratios 79, 122 and 161, the toluene conversions are 11.7, 8.2 and 6.9, respectively and the hydrogen peroxide selectivities are 49.5, 32.4 and 23.4 respectively. With an increase in the content of the vanadium in the sample, the oxidation of the side chain methyl group is more favoured.

Table 13

Oxidation of toluene over vanadium silicate molecular sieves[a]

Catalyst[b]	Conversion[c] (mole, %)	H_2O_2[d] Selectivity	Product distribution, (mole, %)				
			Benzyl alcohol	Benzaldehyde	o-Cresol	p-Cresol	Others
VS-2	11.7	49.5	7.7	52.2	19.7	17.1	3.7
S-2	0	-	-	-	-	-	-
V-imp- S-2	1.2	0.4	-	5.2	-	-	94.8
TS-2	13.2	38.0	-	-	36	59	5.0

[a] Reaction conditions: catalyst = VS-2, (Si/V = 79); toluene (g) = 1; toluene/catalyst (wt. ratio) = 10; tolene/H_2O_2 (mole ratio) = 3; temperature (K) = 353; solvent = acetonitrile; reaction duration = 12 h.

[b] VS-2 : Si/V = 79; S-2 : Si/Al = > 2000; V-imp-S-2 (vanadium impregnated silicalite-2): Si/V = 82; TS-2 : Si/Ti = 77.

[c] $$\text{Conversion} = \frac{\text{No. of moles of toluene converted}}{\text{Total no. of moles of Toluene in reaction mixture}} \times 100$$

[d] H_2O_2 utilized in the formation of benzyl alcohol, benzaldehyde and cresols.

Table 14

Oxidation of toluene over vanadium silicate molecular sieves[a]

Si/V	Conversion[b] (mole, %)	H_2O_2[c] Selectivity	Product distribution (mole, %)				
			Benzyl alcohol	Benzaldehyde	o-Cresol	p-Cresol	Others
79	11.7	49.5	7.7	52.2	19.7	17.1	3.7
122	8.2	32.4	17.0	38.0	24.4	14.2	6.4
161	6.9	23.4	17.7	28.6	26.6	17.7	9.4

[a] Reaction conditions: catalyst = VS-2, (Si/V = 79); toluene (g) = 1; toluene/catalyst (wt. ratio) = 10; tolene/H_2O_2 (mole ratio) = 3; temperature (K) = 353; solvent = acetonitrile; reaction duration = 12 h.

[b] $$\text{Conversion} = \frac{\text{No. of moles of toluene converted}}{\text{Total no. of moles of Toluene in reaction mixture}} \times 100$$

[c] H_2O_2 utilized in the formation of benzyl alcohol, benzaldehyde and cresols.

Vanadium silicate are also active in the oxidation of xylenes and trimethylbenzenes. Both ring hydroxylation and side chain oxidation occur. The relative rates of conversions are, toluene (3.6) > *p*-xylene (2.4) > *m*-xylene (1)= *o*- xylene (1) = 1 3 5 trimethylbenzene (1). The trend parallels the diffusivity of these molecules in the MEL molecular sieves and indicates that the vanadium sites are located inside the channel system.

The influence of solvents on the catalytic activity of the vanadium silicates in the oxidation of toluene is presented in Table 15. The highest activity is found in acetonitrile and follows the order: acetonitrile > methanol > acetone. Unlike in the case of the oxidation of phenol and aniline, vanadium silicates are active even when methanol is used as solvent. However the product selectivity is much lower compared to that in acetonitrile and acetone.

4.3.6 OXIDATION OF ANILINE

Several methods for the oxidation of aniline are reported in the literature. Azobenzene is obtained using MnO_2 as stoichiometric oxidant[66]. Aqueous peracids oxidize aniline to azo and azoxy benzenes[67], while anhydric peracids oxidize aniline to nitrobenzene[68]. Vanadium and molybdenum complexes[69] in the presence of *tert*-butyl hydroperoxide catalyze the oxidation of aniline to nitrobenzene, and titanium complexes[70] to only azoxybenzene. Tungsten oxide[71] in the presence of hydrogen peroxide oxidizes aniline to nitroso and azoxybenzenes. Recently, oxidation of aniline to either azoxybenzene or to nitrobenzene using ruthenium ternary complexes in the presence of hydrogen peroxide has been reported[72]. Vanadium silicate molecular sieves in the presence of aqueous H_2O_2 catalyze the oxidation of aniline to nitrobenzene, azoxybenzene and hydroxy anilines.

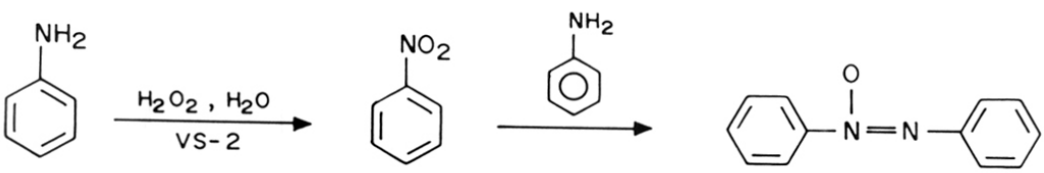

Table 15

Oxidation of toluene over vanadium silicate molecular sieves[a]

Solvent	Conversion[b] (mole, %)	H_2O_2 Selectivity[c]	Product distribution (mole, %)				
			Benzyl alcohol	Benzaldehyde	o-Cresol	p-Cresol	Others
Acetonitrile	11.7	49.5	7.7	52.2	19.7	17.1	3.7
Methanol	7.2	15.0	8.1	21.4	11.7	10.8	48.0
Acetone	5.2	20.8	10.2	45.0	21.0	19.6	4.2

[a] Reaction conditions: catalyst = VS-2, (Si/V = 79); toluene (g) = 1; toluene/catalyst (wt. ratio) = 10; toluene/H_2O_2 (mole ratio) = 3; temperature (K) = 353; reaction duration = 12 h.

[b] $$\text{Conversion} = \frac{\text{No. of moles of toluene converted}}{\text{Total no. of moles of Toluene in reaction mixture}} \times 100$$

[c] H_2O_2 utilized in the formation of benzyl alcohol, benzaldehyde and cresols.

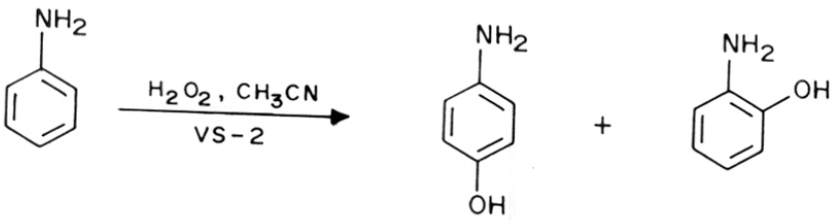

The oxidation of aniline was studied using different solvents and VS-2 as catalyst. The oxidation product distribution strongly depends on the solvent used. As shown in the Table 16, nitrobenzene and azoxy benzene along with small amounts of azobenzene are obtained when water is used as solvent. Hydroxy anilines are obtained as major products using acetonitrile as solvent. Aniline condensed with acetone immediately when hydrogen peroxide was added to the reaction mixture (the condensation reaction also occurred in the absence of catalyst). Minor quantities of hydroxylated products on the aromatic nucleus of the condensed product are also obtained. When methanol is used as the solvent, neither oxidation of the amine group nor hydroxylation of the aromatic nucleus took place. Similarly, in the hydroxylation of phenol, no hydroxylated products are obtained when methanol is used as the solvent[15]. However, hydroxylation of alkanes, benzene and alkyl aromatics occurred in methanol solvent.

4.3.7 OXIDATION OF SULFIDES

The oxidation of sulfides to corresponding sulfoxides and sulfones is generally carried out by using hydroperoxides[73-75], peracids[33,76], diazomethane and SO_2[77] and superoxide anion[78] in stoichiometric quantities. Recently, selective oxidation of sulfides to sulfoxides and sulfones was reported on titanium silicate molecular sieves[79]. Vanadium silicate molecular sieves are more active in the oxidation of sulfides compared to their titanium analogs.

Table 16

Oxidation of aniline on vanadium silicate molecular sieves[a]

Solvent	Conversion[b] (mole, %)	H_2O_2 selectivity[c]	Product distribution (mole, %)				
			PHA[d]	OHA[e]	Nitrobenzne	Azoxybenzene	Others
Acetonitrile	4.3	9.2	21.4	64.3	-	-	14.3
Water	23.9	48.8	-	-	26.9	72.7	0.4
Acetone	18.0	1.4	0.9	2.2	-	-	91.4[f]
Methanol	19.6	0	-	-	-	-	100

[a] Reaction conditions : catalyst = VS-2, Si/V = 79; aniline/catalyst (wt. ratio) = 10; aniline/ H_2O_2 (mole ratio) = 3; temperature (K) = 333; reaction duration (h) = 10

[b] $\text{Conversion} = \frac{\text{No. of moles aniline converted}}{\text{Total no. of moles of aniline in reaction mixture}} \times 100$

[c] H_2O_2 utilized for the formation hydroxy anilines, nitrobenze and azoxy benzene

[d] *para*-hydroxy aniline and [e] *ortho*-hydroxy aniline

[f] Condensation product of aniline with acetone (also formed in the abscence of catalyst) and their hydroxylated products.

[g] Condensation product of aniline with methanol.

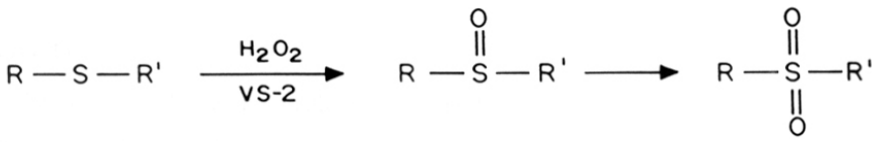

$$R = CH_3,\ C_2H_5,\ C_6H_5$$
$$R' = CH_3,\ C_2H_5$$

The results of the oxidation of various sulfides, *viz.*, dimethylsulfide, diethylsulfide, phenylmethylsulfide and phenylethylsulfide on vanadium silicate (Si/V = 79) using dilute hydrogen peroxide are summarized in Table 17. Oxidation of $(CH_3)_2S$ was carried out at 298 K and other sulfides at 323 K. The products of the reaction are corresponding sulfoxides and sulfones. No other side products are formed in these reactions. Vanadium silicates have high activity and the oxidation of sulfides was completed within 5 to 30 min. The reactivity of the sulfides followed the order $CH_3S > C_2H_5S > PhSCH_3 > PhSC_2H_5$. Table 18 compares the activities of VS-2, TS-2, silicalite-2 and ZSM-11 as catalysts in the oxidation of $PhSCH_3$. The most active catalyst in this sulfoxidation is VS-2. The activity decreased in the order VS-2 > TS-2 > ZSM-11 > silicalite-2. After 30 min of the reaction time under similar conditions the oxidation of methy phenyl sulfide on VS-2, TS-2, silicalite-2 and ZSM-11 are 100, 22, 15, 16 mole %, respectively. On continuing the reaction for 120 min, complete oxidation of sulfide was achieved on TS-2. However, on silicalite-2 and ZSM-11 the conversion levelled off around 50 mole % even after continuing the reaction for 10 h.

Table 17

Oxidation of sulfides over vanadium silicate molecular sieves[a]

Reactant	Conversion[b], (mole, %)	Product distribution (mole, %)		
		Sulfoxide	Sulfone	Others
Dimethyl sulfide[c]	100	71	29	-
Diethyl sulfide	100	81	19	-
Methyl phenyl sulfide	100	84	16	-
Ethyl phenyl sulfide	92	81	12	7

[a] Reaction conditions : catalyst = VS-2, Si/V = 79; sulfide/catalyst (wt. ratio) = 10; sulfide/H_2O_2 (mole ratio) = 1; temperature (K) = 333; solvent = acetonirile; Reaction duration 5 - 30 min.

[b] $$\text{Conversion} = \frac{\text{No. of moles of sulphide conver ted}}{\text{Total no. of moles of sulphides in the reaction mixture}} \times 100$$

[c] Temperature (K) = 298.

Table 18

Oxidation of methyl phenyl sulfide on different catalysts[a]

Catalyst[b]	Reaction Time (min.)	Conversion[c], (mole, %)	Product distribution, (mole, %)	
			$PhSCH_3O$	$PhSCH_3O_2$
VS-2	30	100	84	16
S-2	30	15	72	28
S-2	120	47	84	16
ZSM-11	30	16	84	16
ZSM-11	120	44	89	11
TS-2	30	22	74	26
TS-2	120	100	78	22

[a] Reaction conditions : sulfide/catalyst (wt. ratio) = 10; sulfide/H_2O_2 (mole ratio) = 1; temperature (K) = 333; solvent = acetonirile

[b] VS-2 : Si/V = 79; S-2 : Si/Al = > 2000; ZSM-11 : Si/Al = 82; TS-2 : Si/Ti = 77.

[c] $$\text{Conversion} = \frac{\text{No. of moles of sulphide conver ted}}{\text{Total no. of moles of sulphides in the reaction mixture}} \times 100$$

4.4 CONCLUSIONS

1. Vanadium silicate molecular sieves are active in the oxyfunctionalization of hydrocarbons (hexane, heptane, octane and cyclohexane). hydroxylation of aromatics (benzene, phenol toluene, aniline) and sulfoxidation reactions.

2. Like titanium silicates (TS-1 and TS-2), vanadium silicates are active in the oxyfunctionalization of alkanes yielding alcohols, which undergo further oxidation to carbonyl compounds. However, contrary to the observation on titanium silicates, the vanadium silicates are also able to activate the primary C-H bond of the *n*-alkanes giving primary alcohols and corresponding aldehydes.

3. Solvents have considerable influence on the activity in the oxyfunctionalization of alkanes. Non-protic solvents enhance the rate of reactions. Amongst the non-protic solvents, more polar solvents such as CH_3CN are more effective.

4. The formation of a radical-type intermediate has been inferred from ESR observations. A mechanism involving a peroxo vanadium radical which abstracts a H atom from the hydrocarbon molecule to give a carbon radical which is further hydroxylated to the alcohol is proposed. Only isolated vanadium ions (which exist in VS-2 samples) are probably involved in the oxidation reaction.

5. Vanadium silicate molecular sieves are active in hydroxylation of benzene. Neither silicalite-2 nor vanadium impregnated silicalite-2 are active in this reaction. Acetonitrile is the most suitable solvent among acetone, acetonitrile, methanol.

6. Vanadium silicate molecular sieves are also efficient catalysts in the hydroxylation of phenol.

7. The influence of solvent on the product selectivity in hydroxylation of phenol is significantly different from that observed on titanium silicates. Water is the most suitable solvents in which the activity is comparable to that of titanium silicates.

8. No hydroxylated products of phenol were formed when methanol was used as the solvent, though hydroxylation of alkanes, benzene and alkyl aromatics took place in the presence of methanol. When acetone was used as the solvent hydroquinone and *para*-benzoquinone were the only products; catechol was not formed.

9. In oxidation of toluene, vanadium silicates are active both in ring hydroxylation (to *ortho* and *para* cresols) and side chain oxidation (to benzyl alcohol and benzaldehyde). In this respect they differ from titanium silicates which are active in ring hydroxylation of aromatic nucleus only.

10. Shape selectivity was observed in oxidation of alkyl aromatics (xylenes and trimethybenzene) confirming that most of the vanadium ions are inside the channel system of MEL.

11. In the oxidation of aniline, vanadium silicates are active in both ring hydroxylation (to *ortho* and *para* hydroxyl anilines) and amine group oxidation (to nitrobenzene). Hydroxylation of aromatic nucleus occurred in the presence of acetonitrile and oxidation of amine group took place when water was used as solvent.

12. Vanadium silicates are active catalysts in the oxidation of sulfides to sulfoxides and sulfones. Their activity is about 8 times higher than that of the titanium analogs.

4.5 REFERENCES

1. Taramasso, M. Perego, G. and Notari, B., US Patent 4,441,501 (1983).
2. Esposito, A., Taramasso, M., Neri C. and Buonomo, F., U.K. Patent 2,116,974 (1983); U.S. Patent 4,396,783 (1983);
3. Perego, G., Bellussi, G., Corno, C., Taramasso, M., Buonomo, F.and Esposito A., *Stud. Surf. Sci. Catal.*, **28**, 129 (1989).
4. Reddy, J.S., Kumar, R. and Ratnasamy, P., *Appl. Catal.*, **58**, L1 (1990).
5. Romono, U., Esposito, A., Maspero, F., Neri C. and Clerici, M.G., *Chem. Ind.*, (Milan) **72**, 610 (1990).
6. Notari, B., *Stud. Surf. Sci. Catal.*, **37**, 413 (1987).
7. Thangaraj, A., Kumar, R. and Ratnasamy, P., *Appl. Catal.*, **57**, L1 (1990); *J. Catal.*, **131**, 394 (1991).
8. Tatsmui, T., Nakamura, M., Negishi S., and Tominaga, H., *J. Chem. Soc. Chem. Comm.*, 476 (1990).
9. Huybrechts, D.R.C., Bruycker L.D., and Jacobs, P.A., *Nature*, **345**, 240 (1990).

9a Reddy,J.S., Sivasanker, S. and Ratnasamy, P., *J. Mol. Catal.*, **70**, 335 (1991).

10. Thangaraj, A., Sivasanker, S. and Ratnasamy, P., *J. Catal.*, **131**, 394 (1991).
11. Reddy, J.S., Sivasanker, S., and Ratnasamy, P., *J. Mol. Catal.*, **69**, 383 (1991).
12. Tatsumi, T., Nakamura, M., Yuasa, K. and Tominaga, H., *Chem.. Lett.*, 297 (1990).
13. Hari Prasad Rao, P.R., Thangaraj, A. and Ramaswamy, A.V., *J. Chem. Soc. Chem. Commun.*, 1139 (1991).
14. Hari Prasad Rao, P. R., Ramaswamy, A.V. and Ratnasamy, P., *J. Catal.*, **137**, 225 (1992).

14a. Hari Prasad Rao, P.R., Belhekar, A.A., Hegde, H.G., Ramaswamy, A.V. and Ratnasamy, P., *J. Catal.* (communicated).

15. Hari Prasad Rao, P. R. and Ramaswamy, A.V., *Appl. Catal.*, (in press).
16. Hari Prasad Rao P.R., and Ramaswamy, A.V., *J. Chem. Soc. Chem. Commun.*, 1245 (1992).

16a. Hari Prasad Rao, P.R., Ramaswamy, A.V. and Ratnasamy, P., *J. Catal.* (communicated).

17. Hari Prasad Rao, P.R., Reddy, K.R., Ramaswamy, A.V. and Ratnasamy, P., *3rd Int. Symp. on Heterogeneous Catalysis and Fine Chemicals*, Poitiers, France, April (1993) (Accepted for oral presentation)
18. Inui, T., Medhanavyn, D., Praserthdam, P., Fukuda, K., Ukawa, T., Sakamoto, A. and Miyamoto, A., *Appl. Catal.*, **18**, 311 (1985).
19. Miyamoto, A., Medhanavyn, D. and Inui, T., *Appl. Catal.*, **28**, 89 (1986).

20. Miyamoto, A., Medhanavyn, D. and Inui, T., *Chem. Express,* **1,** 559 (1986).

21. Miyamoto, A. Medhanavyn, D.and Inui, T., *Proc. 9th Intern. Congr. Catal.,* (M.J. Philip and M. Ternan, Eds.) pub. Chem. Inst. of Canada, Ontario, vol. **1**, p. 437 (1988).

22. Cavani, F., Trifiro, F., Habersberger, K. and Tvaruzkova, Z., *Zeolites*, **8**, 12 (1988).

23. Centi, G., Jiru, P. and Trifiro, F., *Stud. Surf. Sci. Catal.*, **44**, 247 (1988).

24. Tvaruzkova, Z., Centi, G., Jiru, P. and Trifiro, F., *Appl. Catal.,* **19**, 307 (1985).

25. Habersberger, K., Jiru, P., Tvaruzkova, Z., Centi, G., and Trifiro, F., *React. Kinet. Catal. Lett.*, **39**, 95 (1989).

26. Centi, G., Habersberger, K., Jiru, P., Trifiro, F. and Tvaruzkova, Z., *Chem. Express,* **1,** 717 (1986).

27. Miyamoto, A., Iwamoto, Y., Matsuda, H. and Inui, T., *Stud. Surf. Sci. Catal.*, **49 B**, 1233 (1989).

28. Zatorski, L.W., Centi, G., Nieto, J.L., Trifiro, F., Bellussi, G. and Fattore, V., *Stud. Surf. Sci. Catal.*, **49 B**, 1243 (1989).

29. Hari Prasad Rao, P.R., Thangaraj, A. and Ramaswamy, A.V., Proc. 10th Natl. Symp. on Catal. and 4th INDO-USSR Symp. on Catal. " *Recent Developments in Catalysis, Theory and Practice*" (Eds. B.Viswanathan and C.N. Pillai), Narosa Pub. New Delhi, India, p. 146 (1989).

30. Kokotailo, G. T., Lawton, S. L., Olson, D. H. and Meier, W. M., *Nature*, **275**, 437 (1978).

31. Flanigen, E. M., Bennett, J. M., Grose, R. W., Cohen, J. P., Patton, R. L., Kirchner, R. M. and Smith, J. V., *Nature*, **271**, 512 (1978)

32. Bibby, D. M., Milestone, N. B. and Aldridge, L. B., *Nature*, **280**, 664 (1979).

33. Sheldon, R. A. and Kochi, J. K., *Metal-Catalyzed Oxidations of Organic Compounds,* Acadamic, New York, (1981).

34. Lyons, J.E., *Appl. Ind. Catal.*, **3**, 131 (1981).

35. Meunier, B., *Bull. Soc. Chim. Fr.,* 578 (1986).

36. Herron, N. and Tolman, C.A., *J. Am. Chem. Soc.*, **109,** 2837 (1987).

37. Weisz, P.B., *Stud. Surf. Sci. Catal.*, **7**, 3 (1980).

38. Mimoun, H., Saussine, L., Daire, E., Postel, M., Fischer, J. and Weiss, R., *J. Amer. Chem. Soc.,* **105**, 3101 (1983).

39. Kirk-Othmer, *Encyclopaedia of Chemical Technology,* 3rd edn, (John Wiley and Sons, New York), **18**, 425 (1978).

40. Reddy, J.S. and Sivasanker, S., *Catal. Lett.*, **11**, 241 (1991).

41. Walling, C., *Acc. Chem. Res.* **8**, 125 (1975).

42. Udenfriend, S., Clark, C.T., Axelord, J. and Bordie, B., *J. Biol. Chem.*, **208**, 731 (1954).

43. Hamilton, G.A. and Friedman, J.P., *J. Amer. Chem. Soc.*, **85**, 1008 (1963).

44. Kinoshita, T., Harada, J., Ito, S. and Sasaki, K., *Angew. Chem. Int. Ed. Engl.*, **22**, 502 (1983).

45. Orita, H., Hayakawa, T., Shimizu, M. and Takehira, K., *J. Mol. Catal.*, **42**, 99 (1987).

46. Suzuki, E., Nakashira, K. and Ono, Y., *Chem. Lett.*, 953 (1988).

47. Panov, G.I., Sheveleva, G.A., Kharitonova, A.S., Romannikov, V.N. and Vostrikova, L.A., *Appl. Catal. A,* **82**, 31 (1992).

48. Sosnovsky, G. and Rawlinson, D.J., in Swern, D. (Editor) *Organic Peroxides,* **II** Wiley Interscience, New York, p. 277 (1971).

49. Olah, G.A. and Ohnishi, R., *J. Org. Chem.*, **43**, 865 (1978).

50. Bourdin, F., Costantini, M., Jouffret, M. and Lartigan, G., Ger. Pat. DE 2,064,497 (1971), assigned to Rhone-Paulenc, France.

51. Maggiono, P., US Pat. 3,914,323 (1972), assigned to Brachima.

52. Krausherar-Czarnetzki, B. and Van Hoof, J.H.C., *Catal. Lett.,* **2**, 43 (1989).

53 Thangaraj, A., Ph.D. Thesis, University of Poona (1991).

54 Reddy J.S., Ph.D. Thesis, University of Poona (1992).

55. Huybrechts,D.R.C., Buskens, P.L. and Jacobs, P.A., *Catal. Lett.*, **8**, 273 (1991).

56. Huybrechts, D.R.C., Buskens, P.L. and Jacobs, P.A., *J. Mol.Catal.,* **71**, 129 (1992).

57. Tuel, A., Moussa-khouzami, Y., Taarit, B. and Naccache, C., *J. Mol. Catal.*, **68**, 45 (1991).

58. Olah, G.A., Keumi, T. and Fung, A.P., *Synthesis,* 536 (1979).

59. Onopchenko, A., Schulz, J.D.D. and Seekircher, R., *J. Org. Chem.*, **37**, 1414 (1972); Hronec, M. and Havsky, J., *Ind. Eng. Chem. Prod. Res. Dev.*, **21**, 455 (1982).

60. Matsuoba, M. and Kokusenya, Y., *Japan Kokai,* J.P. 50/144697, 1975,(Chem. Abs, **84**, 150349u (1975))

61. Buciocchi, E., Rol, C. and Ruzziconi, R., *J. Chem. Res.*, 334 (1984).

62. Walling,C., Zhao, C. and El-Taliawi, G.M., *J. Org. Chem.*, **48**, 4910 (1983).

63. Battioni, P., Renaud, J.P., Bartoli, J.F. and Mansuy, D., *J. Chem. Soc. Chem. Commun.*, 341 (1986).

64. Moiseeva, N.I., Gekhman, A.E., Blymberg, E.A., Moiseeva, I.I., *Kinet. Katal.*, **29**, 970 (1988).

65. Barak, G. and Sasson, Y., *J. Chem. Soc. Chem. Commun.*, 637 (1988).

66. Wheeler, O.D. and Gonzales, D., *Tetrahedron*, **20**, 189 (1964).

67. Gutman, H.R., *Experentia*, **20**, 128 (1964).

68. Emmons, W.D., *J. Amer. Chem. Soc.*, **79**, 5528 (1957).

69. Howe, G.R. and Hiatt, R.R., *J. Org. Chem.*, **25**, 4007 (1970).

70. Kosswig, K., *Justus Liebigs Ann. Chem.*, **749**, 206 (1971).

71. Burchard, P., Fleury, J.P. and Weiss, F., *Bull. Soc. Chim. Fr.*, 2730 (1965).

72. Barak, G. and Sasson, Y., *J. Org. Chem.*, **54**, 3484 (1989).

73. Tezuka,T., Iwaki, M. and Haga, Y., *J. Chem. Soc. Chem. Commun.*, 325 (1984).

74. Bruice, T.C., Noar, J.B., Ball, S.S. and Venkataram, U.V., *J. Amer. Chem. Soc.*, **105**, 2452 (1983).

75. Baumstartk, A.L. and Vasquez, P.C., *J. Org. Chem.*, **48**, 65 (1983).

76. Bortolini, O., Campestrini, S., Furia, F.D. and Modena, G., *J. Org. Chem.*, **52**, 5093 (1987).

77. Thijs, L., Wagennan, A., Van Rens, E.M.M. and Zwanenbug, B., *Tet. Lett.*, 3589 (1973).

78. Sawyer, D.T., Gibian, M.J., Morrison, M.M. and Seo, E.T., *J. Amer. Chem. Soc.*, **100**, 627 (1978).

79. Reddy, R.S., Reddy, J.S., Kumar, R. and Kumar, P., *J. Chem. Soc. Chem. Commun.*, 84 (1992).

CHAPTER 5

SUMMARY AND CONCLUSIONS

Isomorphous substitution of Al or Si in zeolites/molecular sieves with transition metals having redox properties leads to oxidation activity combined with shape selective properties. Ferrisilicates and titanium silicates are two such systems which have been synthesized and their catalytic applications explored. Vanadium incorporated molecular sieves are a new class of materials which can also catalyze various oxidation reactions selectively. They have interesting catalytic properties in ammoxidation of xylenes and propane, oxidative dehydrogenation of propane, oxyfunctionalization of alkanes and hydroxylation of aromatics. **This thesis describes, in detail, the synthesis, characterization and catalytic properties of vanadium silicate molecular sieves with MEL structure. The major objectives of the work are 1) to synthesize vanadium silicate molecular sieves, 2) to characterize the structural environment of the vanadium in them and 3) to study the physico-chemical and catalytic properties.**

Vanadium silicate molecular sieves with MEL structure have been prepared with different Si/V ratios (40 - 300). Tetraethyl orthosilicate and a vanadium salt were used as ingredients and tetrabutyl ammonium hydroxide as templating agent. Three different sources of vanadium with different oxidation states *viz.* VCl_3 (III), $VOSO_4$ (IV) and NH_4VO_3 (V) were tested in the synthesis of vanadium silicates. The gels containing $VOSO_4$ and NH_4VO_3 were clear solution and that with VCl_3 was slightly turbid. The chemical analysis of the sample showed that only a part of the vanadium was retained in the samples after hydrothermal crystallization. The amount of the vanadium retained in the sample depends on the source of vanadium and is approximately 60, 50 and 25 % for VCl_3, $VOSO_4$ and NH_4VO_3, respectively. The oxidation activity of vanadium silicates prepared using $VOSO_4$ as vanadium source was found to be high. Hence, further detailed studies on the synthesis, characterization and activity of vanadium silicates were carried out using $VOSO_4$ as vanadium source.

The effect of various synthesis parameters such as temperature, organic additive, Si/V ratios and water content on the crystallization kinetics of vanadium silicates are presented in Chapter II. An increase in Si/V molar ratio in the reaction mixture enhanced the rate of crystallization. SiO_2/TBA-OH molar ratio of 5 was found to be optimum in the synthesis of vanadium silicates. An increase in the pH of mother liquor with crystallization was observed. This indicates the incorporation of probably both V and Si in the framework. The apparent activation energies for nucleation and crystallization were calculated to be 53.80 kJ mol^{-1} and 56.54 kJ mol^{-1}, respectively.

Physico-chemical characterization of V-silicates was carried out using XRD, spectroscopic (IR/FTIR, ESR, MAS NMR, UV-VIS) and adsorption techniques (Chapter III). The unit cell parameters of VS-2 samples increased uniformly and regularly with the vanadium content in the samples. On steaming the samples, a reduction in the unit cell parameters was observed. An absorption band at around 965 cm^{-1} was observed in the IR spectra of VS-2 samples. This band is absent in the IR spectra of pure silicalite-2 and vanadium impregnated silicalite-2 samples.

It has been proposed that the vanadium ions are probably coordinated at defect sites where the concentration of the Si-OH groups is likely to be high. A broad IR absorption band at 3532 cm^{-1} (due to hydrogen bonded hydroxyl groups) was observed in all VS-2 samples. There is a correlation between the integrated intensity of this band (3532 cm^{-1}) and the vanadium content of the sample. This observation supports the model proposed for vanadium silicates.

The characterization of the surface acidity of the VS-2 samples has been carried out using ammonia and pyridine adsorption. The FTIR spectra on the desorption of ammonia shows two distinct bands at 1680 and 1450 cm^{-1} due to ammonium ions (δ_s and δ_{as} of NH_4, respectively). The spectra of pyridine adsorption showed a weak band at 1547 cm^{-1} due to pyridinium ions. This indicates the presence of Brönsted acid sites. However, the intensity of these bands decreased drastically on evacuation above 373 K indicating that these Brönsted acid sites are weak in nature. These bands are absent in pure silicalite-2 and are probably related to V-OH species of VS-2. This is in agreement with the sodium exchange behavior of the samples.

The ESR spectra of the as-synthesized vanadium silicates have well resolved anisotropic 8-line hyperfine splitting. The hyperfine splitting at room temperature indicates atomically dispersed vanadium in the sample. The 'g' values and hyperfine coupling constants ($g_{\parallel}$= 1.932; $g_{\perp}$ = 1.981; $A_{\parallel}$ = 185 G and $A_{\perp}$ = 72 G) are notably different from those observed for VO^{2+} exchanged into ZSM-5. They are assigned to V^{4+} at framework positions. A linear increase in the ESR signal intensities with vanadium content (of as-synthesized samples) and corresponding parallel increase in unit cell volume (calcined samples) strongly supports the presence of vanadium at framework positions. After calcination no ESR signal was observed indicating complete oxidation of V^{4+} to V^{5+}. After reducing in H_2 as well as after using in catalytic reaction the spectra reappeared. This shows the reversibility of V^{4+} <--> V^{5+} transition.

The ^{51}V MAS-NMR spectra of VS-2 samples reveal that the nature of vanadium strongly depends on the source of vanadium utilized during the synthesis. The ^{51}V NMR spectrum of VS-2 prepared using $VOSO_4$ as source shows a main signal at -573 ppm (relative to $VOCl_3$). The observed line width at half height (approximately 50 ppm) is much narrower than that reported (around 250 ppm) for supported vanadium oxide catalysts. This is similar to those observed in monomeric vanadates with vanadium ions in distorted tetrahedral coordination. The absence of an absorption band around -300 ppm shows that no V_2O_5 like phase and clustered vanadium are present. The UV-VIS spectrum of VS-2 shows an absorption band at 310 nm, which also indicate distorted tetrahedral environment for V^{5+} ions. Adsorption of *n*-hexane and cyclohexane also show the absence of occluded amorphous material. A possible environment of vanadium in VS-2 has been proposed consistent with our results.

Vanadium silicates are found to have interesting catalytic properties in various oxidation reactions. They are active in the oxidation of alkanes, benzene, phenol, alkyl aromatics, aniline and sulfides (Chapter IV).

Vanadium silicate-2 (VS-2) molecular sieves in the presence of dilute hydrogen peroxide oxidized alkanes (*n*-hexane, *n*-heptane, *n*-octane and cyclohexane) to corresponding alcohols and carbonyl compounds. They are also able to activate the primary C-H bond of the *n*-alkanes giving primary alcohols and aldehydes. However, the activation of the carbon atom at the second position is preferred to others and follows the order 2 > 3 > 4 > 1. The oxidation conversions and H_2O_2 selectivities decreased in the order *n*-hexane > *n*-heptane > *n*-octane > cyclohexane. This order is consistent with the large decrease in diffusivities with increase in chain length and molecular size of the paraffin molecules. Solvents have considerable influence in the oxy-functionalization of alkanes. Acetonitrile is found to be the most effective solvent with highest selectivity to the monosubstituted products. The activity and selectivity seems to be related to the polarity of the solvent and decreased in the order: acetonitrile > methanol > acetone. The formation of the radical type intermediate has been inferred from the ESR observations. A mechanism involving vanadium peroxo-radical which abstracts a H atom from the hydrocarbon molecule to give a carbon radical, which is further hydroxylated to alcohol is proposed.

Vanadium silicates are active in the hydroxylation of benzene. The product distribution contains phenol and *para*-benzoquinone (PBQ). Formation of PBQ was also observed when

titanium silicates were used as catalysts, but not when acidic zeolites were used. Hence, as in titanium silicates, in vanadium silicates also peroxo species may be involved in the hydroxylation.

VS-2 is an efficient catalyst in hydroxylation of phenol to hydroquinone and catechol. Solvents have interesting influence in this reaction. Water is the most suitable solvent in which the activity is comparable to that of titanium silicates. The phenol conversions and H_2O_2 selectivities decreased in the order water > acetonitrile > acetone. When acetone is the solvent, only hydroquinone along with small quantities of *para* benzoquinone were the products. No hydroxylated products of phenol are formed when methanol is used as a solvent.

In the oxidation of alkyl aromatics, VS-2 is active in both the hydroxylation of aromatic nucleus as well as the oxidation of side chain alkyl groups. Benzyl alcohol, benzaldehyde and *ortho*- and *para*-cresols were the products in the oxidation of toluene. The formation of benzaldehyde as the major product shows their ability to oxidize side chain methyl groups more effectively. In contrast, on titanium silicates, only ring hydroxylation takes place giving cresols as products.

VS-2 is active in oxidation of aniline. As with alkyl aromatics, both ring hydroxylation and oxidation of amino group are possible. However, product distribution depends on the solvent used. Hydroxy anilines are the products when acetonitrile is used as solvent. Nitrobenzene and azoxybenzenes are the products when water is used as solvent. Thus solvents have a profound influence on the conversion and selectivity. VS-2 is found to be the most effective catalyst in the oxidation of sulfides to sulfoxides and sulfones, among VS-2, TS-2, silicalite-2 and ZSM-11.

PUBLICATIONS

1. "Oxidative dehydrogenation of aqueous ethanol over the molecular sieve TS-1", P.R. Hari Prasad Rao, A. Thangaraj and A.V. Ramaswamy, *J. Chem. Soc. Chem. Commun.*, 1139 (1991).
2. "Synthesis and catalytic properties of crystalline, microporous vanadium silicates with MEL structure", P.R. Hari Prasad Rao, A.V. Ramaswamy, and P. Ratnasamy, *J. Catal.*, **137**, 225 (1992).
3. "Catalytic hydroxylation of phenol over vanadium silicate molecular sieve with MEL structure", P.R. Hari Prasad Rao, and A.V. Ramaswamy, *Appl. Catal.*, (in press).
4. "Oxyfunctionalization of alkanes with H_2O_2 catalyzed by vanadium silicates", P.R. Hari Prasad Rao, and A.V. Ramaswamy, *J. Chem. Soc. Chem. Commun.*, 1245 (1992).
5. "Oxidative dehydrogenation of aqueous ethanol over non-acidic pentasil type zeolites", P.R. Hari Prasad Rao, A. Thangaraj and A.V. Ramaswamy, *Recent Developments in Catalysis, Theory and Practice,* (Eds. B.Viswanathan and C.N. Pillai), Narosa, New Delhi p. 146, 1989.
6. "Selective oxidation reactions over vanadium silicate molecular sieves", P.R. Hari Prasad Rao, K.R. Reddy, A.V. Ramaswamy and P. Ratnasamy, *3rd Int. Symp. on Heterogeneous Catalysis and Fine Chemicals*, Poitiers, France, April (1993) (Accepted for oral presentation).
7. "Synthesis and characterization of vanadium silicate with MEL structure", P.R. Hari Prasad Rao, R. Kumar, A.V. Ramaswamy, and P. Ratnasamy, *Zeolites*, (communicated).
8. "Studies on the crystalline microporous vanadium silicates, II. FTIR, NMR and ESR spectroscopy and catalytic oxidation of alkyl aromatics over VS-2", P.R. Hari Prasad Rao, A.A. Belhekar, S.G. Hegde, A.V. Ramaswamy and P. Ratnasamy, *J. Catal.*, (communicated).
9. "Studies on the crystalline microporous vanadium silicates, III. Selective oxidation of n-alkanes and cyclohexane on VS-2", P.R. Hari Prasad Rao, A.V. Ramaswamy and P. Ratnasamy, *J. Catal.*, (communicated).
10. "Theoretical studies on the isomorphous substitution of vanadium into molecular sieves", R. Vetrivel, P.R. Hari Prasad Rao and A.V. Ramaswamy, (to be communicated).
11. "Selective oxidation of N and S containing compounds on vanadium silicate molecular sieves", P.R. Hari Prasad Rao, A.V. Ramaswamy and P. Ratnasamy (to be communicated).

Patents

1. "A process for the preparation of vanadium titanium silicate molecular sieve",
   P.R. Hari Prasad Rao, A. Thangaraj and A.V. Ramaswamy, 1025/DEL/91
2. "A process for the preparation of a novel porous crystalline material vanadium silicate, VS-2",
   P.R. Hari Prasad Rao, A.V. Ramaswamy, and P. Ratnasamy, (applied).
3. "A process for the preparation of large pore vanadium silicate molecular sieve",
   A.P. Singh, K.R.Reddy, P.R. Hari Prasad Rao and P. Ratnasamy, (applied).